MODELING OF CONTINUOUS BIODIESEL PRODUCTION FROM ESTERIFICATION OF OLEIC ACID IN THE PRESENCE OF SOLID CATALYSTS

MR. KIATTISAK PINMAI
ID: 55300700510

A THESIS SUBMITTED AS A PART OF THE REQUIREMENTS FOR THE DEGREE OF MASTER OF ENGINEERING IN ENERGY TECHNOLOGY AND MANAGEMENT

THE JOINT GRADUATE SCHOOL OF ENERGY AND ENVIRONMENT AT KING MONGKUT'S UNIVERSITY OF TECHNOLOGY THONBURI

1ST SEMESTER 2014

COPYRIGHT OF THE JOINT GRADUATE SCHOOL OF ENEGY AND ENVIRONMENT

Modeling of Continuous Biodiesel Production from Esterification of Oleic Acid in The Presence of Solid Catalyst

Mr. Kiattisak Pinmai
ID: 55300700510

A Thesis Submitted as a Part of the Requirements
for the Degree of Master of Engineering
in Energy Technology and Management

The Joint Graduate School of Energy and Environment
at King Mongkut's University of Technology Thonburi

1st Semester 2014

Thesis Committee

(Assoc. Prof. Dr. Navadol Laosiripojana)	Advisor
(Dr. Boonrod Sajjakulnukit)	Member
(Asst. Prof. Dr. Worapon Kiatkittipong)	Member
(Assoc. Prof. Dr. Gumpon Prateepchaikul)	External

Thesis Title: Modeling of Continuous Biodiesel Production from Esterification of Oleic Acid in the Presence of Solid Catalysts

Student's name, organization and telephone/fax numbers/email

Mr. Kiattisak Pinmai

The Joint Graduate School of Energy and Enviroment (JGSEE)

King Mongkut's University of Technology Thonburi (KMUTT)

126 Pracha Uthit Rd., Bangmod, Tungkru, Bangkok 10140, Thailand

Tel. 0-86-368-6216

Email: extrared_x1@hotmail.com

Supervisor's name, organization and telephone/fax numbers/email

Assoc. Prof. Dr. Navadol Laosiripojana

The Joint Graduate School of Energy and Environment (JGSEE)

King Mongkut's University of Technology Thonburi (KMUTT)

91 Pracha Uthit Rd., Bangmod, Tungkru, Bangkok 10140, Thailand

Tel: 02-872-6978 Ext. 4146

Email: navadol_l@jgsee.kmutt.ac.th

Topic: Modeling of Continuous Biodiesel Production from Esterification of Oleic acid in the Presence of Solid Catalysts

Name of student: Mr. Kiattisak Pinmai **Student ID:** 55300700510

Name of Supervisor: Assoc. Prof. Dr. Navadol Laosiripojana

ABSTRACT

The continuous packed bed operation of biodiesel production toward the esterification of fatty acid was studied by a simulation using COMSOL software in order to optimize the operate conditions for maximizing FAME yield. The factors studied in the present work included the effects of temperature, methanol/oleic acid molar ratio and feed flow rate. Additionally, the effects of catalyst amount and molecular sieve adding on the system performance were also investigated. The developed models were based on isothermal, no pressure drop, heterogeneous and tree- dimensional continuous packed bed. The simulation results generally consisted of the percent conversion of oleic acid and concentration profiles along the reactor length at different conditions of each factors.

The simulation results revealed that the conversion had increased with increasing amounts of the catalyst, from which the conversion reached to around 93 % and remained constant when the mass percent of catalyst rose up to 10% base on oleic acid weight. For the effects of temperature and methanol/ oleic acid molar ratio, the simulation indicated that the increments of temperature and methanol/ oleic acid molar ratio can increase and speed up the conversion rate of oleic acid. On the contrary, the simulation results of effect of feed flow rate showed that the conversion increased with decreasing of flow rate due to at the lower flow rate, the oleic acid has longer residence time in the reactor. The highest conversion was 98% which obtained by simulation at 120°C, methanol/ oleic acid molar ratio of 16:1 and 1L/h of feed flow rate. Lastly, when molecular sieve was added inside the reactor, the conditions could be optimized to 100 °C with methanol/ oleic acid molar ratio of 5:1 which the conversion of oleic acid can reach to 99% due to water as by-product that produced during operating process was adsorbed by molecular sieve, resulting the equilibrium of the esterification reaction more shifted to the side of the products.

Keywords: Biodiesel, Free fatty acid, Esterification, Molecular sieve.

ACKNOWLEDGEMENTS

I would like to express my appreciation to Assoc. Prof. Dr. Navadol Laosiripojana, my supervisor, for the opportunity of working with him, and for his kind advice and encouragement throughout the course of my M.Eng program.

Sincere thanks to my committee members, Assoc. Prof. Dr. Worapon Kiatkittipong and Dr. Boonrod Sajjakulnukit, for their valuable time and kind comments. I also wish to thank my external committee member, Assoc. Prof. Dr. Gumpon Prateepchaikul for his valuable time and suggestions.

I would like to express my gratitude to the Joint Graduate School of Energy and Environment (JGSEE) for financial support throughout my study.

Finally, I wish to express my warm thanks to my family for their love, encouragement and financial support throughout my study.

CONTENTES

CONTENTES (Cont')

LIST OF TABLES

LIST OF FIGURES

LIST OF FIGURES (Cont')

LIST OF FIGURES (Cont')

CHAPTER 1

INTRODUCTION

1.1 Rational and Problem Statement

Currently, the problem related to the energy crisis are rising due to limited energy resources. Hence, several researchers have been attempting to survey the new energy resources, which are sustainable and low cost. Among the renewable fuel, biodiesel is known to be the promising alternative to petroleum diesel that most used in transportation section. Biodiesel consists of long-chain fatty acid methyl ethers (FAME), which can be obtained from renewable feedstock, such as vegetable oils palm oil, rapeseed oil, soybean oil or animal fats. Compared to fossil-based diesel fuels, it possesses many advantages, *i.e*. cleaner engine emissions, biodegradable, renewable and superior lubricating property (R. Alcantara et al., 2000), which makes it an excellent substitute or additive to conventional diesel fuels. However, biodiesel is not commercialized all over the world because of the high cost of the raw materials; the raw materials cost contributes more than 70% of the overall production cost (S. Zullaikah et al., 2005). Additionally, the biodiesel industry faces pressure in "food versus fuel" crisis. Hence, selection raw material is important factor, which waste cooking oil (WCO) or mixture of oils from various sources is a promising alternative to refined vegetable oils due to its low price. The disadvantage of using WCO is its high free fatty acid (FFA) content.

Generally, it is well known that the transesterification method by using an alkali as a catalyst is the most wildly used technique for producing biodiesel. The alkali catalytic has received much more attention because of the shorter reaction time and lower cost of catalyst as compared with acid catalytic. Nevertheless, this method is not suitable for raw material is its high FFA content, because FFA can react with the alkali catalyst to release soap and water during the process which also consumes the catalyst and lowers the yield of biodiesel (M. Canakci et al., 2007). A possible solution to this drawback could be the development of new technologies enabling to employ waste raw materials such as supercritical methanol (D. Kusdiana and S. Saka, 2001) or the two-stage process (esterification and transesterification reaction) (C. Lacaze-Dufaure and Z. Mouloungui et

al., 2000). In the first step the FFA is generally esterified with methanol under sulfuric acid catalysis, which produced FAME and water. When the FFA concentration decreases to less than 0.5% (by mass), sulfuric acid is then removed by phase separation after the system at rest for approx. 30 min. Subsequently the alkali is introduced into the system to further complete the transesterification. However, this route still has some drawbacks: difficult recovery of the acid catalyst, corrosiveness of sulfuric acid, and high the cost of equipment required for the reaction system. The esterification reaction of acid oils or fats can then be used both as biodiesel direct production and as pre-treatment step in the conventional transesterification and can also use both homogeneous acid catalyst and solid acid as heterogeneous catalysts. (Wang *et al*., 2006 has been reported that solid acid catalyst can be easily separated for reuse) Hence, the esterification is interesting to produced biodiesel nowadays.

Most biodiesel production is operated by batch reactors, which can produce only on a small-scale. The current situation of renewable fuel demand increase was reason to develop a reactor that can produce biodiesel in large-scale.

The purpose of this work is study the feasibility and suitability of changing the biodiesel production process from batch operation into packed bed operation. The packed bed reactor model was simulated to find the optimal conditions that can obtain highest yield of product. Biodiesel production of this work used the esterification reaction. FFA and methanol have been chosen as esterification agent, while, selected acid solid catalyst are: Amberlyst 15 and ferric sulfate/active carbon.

1.2 Literature Review

Literature regarding the esterification of free fatty acid with methanol in the presence of solid acid catalyst which is operated in batch reactor is reviewed here. This section shows some factors affecting conversion of reactants including types of catalyst, effects of catalyst loading, methanol/FFA molar ratio, reaction temperature and type of kinetic model. Details of each topic are presented below:

1.2.1 Types of catalyst

Wang *et al*. (2006) found that using ferric sulfate was a good alternative in the esterification reaction, but small ferric sulfate particles tended to adhere to oil, making it difficult to separate from the oil after the reaction was reused. Mengyu et al. (2009)

developed ferric sulfate/active carbon from ferric sulfate and they also studied the esterification reaction by operating with different types of catalyst; non-catalyst, homogenous catalyst (sulphuric acid) and heterogeneous catalyst (ferric sulfate/active carbon). In Figure 1.1 shows that the reaction had hardly occurred in the absence of a catalyst. After the reaction took place 4 hour, the conversion was constant and gave 90% maximum conversion with the presence of sulphuric acid catalyst while $Fe_2(SO_4)_3$/C (ferric sulfate/active carbon) given conversion reached to 96% which was 6% higher than sulphuric acid. Moreover, using ferric sulfate as solid acid catalyst was easy recycling and could be used for longer than liquid catalyst. R. Tesser,et al., 2010 also studied the catalytic activity of different solid acid catalysts as shown in figure 1.2. They found that each catalyst gave similar conversion at the end of reaction. The conversion of different catalysts including Amberlyst 15 and ferric sulfate active carbon were compared in Figure 1.2 and Figure 1.3 in similar condition (operating time at 3 h, molar ratio 8:1 – 9:1, range of temperature 95-100ºC). It showed that using ferric sulfate/active carbon and Amberlyst 15 as catalysts gave similar percent conversion.

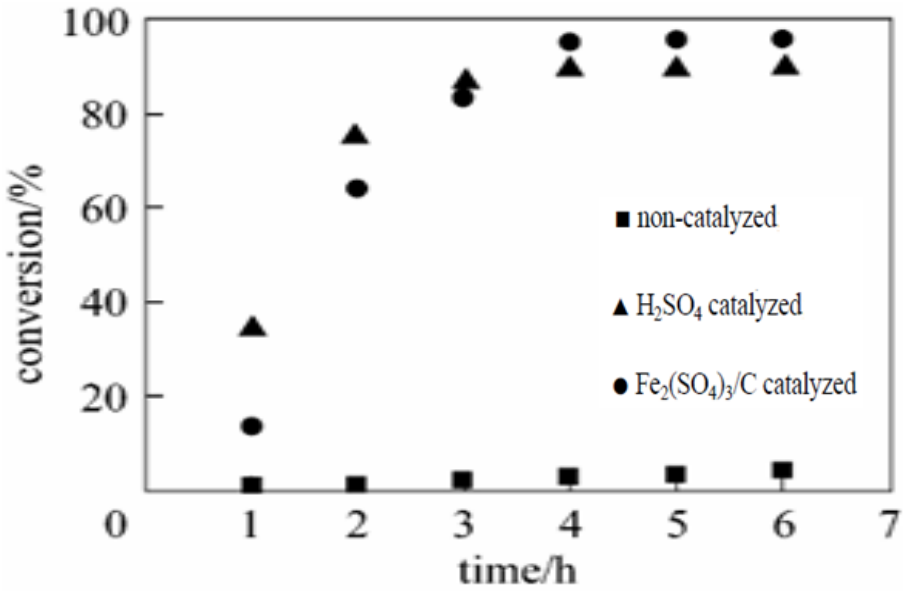

Figure 1.1 Catalytic activity of $Fe_2(SO_4)_3$/C solid catalyst and sulphuric acid [11].

1.2.2 Effects of amount of catalyst on FFA conversion

Mengyu et al. (2009) studied the effect of catalyst loading, which was operated by varying the mass percent of catalyst used in the reaction from 0 to 7.5 % (Reaction temperature 368.15 K, reaction time 3 h and methanol/FFA mole ratio 18:1). Figure 1.4

shows that the esterification reaction had taken place without any catalyst. The conversion increased with increments of catalyst and the maximum conversion was 98 % when the mass percent of catalyst rose up to 3.5%, which was an optimal value.

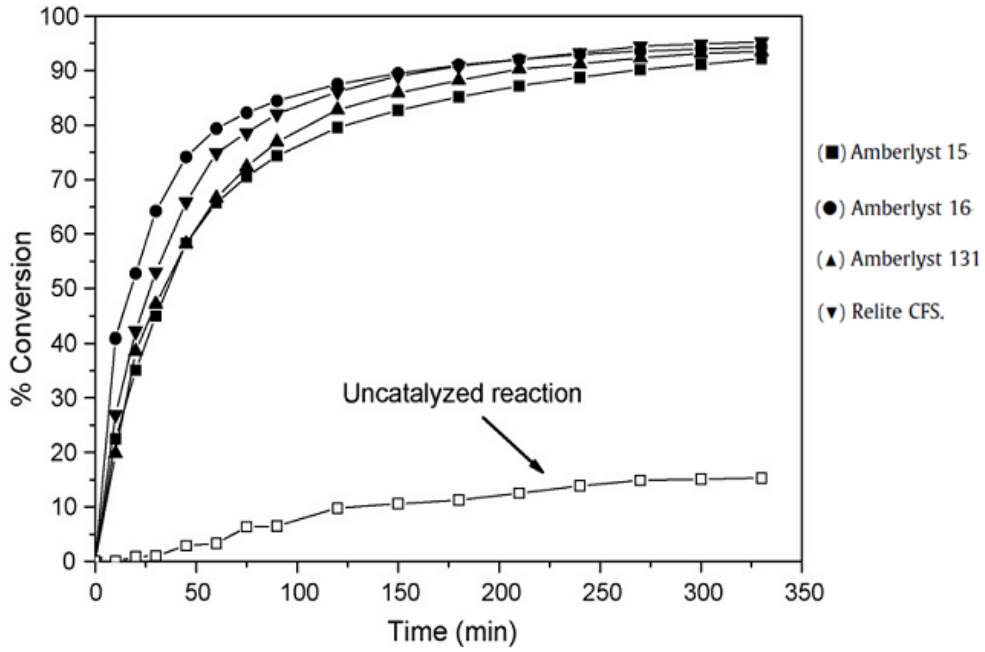

Figure 1.2 Experimental batch run for catalytic screening [15].

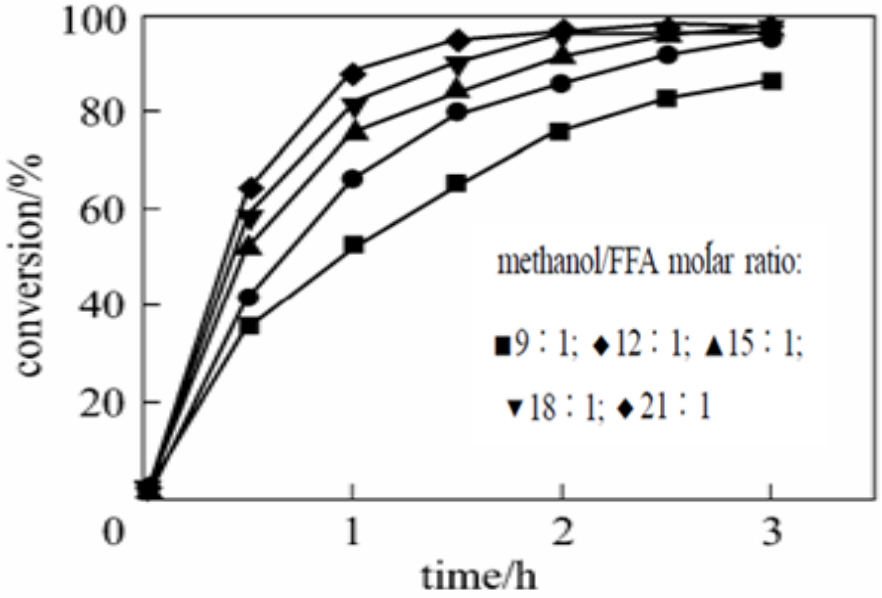

Figure 1.3 Conversion of FFA *vs.* methanol/FFA molar [11].

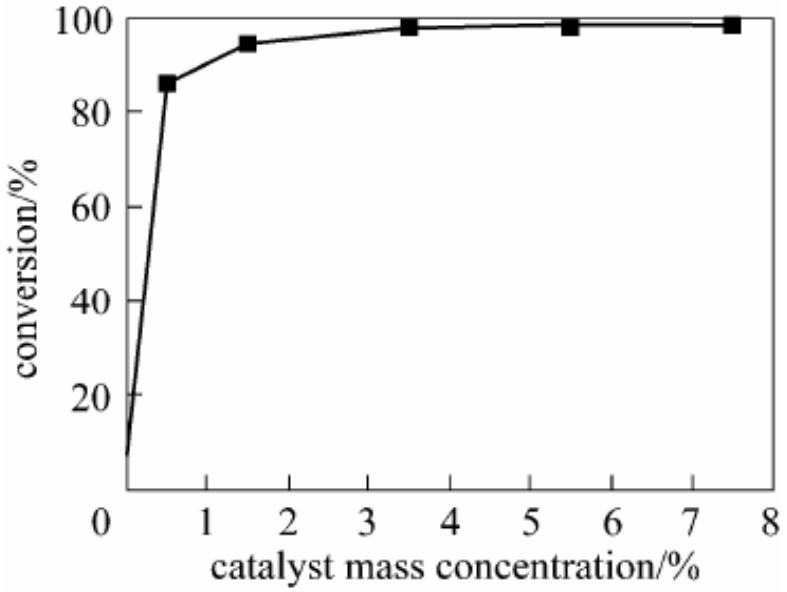

Figure 1.4 Conversion of FFA *vs*. amount of catalyst [11].

1.2.3 Effect of methanol/FFA molar ratio on FFA Conversion

Titiong et al. (2007) reported that an excess of methanol could speed the reaction. Figure 1.3 shows the effects of methanol/FFA molar ratio in terms of FFA conversion. The conversion increased with increasing mole ratio. When methanol concentration increased, the equilibrium of the esterification reaction shifted towards the side of the products i.e. methyl esters and water yielding higher conversion of FFA to methyl esters. Furthermore, by increasing the methanol to molar ratio, the viscosity of the reacting mixture decreased. This in turn promoted better mixing between reactants and catalyst and enhanced the mass transfer rate leading to a higher conversion within a fixed reaction time.

1.2.4 Effect of reaction temperature on FFA conversion

Liu et al. (2006) reported that the reaction temperature was one factor that may influence the esterification rate. Figure 1.5 indicates the effects of temperature from 338.15 K to 368.15 K on FFA conversion and it demonstrated that the reaction rate (conversion) could be rapidly sped up by rising the temperature. The conversion increased up to 98% when esterified at 368.15 K.

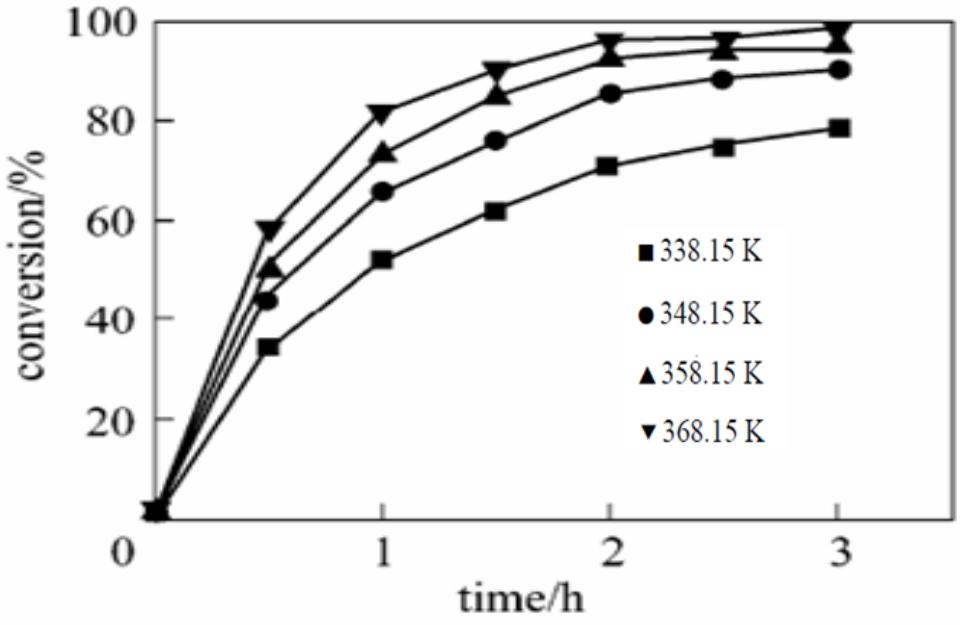

Figure 1.5 Conversion of FFA *vs*. reaction temperature [11].

1.2.5 Type of kinetic model

Tesser et al. (2010) studied a kinetic model by using a simulation of two kinetic models. They compared the simulated data with the experimental data. Each model used different assumptions, thus resulting in different rates of reaction.

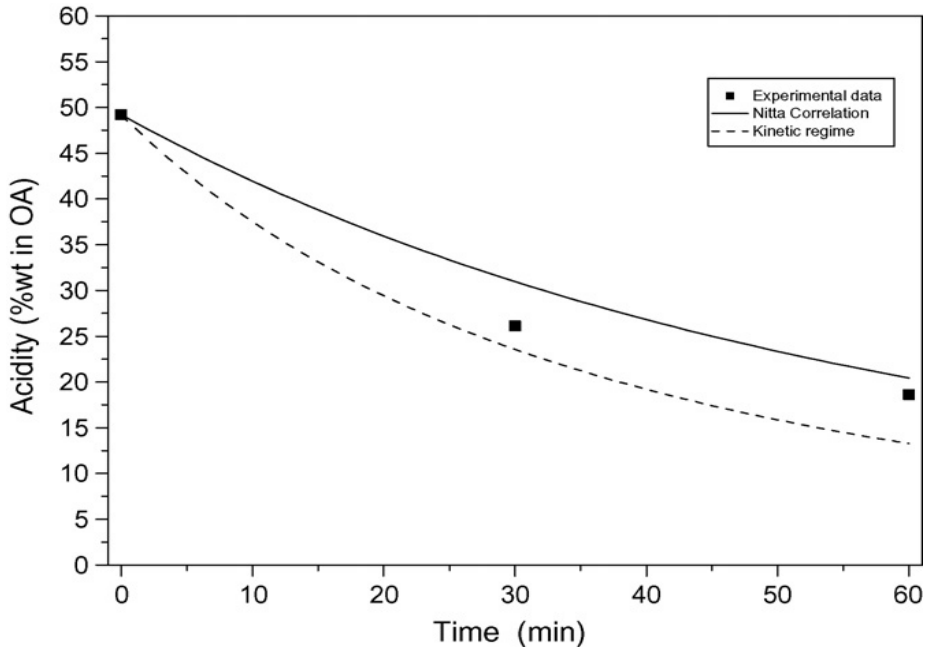

Figure 1.6 Acidity profiles of experimental data and simulation [13].

1.3 Research objective

The goal of this research is to develop a model for a packed bed reactor for biodiesel production that can obtain a yield of product with a quantity that can be maximized. The specific objectives are:

1. To study and select the proper kinetic models of the esterification reaction and develop a mathematical model for biodiesel production via esterification under continuous packed bed operation.
2. To determine the proper conditions (i.e. temperature, methanol/fatty acid ratio, and reactor size) for operating a process that can maximize the conversion of oleic acid.

1.4 Scope of research work

The scope of this work is to study and select the kinetic equations, as well as the kinetic parameters of the esterification reaction, over several solid catalysts i.e. Amberlyst 15 and sulfated zirconia for applying in the mathematical modeling. Then, several sensitivity analyses were performed to determine the effects of temperature, methanol/fatty acid ratio, and reactor size on the conversion of oleic acid at the end of the reactor.

CHAPTER 2

THEORIES

2.1 Biodiesel Production

Biodiesel is renewable fuel for petroleum diesel, which consists of long-chain alkyl esters. It can be produced from renewable feedstocks, such as vegetable oils or animal fats, in several processes, e.g. micro-emulsion, pyrolysis, supercritical, transesterification and esterification (Ma and Hanna, 1999; Fukuda et al., 2001; Jitputti et al., 2005; Meher et al., 2004; Marchetti et al., 2005). However, the selection of each process to produce biodiesel depending on types of raw material, sources of raw material and prices of raw material. As mentioned above, details of biodiesel production methods are described below**:**

2.1.1 Micro-emulsion Process

Micro-emulsion is the dispersion of colloids in equilibrium. Colloidal particles in the range 1-150 nm are used in conjunction with a solvent, such as methanol, ethanol and butanol, which is also one way to solve the problem of high viscosity in vegetable oils to create lower viscosity (Srivasyava and Prasad, 1999). Micro-emulsion arising from methanol and vegetable oil can obtain the oil that has similar properties to petroleum diesel fuel. However, when test with the diesel engine found that the accumulation of stain (carbon compounds) around the nozzles and valves of the engine, which is a disadvantage of the oil produced by this method (Ma and Hanna, 1999).

2.1.2 Pyrolysis Process

Pyrolysis is a thermochemical process that converts one compound to other compounds by heat (450 to 600ºC in the absence of oxygen to prevent complete combustion). Renewable feedstocks, such as vegetable oils, animal fats and natural fatty acids, can be treated by pyrolysis to create biodiesel (Ma and Hanna, 1999). This process is difficult control in order to obtain desire product due to several reaction and by-product. Mechanisms of pyrolysis process are shown in Figure 2.1.

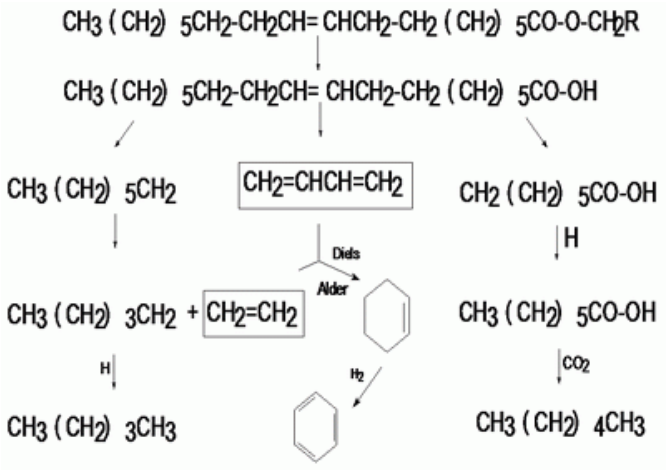

Figure 2.1 Mechanisms of pyrolysis processes [10].

2.1.3 Supercritical Process

An alternative process, a catalyst-free method for transesterification, uses supercritical methanol at high temperatures (512.2 K) and pressures (8.1 MPa) in a continuous process. In the supercritical state, the oil and methanol are in a single phase and reaction rapidly occurs spontaneous. This process can tolerate water in the feedstock. Free fatty acids are converted to methyl esters instead of soap (Demirbas, 2002) therefore a wide variety of feedstocks can be used and the catalyst removal step is also eliminated. High temperature and pressure are required but the production cost of energy is similar or less than catalytic production routes.

2.1.4 Transesterification Process

The most common way to obtain biodiesel is the transesterification reaction of vegetable oils in the presence of a low molecular weight alcohol and a catalyst. The transesterification reaction involves the exchange of organic groups R1, R2, R3 belonging to a glyceride with the organic group of an alcohol R' (Figure 2.2).

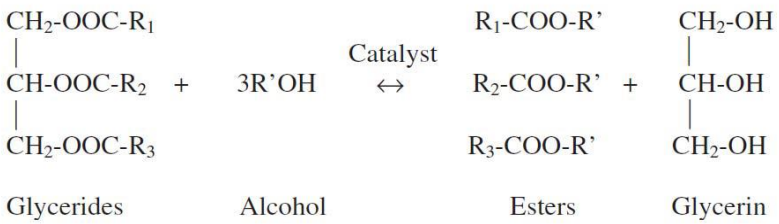

Figure 2.2 The transesterification reaction. R1, R2 and R3 are a mixture of various fatty acid chains. The alcohol used for producing biodiesel is usually methanol (R′ = CH3) [17]**.**

The overall process is normally a sequence of three consecutive steps, which are all reversible reactions. In the first step, diglyceride is obtained from triglycerides, from diglyceridemonoglyceride is produced and in the last step from monoglyceridesglycerine is formed (Figure 2.3). In all these reactions fatty acid methyl esters (FAME) are produced. However, an excess of alcohol is usually more appropriate to improve the reaction towards the desired product:

$$\text{Triglycerides (TG)} + \text{R}'\text{OH} \underset{k_2}{\overset{k_1}{\leftrightarrow}} \text{Diglycerides (DG)} + \text{R}'\text{COOR}_1,$$

$$\text{Diglycerides (DG)} + \text{R}'\text{OH} \underset{k_4}{\overset{k_3}{\leftrightarrow}} \text{Monoglycerides (MG)} + \text{R}'\text{COOR}_2,$$

$$\text{Monoglycerides (MG)} + \text{R}'\text{OH} \underset{k_6}{\overset{k_5}{\leftrightarrow}} \text{Glycerin (GL)} + \text{R}'\text{COOR}_3.$$

Figure 2.3 The three consecutive and reversible steps of the transesterification reaction.

The reaction product is an immiscible two-phase mixture of biodiesel, including excess methanol and glycerine. During separation (e.g. centrifuge) the hydrophilic and denser glycerine migrates to the bottom of the mixture creating a separate layer, while the less dense biodiesel stays on top together with the unconverted oil.

2.1.4.1 Transesterification Mechanism

The mechanism of the base-catalyzed transesterification of vegetable oils is shown in Figure 2.4. The first step is the reaction of the base with the alcohol, producing an alkoxide and the protonated catalyst. The nucleophilic attack of the alkoxide at the carbonyl group of a triglyceride generates a tetrahedral intermediate, from which the alkyl ester and the corresponding anion of the diglyceride are formed. The latter deprotonates the catalyst and reacts with a second molecule of alcohol starting a new catalytic cycle. Diglycerides and monoglycerides are converted by the same mechanism to a mixture of alkyl esters and glycerine.

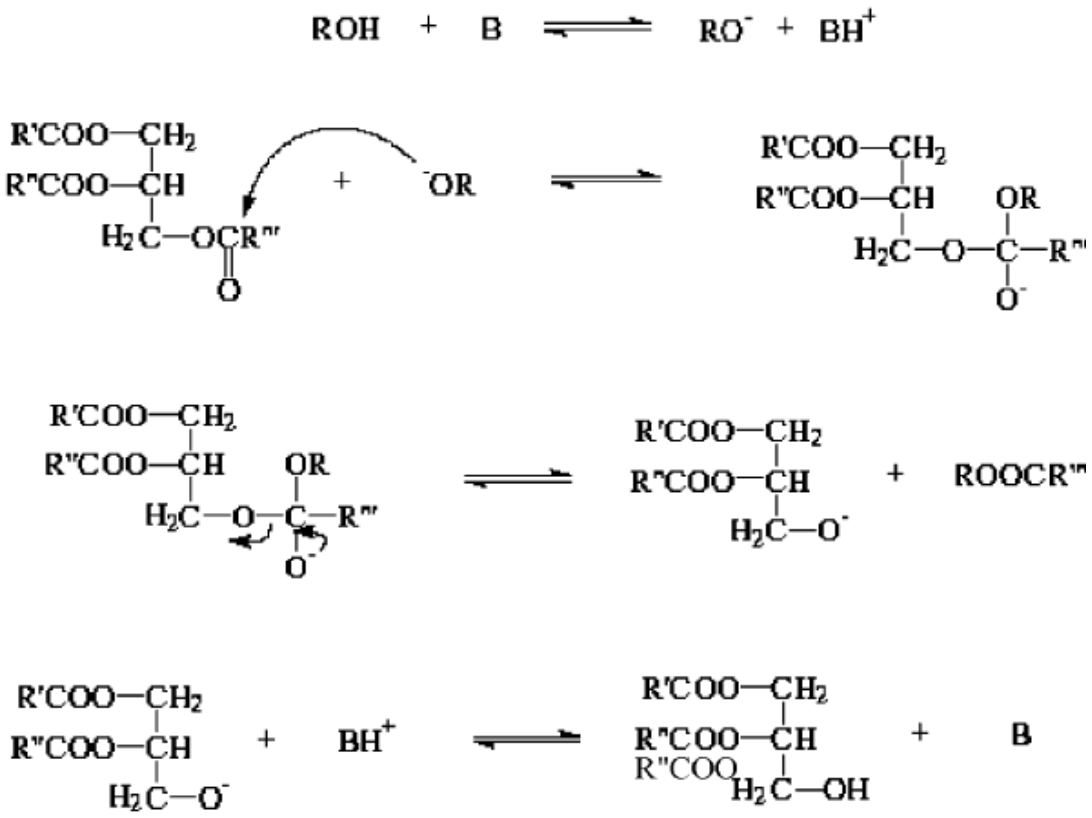

Figure 2.4 Mechanism of the alkali-catalyzed transesterification of vegetable oils (B:base) [18].

Alkaline-catalyzed transesterifications proceed at considerably higher rates than do acid catalyzed transesterifications. Due to this fact and also because alkaline catalysts are less corrosive to industrial equipment, most commercial transesterifications are conducted with alkaline catalysts. However, this process is not suitable for raw materials that has high free fatty acids (FFA). The FFA of the raw materials that used in alkaline-catalyzed transesterification should be restricted down to ~0.5% (by mass), equivalent to ~1(mg KOH)g^{-1}due to the FFA in the raw materials can react with the alkali catalyst during the process to release soap and water, so the raw material must refinery resulting in high price of the commercial product.

2.1.5 Esterification Process

To remedy the drawbacks of tranesterification, values the products more expensive. It has been reported that FFA does not react with acid catalyst. Therefore, esterification process used solid acid served as catalyst is be a good alternative, which developed to biodiesel production. The general esterification is the dehydration of carboxylic acid with

an alcohol to produced ester and water, main reaction is shown in Figure 2.5. Figure 2.6 shows the esterification of FFA with methanol, which is catalyzed by a solid acid. In this work, R1 represents an unsaturated linear chain of 11 - 17 carbon atoms which varies as the raw materials resource.

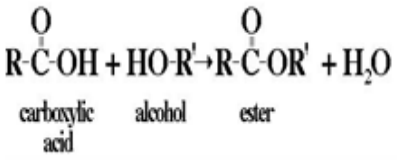

Figure 2.5 The general esterification of carboxylic acid with an alcohol. [13].

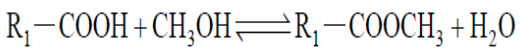

Figure 2.6 The esterification reaction of a free fatty acid with methanol. [13]**.**

2.1.5.1 Esterification mechanism

Carboxylic acids (FFA) can be esterified by alcohols in the presence of a suitable catalyst. An acidic catalyst as shown in Figure 2.7. The initial step is protonation of the acid to give an oxonium ion, which can undergo an exchange reaction with an alcohol to give the intermediate, and this in turn can lose a proton to become an ester. Each step in the process is reversible but in the presence of a large excess of the alcohol, the equilibrium point of the reaction is displaced so that esterification proceeds virtually to completion. However, in the presence of water, which is a stronger electron donor than are aliphatic alcohols, formation of the intermediate is not favored and esterification will not proceed fully.

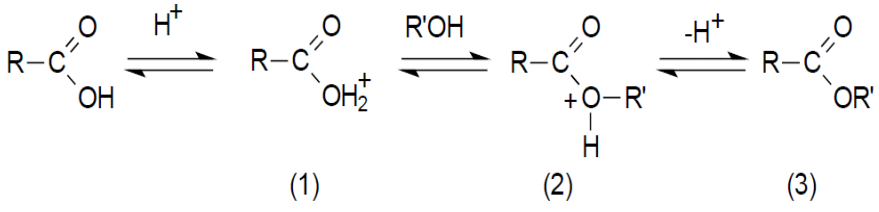

Figure 2.7 Acid-catalyzed esterification of fatty acid. [19]

2.2 Kinetic Theory

The kinetic theory is a theory that describes a chemical reaction involving between 2 or more substances. The theory consists of a collision theory and an activated–complex theory. Both theories discussed efficiency collision between molecules of the substances, but activated–complex theory discussed in detail while collision of 2 substances and the formation of products.

2.2.1 Collision Theory

The collision theory is best explained with substances in the gas phase and assumes that reactions occur when there are efficiency collision between reactants. Moreover, it postulates that the majority of collisions do not lead to a reaction, but only those in which the colliding species have: a kinetic energy greater than a certain minimum (called the activation energy, Ea) and the correct special orientation with respect to each other. Figure 2.8 shows that (a) the direction in collision is most appropriate, if energy greater than Ea, the reaction occur. While the (b) (c) and (d) direction in the collision is inappropriate. Although the energy in collision energy is greater than Ea, the reaction does not occur.

2.2.2 Activated–complex Theory

The activated-complex theory, or transition state theory, describes the collision theory in detail. When collision of reactants, the substances that unstable and have high energy (called activated complex) will be occur. Then, this activated complex is in equilibrium with the reactants and converted to product. The activated complex is unstable and have high energy due to breaking the chemical bond of reactants and a rearranging of bonds to form the products, the state of activated complex called transition state. When activated complex convert to product, energy will decrease and stable. In addition, the difference between the energy of transition state with energy of product equal to the activation energy.

In Figure 2.9, reactant (A and BC) change to activated complex (A----B----C), and then convert to product (AB and C), which Activation energy equal to Ea and energy of reaction equal to ΔE.

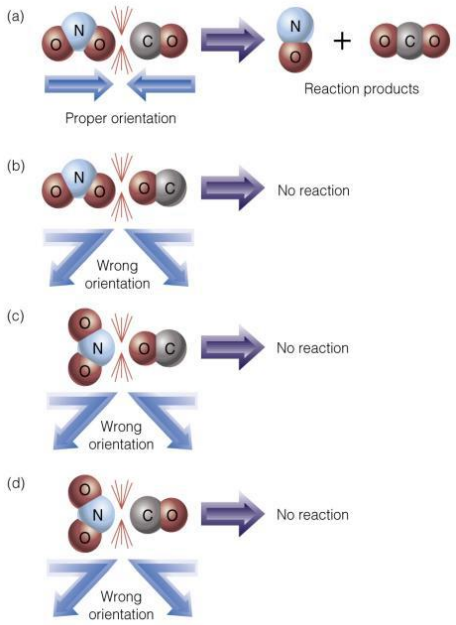

Figure 2.8 The direction of collisions of particles in the reaction. [20].

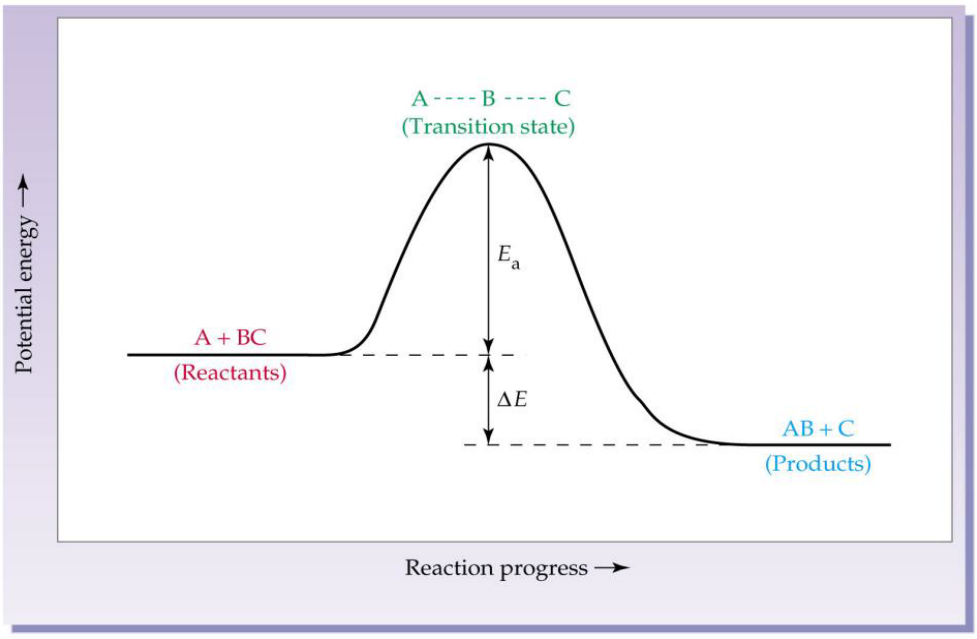

Figure 2.9 The changes in the energy of the reaction A + BC ➔AB + C. [20].

2.2.3 The rate laws and the reaction order

In the chemical reactions described in the following paragraphs, we take as the basis of calculation a species A, which is one of the reactants that disappears as a result of the reaction. The limiting reactant is usually chosen as our basis for calculation. The rate of disappearance of A, $-r_A$, depends on temperature and composition. For many reactions, it

can be written as the product of a *reaction rate constant*, k_A, and a function of the concentrations (activities) of the various species involved in the reaction:

$$-r_A = [k_A(T))][fn(C_A,C_B,\ldots)] \qquad (2\text{-}1)$$

The algebraic equation that relates $-r_A$, to the species concentrations is called the kinetic expression or rate law. The specific rate of reaction (also called the rate constant), k_A, like the reaction rate $-r_A$, always refers to a particular species in the reaction, and normally, should be subscripted with respect to that species. However, for reactions in which the stoichiometric coefficient is 1 for all species involved in the reaction, for example,

$$1NaOH + 1HCl ==> 1NaCI + 1H_2O$$

we shall delete the subscript on the specific reaction rate, (e.g., A in k_A), to let

$$k = k_{NaOH} = k_{HCl} = k_{NaCl} = k_{H2O}$$

2.2.3.1 Power Law Models and Elementary Rate Laws

The dependence of the reaction rate, $-r_A$, on the concentrations of the species present, fn (C_j), is almost without exception determined by experimental observation. Although the functional dependence on concentration may be postulated from theory, experiments are necessary to confirm the proposed form. One of the most common general forms of this dependence is the power law model. Here, the rate law is the product of concentrations of the individual reacting species, each of which is raised to a power, for example:

$$-r_A = kAC^{\alpha}{}_A,C^{\beta}{}_B \qquad (2\text{-}2)$$

The exponents of the concentrations in Equation (2-2) lead to the concept of the reaction order. The order of a reaction refers to the powers to which the concentrations are raised in the kinetic rate law. In Equation (2-2), the reaction is α order with respect to reactant A, and β order with respect to reactant B. The overall order of the reaction, n, is

$$n = \alpha + \beta$$

The units of $-r_A$, are always in terms of concentration per unit time while the units of the specific reaction rate, k_A, will vary with the order of the reaction. Consider a reaction involving only one reactant, such as:

A ==>Product

with a reaction order *n.* The units of the specific reaction rate constant are:

$$k = \frac{(Concentration)^{1-n}}{Time}$$

Consequently, the rate laws corresponding to a zero-, first-, second-, and third-order reaction, together with typical units for the corresponding rate constants are:

Zero-order (n = 0): $-r_A = k_A$: (2-3)
$\{k\} = mol/dm^3 \cdot s$

First-order (n = 1): $-r_A = k_A C_A$: (2-4)
$\{k\} = s^{-1}$

Second-order (n = 2): $-r_A = k_A C^2_A$: (2-5)
$\{k\} = dm^3/mol \cdot s$

Third-order (n = 3): $-r_A = k_A C^3_A$ (2-6)
$\{k\} = (dm^3/mol)^2 \cdot s^{-1}$

An elementary reaction is one that evolves a single step, such as the bimolecular reaction, between oxygen and methanol:

$$O\bullet + CH_3OH \Longrightarrow CH_3O\bullet + OH\bullet$$

The stoichiometric coefficients in this reaction are *identical* to the powers in the rate law. Consequently, the rate law for the disappearance of molecular oxygen is:

$$-r_{O\bullet} = kC_{O\bullet}C_{CH3OH}$$

The reaction is the first order in molecular oxygen and the first order in methanol. Therefore, we say that both the reaction and the rate law are elementary. There are many reactions where the stoichiometric coefficients in the reaction are identical to the reaction orders, but the reactions are not elementary owing to such things as pathways involving active intermediates and series reactions. For these reactions that are not elementary but whose stoichiometric coefficients are identical to the reaction orders in the rate law, we say that the reaction follows an elementary rate law. For example, the oxidation reaction of nitric oxide discussed earlier,

$$2NO + O_2 ==> 2NO_2$$

is not elementary but follows the elementary rate law

$$-r_{NO} = k_{NO}C^2_{NO}C_{O2}$$

Another non-elementary reaction that follows an elementary rate law is the gas-phase reaction between hydrogen and iodine

$$H_2 + I_2 ==> 2HI$$
$$-r_{H2} = k_{H2}C_{H2}C_{I2}$$

In summary, far many reactions involving multiple steps and pathways, the powers in the rate laws surprisingly agree with the stoichiometric coefficients. Consequently, to facilitate describing this class of reactions, we say a reaction follows an elementary rate law when the reaction orders are identical with the stoichiometric coefficients of the reacting species for the reaction as written. It is important to remember that the rate laws are determined by experiment observation! They are a function of the reaction chemistry and not the type of reactor in which the reactions occur. Table 2.1 gives examples of rate laws for a number of reactions.

Table 2.1 Example of Reaction Rate Laws [21].

First-Order Rate Laws	(1) C_2H_6 ==> $C_2H_4 + H_2$ (2) nC_4H_{10}<==> iC_4H_{10}	$-r_A = kC_{C2H6}$ $-r_n = k[Cn_{C4} - C_{iC4}/K_C]$
Second-Order Rate Laws	(1) CNBr + CH_3NH_2 ==> CH_3Br + $NCNH_2$ (2) A + B <==> C +D	$-r_A = kC_{CNBr}C_{CH3NH2}$ $-r_A = k[C_AC_B - C_CC_D/K_C]$

2.2.3.2 Reversible Reaction

All rate laws for reversible reactions must reduce to the thermodynamic relationship relating the reacting species concentrations at equilibrium. At equilibrium, the rate of the reaction is identically zero for all species (i.e., $-r_A$, = O). That is, for the general reaction

$$aA + bB \rightleftharpoons cC + dD$$

the concentrations at equilibrium are related by the thermodynamic relationship for the equilibrium constant K_C

$$K_C = \frac{C^c{}_{Ce}C^d{}_{De}}{C^a{}_{Ae}C^b{}_{Be}}$$

The units of the thermodynamic equilibrium constant, $\boldsymbol{K_C}$, are $(mol/dm^3)^{d+c-b-a}$

To illustrate how to write rate laws for reversible reactions, we will use the combination of two benzene, B, molecules to form one molecule of hydrogen and one of diphenyl, D. In this discussion, we shall consider this gas-phase reaction to be elementary and reversible:

$$2C_6H_6 \underset{k_{-B}}{\overset{k_B}{\rightleftharpoons}} C_{12}H_{10} + H_2$$

The forward and reverse specific reaction rate constants, k_B, and k_{-B}, respectively, will be defined with respect to benzene.

Benzene (B) is being depleted by the forward reaction:

$$2C_6H_6 \xrightarrow{k_B} C_{12}H_{10} + H_2$$

in which the rate of disappearance of benzene is:

$$-r_{B,forward} = k_B C^2_B$$

If we multiply both sides of this equation by -1, we obtain the expression for the rate of the formation of benzene for the forward reaction:

$$r_{B,forward} = -k_B C^2_B \qquad (2\text{-}7)$$

For the reverse reaction between diphenyl (D) and hydrogen (H_2):

$$C_{12}H_{10} + H_2 \xrightarrow{k\text{-}_B} 2C_6H_6$$

The rate of formation of benzene is given as:

$$r_{B,\,reverse} = k_{-B} C_D C_{H2} \qquad (2\text{-}8)$$

Again, both the rate constants kB, and k-B, are defined with respect to benzene.

The net rate of the formation of benzene is the sum of the rates of the formation from the forward reaction [Equation (2-7)] and the reverse reaction [Equation [2-8)]:

$$r_B = r_{B,\,net} = r_{B,\,forward} + r_{B,\,reverse}$$
$$r_B = -k_B C^2_B + k_{-B} C_D C_{H2} \qquad (2\text{-}9)$$

Multiplying both sides of Equation (2-9) by -1, we obtain the rate law for the rate of the disappearance of benzene, $-r_B$:

$$-r_B = k_B C^2_B - k_{-B} C_D C_{H2} = k_B [C^2_B + (k_{-B}/k_B) C_D C_{H2}]$$

Replacing the ratio of the reverse to forward rate law constants by the equilibrium constant, we obtain:

$$\boxed{-r_B = k_B \left(C^2_B - \frac{C_D C_{H2}}{K_C} \right)}$$

Where:

$$\frac{k_B}{k_{-B}} = Kc = \text{Concentration equilibrium constant}$$

The equilibrium constant decreases with increasing temperature for exothermic reactions and increases with increasing temperature for endothermic reactions.

2.2.4 Catalysis and Catalytic Reactors

A catalyst is a substance that speeds up a chemical reaction, but is not consumed by the reaction. Hence, a catalyst can be recovered chemically unchanged at the end of the reaction it has been used to speed up or catalyze**.** Catalysts work by providing an (alternative) mechanism involving a different transition state and lower activation energy. Consequently, more molecular collisions have the energy needed to reach the transition state. Hence, catalysts can enable reactions that would otherwise be blocked or slowed by a kinetic barrier. The catalyst may increase reaction rate or selectivity, or enable the reaction at lower temperatures. This effect is shown in Figure 2.10.

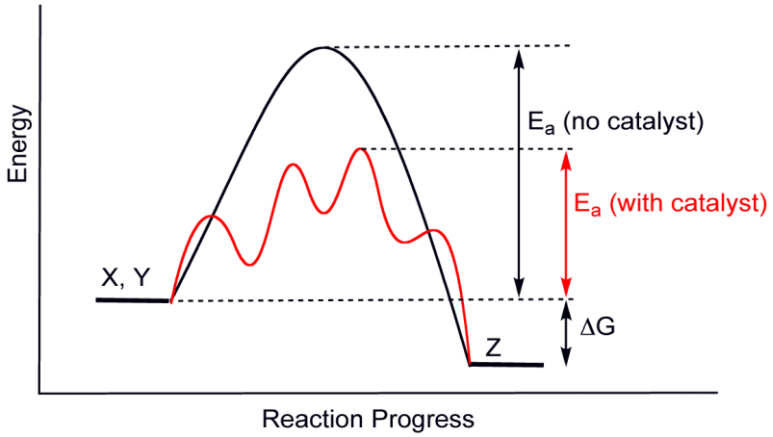

Figure 2.10 Energy profile diagram. [21].

2.2.4.1 Adsorption Isotherms

Since chemisorption is usually a necessary part of a catalytic process, we shall discuss it before treating catalytic reaction rates. The letter S will represent an active site. Alone, it will denote a vacant site, with no atom, molecule, or complex adsorbed on it. The combination of S with another letter (e.g. A·S) will mean that one unit of species A will be adsorbed on the site S. Species A can be an atom, molecule, or some other atomic combination, depending on the circumstances. Consequently, the adsorption of A on a site Sis represented by: A + S <====> A·S

The total molar concentration of active sites per unit mass of catalyst is equal to the number of active sites per unit mass divided by Avogadro's Number and will be labeled C_v, (mol/g·cat). The molar concentration of vacant sites, C_v, is the number of vacant sites per unit mass of catalyst divided by Avogadro's number. In the absence of catalyst deactivation, we assume that the total concentration of active sites remains constant. Some further definitions include:

P_i partial pressure of species *i* in the gas phase, atm or kPa

$C_{i·S}$ surface concentration of sites occupied by species *i*, mol/g·cat

A conceptual mode1 depicting species A and B on two sites is shown in Figure 2.11.

Figure 2.11 Vacant and occupied sites. [21].

For the system shown, the total concentration of sites is:

$$C_t = C_v + C_{A·S} + C_{B·S} \qquad (2\text{-}10)$$

This equation is referred to as a site balance.

Two models will be postulated for the adsorption of carbon monoxide on metal surfaces. In one model, CO is adsorbed as the molecule, CO:

$$CO + S <====> CO·S$$

In the other, carbon monoxide is adsorbed as O and C atoms instead of molecular CO.

$$CO + 2S <====> C·S + O·S$$

The former is called molecular or non-dissociated adsorption (e.g. CO), and the latter is called dissociative adsorption (e.g. C and 0). Whether a molecule adsorbs non-dissociatively or dissociatively depends on the surface.

The adsorption of carbon monoxide molecules will be considered first. Since the carbon monoxide does not react further after being adsorbed, we need only to consider the adsorption process:

$$CO + S <====> CO \cdot S \qquad (2\text{-}11)$$

In obtaining a rate law for the rate of adsorption, the reaction in Equation (2-11) can be treated as an elementary reaction. The rate of attachment of the carbon monoxide molecules to the active site on the surface is proportional to the number of collisions that these molecules make with a surface active site per second. In other words, a specific fraction of the molecules that strike the surface become adsorbed. In turn, the collision rate is directly proportional to the carbon monoxide partial pressure, P_{CO}. As carbon monoxide molecules adsorb only an vacant sites and not on sites already occupied by other carbon monoxide molecules, the rate of attachment is also directly proportional to the concentration of vacant sites, C_V. Combining these two facts means that the rate of attachment of carbon monoxide molecules to the surface is directly proportional to the product of the partial pressure of CO and the concentration of vacant sites; that is:

$$\text{Rate of attachment} = k_A P_{CO} C_V$$

The rate of detachment of molecules from the surface can be a first-order process; that is, the detachment of carbon monoxide molecules from the surface is usually directly proportional to the concentration of sites occupied by the adsorbed molecules (e.g. $C_{CO \cdot S}$):

$$\text{Rate of detachment} = k_{-A} C_{CO \cdot S}$$

The net rate of adsorption is equal to the rate of molecular attachment to the surface minus the rate of detachment from the surface. If k_A and k_{-A}, are the constants of proportionality for the attachment and detachment processes, then:

$$r_{AD} = k_A P_{CO} C_V - k_{-A} C_{CO \cdot S} \qquad (2\text{-}12)$$

The ratio $K_A = k_A/k_{-A}$, is the adsorption equilibrium constant. Using it to rearrange Equation (2-12) gives:

$$r_{AD} = k_A \left(P_{CO} C_V - \frac{C_{CO \cdot S}}{K_A} \right) \quad (2\text{-}13)$$

The adsorption rate constant, k_A, for molecular adsorption is virtually independent of temperature, while the desorption constant, k_{-A}, increases exponentially with increasing temperature. The equilibrium adsorption constant, K_A, decreases exponentially with increasing temperature.

Since carbon monoxide is the only material adsorbed on the catalyst, the site balance gives

$$C_t = C_V + C_{CO \cdot S} \quad (2\text{-}14)$$

At equilibrium, the net rate of adsorption equals zero. Setting the left-hand side of Equation (2-13) equal to zero and solving for the concentration of CO adsorbed on the surface, we get:

$$C_{CO \cdot S} = K_A C_V P_{CO}$$

Using Equation (2-14) to give C_V in terms of $C_{CO \cdot S}$ and the total number of sites C_t, we can solve for $C_{CO \cdot S}$ in terms of constants and the pressure of carbon monoxide:

$$C_{CO \cdot S} = K_A C_V P_{CO} = K_A P_{CO} (Ct - C_{CO \cdot S})$$

Rearranging gives us:

$$C_{CO \cdot S} = \frac{K_A P_{CO} C_t}{1 + K_A P_{CO}}$$

Thus, this equation gives the concentration of carbon monoxide adsorbed on the surface, $C_{CO \cdot S}$as a function of the partial pressure of carbon monoxide, and is an equation for the adsorption isotherm.

2.2.4.2 Surface Reaction

After a reactant has been adsorbed onto the surface, it is capable of reacting in a number of ways to form the reaction product. Three of these ways are:

1. Single site. The surface reaction may be a single-site mechanism in which only the site on which the reactant is adsorbed is involved in the reaction. For example, an adsorbed molecule of A may isomerize (or perhaps decompose) directly on the site to which it is attached, such as:

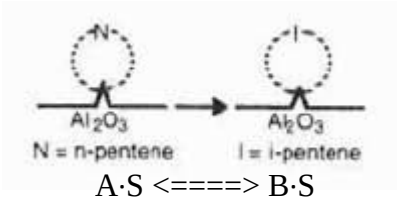

A·S <====> B·S

Since in each step the reaction mechanism is elementary, the surface reaction rate law is:

$$r_S = k_S\left(P_{A\cdot S} - \frac{C_{B\cdot S}}{K_S}\right)$$

where *Ks* is the surface reaction equilibrium constant $Ks = k_s lk_{-s}$

2. Dual site. The surface reaction may be a dual-site mechanism in which the adsorbed reactant interacts with another site (either unoccupied or occupied) to form the product.

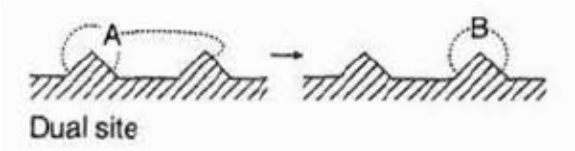

For example, adsorbed A may react with an adjacent vacant site to yield a vacant site and a site on which the product is adsorbed, for the generic reaction:

A·S + S <====> B·S + S

the corresponding surface reaction rate law is

$$r_S = k_S\left(C_{A\cdot S}C_V - \frac{C_{B\cdot S}C_V}{K_S}\right)$$

Another example of a dual-site mechanism is the reaction between two adsorbed species.

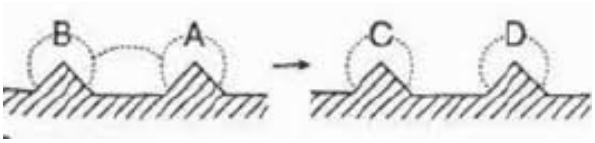

For the generic reaction:

$$A{\cdot}S + B{\cdot}S <====> C{\cdot}S + D{\cdot}S$$

the corresponding surface reaction rate law is:

$$r_S = k_S \left(C_{A\cdot S} C_{B\cdot S} - \frac{C_{C\cdot S} C_{D\cdot S}}{K_S} \right)$$

A third dual-site mechanism is the reaction of two species adsorbed on different types of sites S and S'.

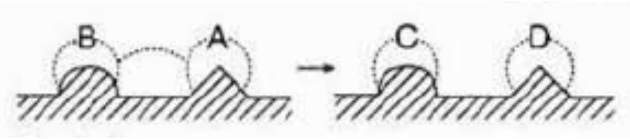

For the generic reaction:

$$A{\cdot}S + B{\cdot}S' <====> C{\cdot}S' + D{\cdot}S$$

the corresponding surface reaction rate law is:

$$r_S = k_S \left(C_{A\cdot S} C_{B\cdot S'} - \frac{C_{C\cdot S'} C_{D\cdot S}}{K_S} \right)$$

Reactions involving either single- or dual-site mechanisms described earlier are sometimes referred to as following Lmuir-Hirsshelwood kinetics.

3. Eley-Rideal. A third mechanism is the reaction between an adsorbed molecule and a molecule in the gas phase:

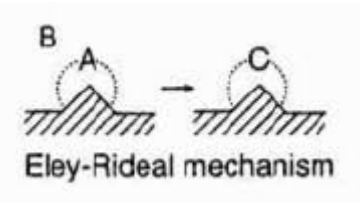

For the generic reaction:

$$A{\cdot}S + B(g) \text{ <====> } C{\cdot}S$$

the corresponding surface reaction rate law is:

$$r_S = k_S\left(C_{A\cdot S}P_B - \frac{C_{C\cdot S}}{K_S}\right)$$

This type of mechanism is referred to as an Eley-Rideal mechanism.

2.2.4.3 Desorption

In each of the preceding cases, the products of the surface reaction adsorbed on the surface are subsequently desorbed into the gas phase. For the desorption of a species (e.g. C):

$$C{\cdot}S + \text{ <====> } C + S$$

the rate of desorption of C is:

$$r_D = k_D\left(C_{C\cdot S} - \frac{P_C C_V}{K_D}\right)$$

where K_D is the desorption equilibrium constant. We note that the desorption step for C is just the reverse of the adsorption step for C, and that the rate of desorption of C, r_D, is just opposite in sign to the rate of adsorption of C, $r_{AD,C}$:

$$r_{D,C} = -r_{AD,C}$$

In addition, we see that the desorption equilibrium constant $K_{D,C}$ is just the reciprocal of the adsorption equilibrium constant for C, $K_{AD,C}$:

$$K_{D,C} = \frac{1}{K_{AD,C}}$$

$$r_D = k_D(C_{C\cdot S} - K_{AD,C}P_C C \qquad (2\text{-}15)$$

In the material that follows, the form of the equation for the desorption step that we will use will be similar to Equation (2-15).

2.2.4.4 Rate-Limiting Step

We now wish to develop rate laws for catalytic reactions that are not diffusion-limited. In developing the procedure to obtain a mechanism, we shall discuss a particular catalytic reaction, the decomposition of cumene to form benzene and propylene. The overall reaction is:

$$C_6H_5CH(CH_3)_2 \text{ ====> } C_6H_6 + C_3H_6$$

A conceptual model depicting the sequences of steps in this platinum-catalyzed reaction is shown in Figure 2.12.

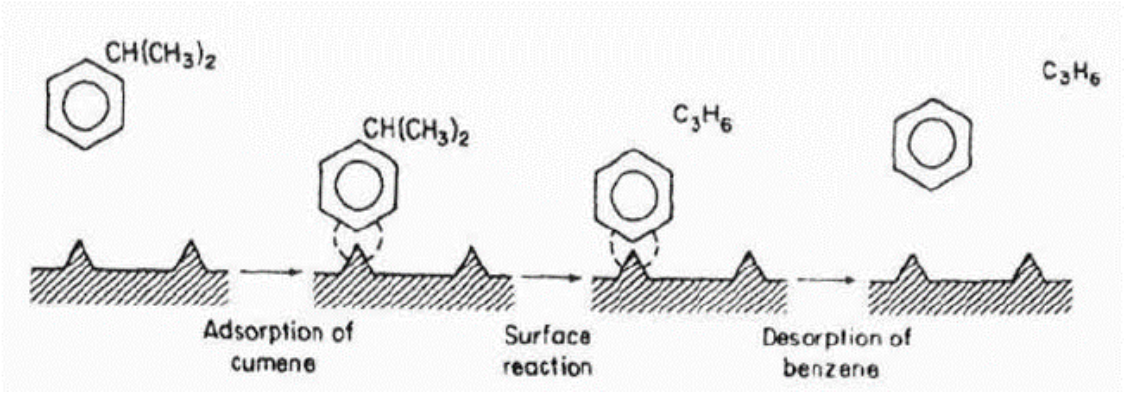

Figure 2.12 Sequence of steps in reaction-limited catalytic reaction [21].

The nomenclature in Table 2.2 is used to denote the various species in this reaction: C = cumene, B = benzene, and P = propylene. The reaction sequence for this decomposition is:

Table 2.2 Steps in a Langmuir-Hinshelwood Kinetic Mechanism

$C + S \underset{k_{-A}}{\overset{k_A}{\Longleftrightarrow}} C\cdot S$	Adsorption of cumene on surface	(2-16)
$C\cdot S \underset{k_{-S}}{\overset{k_S}{\Longleftrightarrow}} B\cdot S + P$	Surface reaction to form adsorbed benzene and propylene in the gas phase	(2-17)
$B\cdot S \underset{k_{-D}}{\overset{k_D}{\Longleftrightarrow}} B + S$	Desorption of benzene from surface	(2-18)

Equations (2-16) through (2-18)) represent the mechanism proposed for this reaction.

The rate expression for the adsorption of cumene as given in Equation (2-16) is

$$r_{AD} = k_A\left(P_C C_V - \frac{C_{C\cdot S}}{K_{AD}}\right) \tag{2-19}$$

The rate law for the surface reaction step producing adsorbed benzene and propylene in the gas phase.

$$r_S = k_S\left(C_{\mathrm{C\cdot S}} - \frac{P_P C_{B\cdot S}}{K_S}\right) \tag{2-20}$$

The rate of benzene desorption [see Equation (2-18)] is

$$r_D = k_D\left(C_{\mathrm{B\cdot S}} - K_{AD,B} P_B C_V\right) \tag{2-21}$$

(a) <u>Is the Adsorption Reaction Rate-Limiting?</u>

To answer this question, we shall assume that the adsorption of cumene is indeed rate-limiting, derive the corresponding rate law, and then check to see if it is consistent with experimental observation. For adsorption-limited reactions, k_A is small and k_S and k_D are large. Consequently, the ratios r_S/k_S and r_D/k_D very small (approximately zero), whereas the ratio $r_{AD}/k_A$is relatively large. That is, the rate for he adsorption step[$k_A P_C$](s^{-1})

is small with respect to the other rate constants: $k_S(s^{-1})$ for the surface reaction step and $k_D(s^{-1})$ for the desorption step.

Again, for adsorption-limited reactions the surface specific reaction rate k_S is large by comparison, and we can set

$$\frac{r_S}{k_S} \cong 0$$

and solve Equation (2-20) for $C_{C\cdot S}$:

$$C_{C\cdot S} = \frac{C_{B\cdot S} P_P}{K_S} \tag{2-22}$$

To be able to express $C_{C\cdot S}$ solely in terms of the partial pressures of the species present, we must evaluate $C_{B\cdot S}$, for adsorption-limited reactions, k_D is large by comparison, we can set

$$\frac{r_D}{k_D} \cong 0$$

and then solve Equation (2-21) for $C_{B\cdot S}$:

$$C_{B\cdot S} = K_B P_B C_V \tag{2-23}$$

After combining Equations (2-22) and (2-23), we have:

$$C_{C\cdot S} = K_B \frac{P_B P_P}{K_S} C_V \tag{2-24}$$

Replacing $C_{C\cdot S}$ in Equation (2-14) into Equation (2-19) and then factoring C_V, we obtain:

$$r_{AD} = k_A \left(P_C - \frac{K_B P_B P_P}{K_S K_{AD}}\right) C_V = k_A \left(P_C - \frac{P_B P_P}{K_P}\right) C_V \tag{2-25}$$

where the term $(K_S K_{AD}/K_B)$ is simply the overall partial pressure equilibrium constant, K_P.

The concentration of vacant sites, C_V, can now be eliminated from Equation (2-25) by utilizing the site balance to give the total concentration of sites, Ct, which is assumed to be constant:

Total sites = Vacant sites + Occupied sites

Since cumene and benzene are adsorbed on the surface, the concentration occupied sites is ($C_{C\cdot S}$+$C_{B\cdot S}$), and the total concentration of sites is:

$$Ct = C_V + C_{C\cdot S} + C_{B\cdot S} \tag{2-26}$$

Substituting Equations (2-23) and (2-24) into Equation (2-26), we have:

$$Ct = C_V + K_B \frac{P_B P_P}{K_S} C_V + K_B P_B C_V$$

Solving for C_V, we have:

$$C_V = \frac{C_t}{1 + K_B \frac{P_B P_P}{K_S} + K_B P_B} \tag{2-27}$$

Combining Equations (2-25) and (2-27), we find that the rate law for catalytic decomposition of cumene, assuming that the adsorption of cumene is the rate-limiting step, is:

$$\boxed{r_{AD} = \frac{C_t k_A \left(P_C - \frac{P_B P_P}{K_P}\right)}{1 + K_B \frac{P_B P_P}{K_S} + K_B P_B}}$$

Initially, no products are present; consequently, $P_P = P_B = 0$. The initial rate is given by:

$$-r_{C0} = C_t k_A P_{C0} = k_{PC0}$$

(b) Is the Surface Reaction Rate-Limiting ?

From Equation (2-20), we cannot readily measure the concentrations of the adsorbed species, we must utilize the adsorption and desorption steps to eliminate $C_{C\cdot S}$ and $C_{B\cdot S}$ from this equation. From the adsorption rate expression in Equation (2-19) and the condition that k_A and k_D are very large by comparison with k_S when surface reaction is controlling we obtain a relationship for the surface reaction for adsorbed curnene:

$$C_{C\cdot S} = K_{AD} P_C C_V \tag{2-28}$$

In a similar manner, the surface concentration of adsorbed benzene can be evaluated from the desorption rate expression [Equation (2-21)] together with the approximation:

When $\dfrac{r_D}{k_D} \cong 0$ then $C_{B\cdot S} = K_B P_B C_V$

Substituting for $C_{C\cdot S}$ and $C_{B\cdot S}$ into Equation (2-20), give

$$r_S = k_S \left(P_C K_{AD} - \frac{K_B P_B P_P}{K_S} \right) C_V = k_A K_{AD} \left(P_C - \frac{P_B P_P}{K_P} \right) C_V$$

Substituting for concentrations of the adsorbed species, $C_{C\cdot S}$ and $C_{B\cdot S}$, yields:

$$C_V = \frac{C_t}{1 + P_B K_B + K_{AD} P_C}$$

$$\boxed{r_S = \frac{k_S C_t k_{AD} \left(P_C - \dfrac{P_B P_P}{K_P} \right)}{1 + K_B P_B + K_C P_C}}$$

The initial rate is:

$$\boxed{-r_{C0} = \frac{k_S C_t K_{AD} P_{C0}}{1 + K_S P_{C0}}}$$

(c) Is the Desorption of Benzene Rate-Limiting?

The rate expression for the desorption of benzene is:

$$r_D = k_D\left(C_{\mathrm{B\cdot S}} - K_{AD,B}P_B C_V\right)$$

From the rate expression for the surface reaction, solve Equation (2-22) for $C_{B\cdot S}$, then substitute Equation (2-28) to obtain:

$$C_{B\cdot S} = \frac{K_S K_{AD} P_C C_V}{P_P} \tag{2-29}$$

Combining Equations (2-29) and (2-21) gives us:

$$r_D = k_D K_{AD} K_S \left(\frac{P_C}{P_P} - \frac{P_B}{K_p}\right) C_V \tag{2-30}$$

After substituting $C_{C\cdot S}$ and $C_{B\cdot S}$ to site balance, we solve the site balance for C_V:

$$C_V = \frac{C_t}{1 + \frac{K_{AD}K_S P_C}{P_P} + K_{AD}P_C} \tag{2-31}$$

Replacing $C_V$in Equation (2-30) by Equation (2-31), and multiplying the numerator and denominator by Pp, we obtain the rate expression for desorption control:

$$r_S = \frac{C_t k_D K_{AD} K_S \left(P_C - \frac{P_B P_P}{K_P}\right)}{P_P + P_P K_{AD} K_S + K_{AD} P_P P_C}$$

To determine the dependence of the initial rate on partial pressure of cumene, we again set P_P and $P_B = 0$, the rate law reduces to: $-r_{CO} = k_D C_t$

2.2.5 Factors Affecting Rate of Reaction

The following are the main factors that influence the rate of a chemical reaction.

2.2.5.1 Nature of Reactants

Different reactants have different energies of activation. Reactions between polar or ionic molecules are very fast. Oxidation-Reduction reactions are slower than ionic

reactions because they involve transfer of electrons and bond rearrangement. The physical state of reacting substances are important in determining their reactivity. The reaction in which ionic solutions are involved also take place at high speed

2.2.5.2 Concentration of reactants

The concentrations of reactants play an important role in chemical kinetics. It is usually true that by increasing the amount of reactants, the rate of reaction is increased. As we know that an increase in concentration of reactants increases the number of molecules. According to collision theory, the greater the number of molecules the higher is the collision ratio, consequently faster is the rate of reaction.

2.2.5.3 Surface area of reactants

In heterogeneous reactions, the rate of the reaction depends upon the surface area of the solid reactant. Greater the surface area, higher is the rate of reaction. For example finely divided calcium carbonate (marble) reacts more quickly with hydrochloric acid than calcium carbonate chips. It is due to the fact that powered calcium carbonate offers larger surface area to the reacting acid. In other words, by increasing the surface area of reactant, rate of reaction increases due to greater contact between individual particles and also due to the fact that the surface molecules reacts more quickly.

2.2.5.4 Temperature

The rate of a reaction increases with the rise of temperature. This can be explained by the fact that at higher temperatures, a greater fraction of colliding molecules possess the necessary energy of activation. Generally an increase of every 10K in temperature doubles the rate.As the temperature increases the velocity of molecules also increases which results in the increase in the frequency of collision. The rise in temperature rises the kinetic energy of each molecule. It has been found that by raising the temperature by 10k,the fraction of molecule possessing threshold or activation energy becomes double. As a result the no of effective collision is also double,hence rate is doubled

2.2.5.5 Presence of Catalyst

A catalyst is a substance that controls the rate of reaction without itself undergoing a permanent chemical change. There are two types of catalysts:

Positive Catalyst: A positive catalyst increases the rate of a reaction by lowering the energy of activation. Thus in the presence of a positive catalyst, the greater fraction of the total molecule will posses lower energy of activation and collided successfully in a short period of time, there by increasing the rate of reaction. Role of positive catalyst; A

positive catalyst functions by providing an alternate path to the reaction or by the formation of a transition (intermediate) compound having low energy of activation. The activation energy of this path is lower. As a result rate of reaction is increased.

Negative Catalyst: A negative catalyst retards the rate of a reaction. Negative catalysts do not lower the energy of activation, rather they are combined with reactant molecules, thus decreasing the number of colliding reactant molecules. This decreases the effective collisions, hence rate of reaction. Role of negative catalyst; A negative catalyst does not lower the energy of activation rather it combines with the reactant molecules, thus decreasing the number of colliding reactant molecules. This decreases the effective collisions, hence, decreasing the rate of reaction.

2.2.5.6 Light or Radiation

Not all reactions are affected by light or radiation, but a few reactions, which are usually free radicals or photo chemical reactions, are influenced by light. Light activates some of the reactant molecules producing free radicals. Since free radicals are very excited, therefore, they react immediately with other molecules to form products. The concentration of reactants does not influence the rate of such reactions, so they are zero order reaction. We know that that light consists of photon. When photons strike the reactant molecule, they provide necessary activation energy to the reactant molecules.

2.3 Reactor definitions and Reactor sizing

2.3.1 Batch Reactor

A batch reactor is used for small-scale operations, for testing new processes that have not been fully developed, for the manufacture of expensive products, and for processes that are difficult to convert to continuous operations. The reactor can be charged (i.e. filled) through the holes at the top (Figures 2.13a and 2.13b). The batch reactor has the advantage of high conversions that can be obtained by leaving the reactant in the reactor for long periods of time, but it also has the disadvantages of high labor costs per batch, the variability of products from batch to batch, and the difficulty of large-scale production.

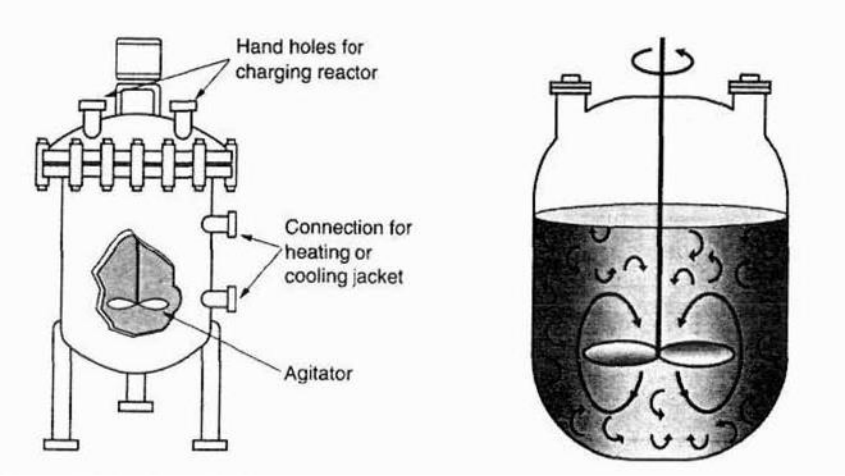

Figure 2-13a Simple batch homogeneous reactor [21].

Figure 2-13b Batch reactor mixing patterns [21].

A batch reactor has neither inflow nor outflow of reactants or products while the reaction is being carried out: $F_{j0} = F_j = 0$. The resulting general mole balance on species *j* is:

$$\frac{dN_j}{dt} = \int_0^v r_j dV$$

If the reaction mixture is perfectly mixed (Figure 2-12b) so that there is no variation in the rate of reaction throughout the reactor volume, we can take r_j out of the integral, integrate, and write the mole balance in the form:

$$\frac{dN_j}{dt} = r_j V \tag{2-32}$$

Let us consider the isomerization of species A in a batch reactor:

A =====> B

As the reaction proceeds, the number of moles of A decreases and the number of moles of B increases, as shown in Figure 2-13.

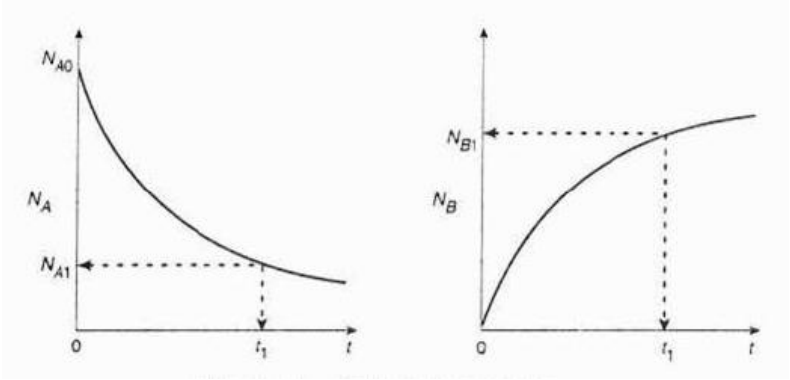

Figure 2.14 Mole-time trajectories [21].

We might ask what time, t_1, is necessary to reduce the initial number of moles from N_{A0} to a final desired number N_{A1}. Applying Equation (2-32) to the isomerization:

$$\frac{dN_A}{dt} = r_A V$$

Rearranging:

$$dt = \frac{dN_A}{r_A V}$$

and integrating with limits that at $t = 0$, then $N_A = N_{A0}$, and at $t = t_1$, then $N_A = N_{A1}$, we obtain:

$$t_t = \int_{N_{A1}}^{N_{A0}} \frac{dN_A}{r_A V} \tag{2-33}$$

This equation is the integral form of the mole balance on a batch reactor. It gives the time, t_1, necessary to reduce the number of moles from N_{A0} to N_{A1} and also to form N_{B1} moles of B.

2.3.2 Continuous-Flow Reactors

Continuous flow reactors are almost always operated at steady state. We will consider three types: the continuous stirred tank reactor (CSTR), the plug flow reactor (PFR), and the packed bed reactor (PBR).

2.3.2.1 Continuous-Stirred Tank Reactor

A type of reactor used commonly in industrial processing is the stirred tank operated continuously (Figure 2.15). It is referred to as the continuous-stirred tank reactor

(CSTR) or vat, or backmix reactor, and is used primarily for liquid phase reactions. It is normally operated at steady state and is assumed to be perfectly mixed. Consequently, there is no time dependence or position dependence of the temperature, the concentration, or the reaction rate inside the CSTR. That is, every variable is the same at every point inside the reactor. Because the temperature and concentration are identical everywhere within the reaction vessel, they are the same at the exit point as they are elsewhere in the tank. Thus the temperature and concentration in the exit stream are modeled as being the same as those inside the reactor. In systems where mixing is highly non-ideal, the well-mixed model is inadequate and we must resort to other modeling techniques, such as residence-time distributions, to obtain meaningful results.

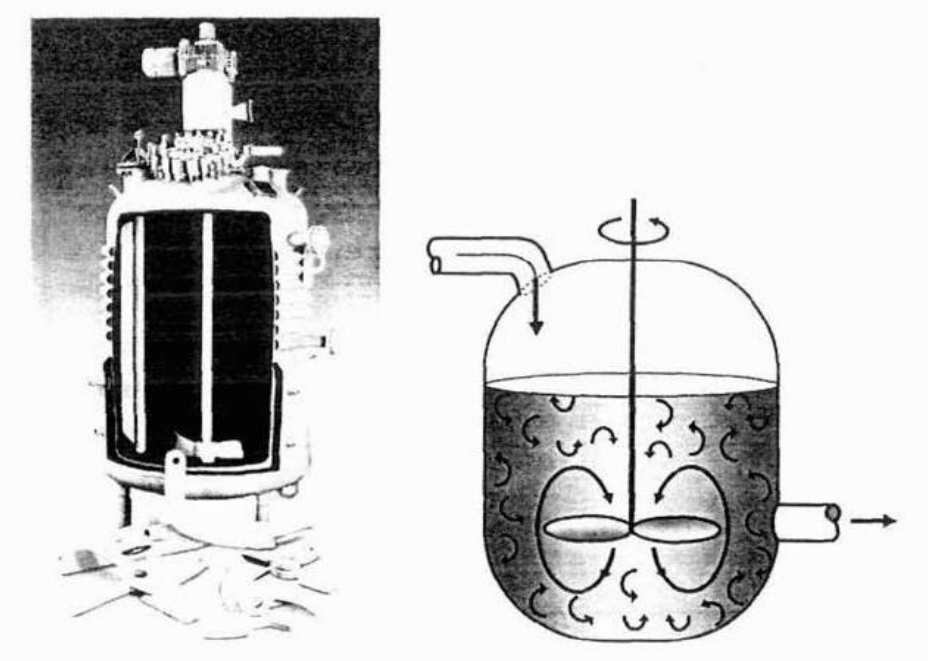

Figure 2-15a CSTR/batch reactor [21]. **Figure 2-15b** CSTR mixing patterns [21].

When the general mole balance equation:

$$F_{j0} - F_j + \int_0^v r_j \, dV = \frac{dN_j}{dt} \tag{2-34}$$

is applied to a CSTR operated at steady state (i.e. conditions do not change with time):

$$\frac{dN_j}{dt} = 0$$

in which there are no spatial variations in the rate of reaction (i.e. perfect mixing):

$$\int_0^V r_j \, dV = V r_j$$

it takes the familiar form known as the *design equation* for a CSTR:

$$V = \frac{F_{j0} - F_j}{-r_j} \tag{2-35}$$

The CSTR design equation gives the reactor volume V necessary to reduce the entering flow rate of species j, from F_{j0}, to the exit flow rate F_j, when species j is disappearing at a rate of $-r_j$. We note that the CSTR is modeled such that the conditions in the exit stream (e.g. concentration, temperature) are identical to those in the tank. The molar flow rate F_j is just the product of the concentration of species j and the volumetric flow rate v :

$$F_j = C_j \cdot v$$

$$\frac{moles}{time} = \frac{moles}{volume} \cdot \frac{volume}{time} \tag{2-36}$$

Consequently, we could combine Equations (2-35) and (2-36) to write a balance on species A:

$$V = \frac{V_0 C_{A0} - v C_A}{-r_A} \tag{2-37}$$

2.3.2.2 Tubular Reactor

In addition to the CSTR and batch reactors, another type of reactor commonly used in industry is the tubular reactor. It consists of a cylindrical pipe and is normally operated at steady state, as is the CSTR. Tubular reactors are used most often for gas-phase reactions. A schematic and a photograph of industrial tubular reactors are shown in Figure 2.15. In the tubular reactor, the reactants are continually consumed as they flow down the length of the reactor. In modeling the tubular reactor, we assume that the concentration varies continuously in the axial direction through the reactor. Consequently, the reaction rate, which is a function of concentration for all but zero-order reactions, will also vary axially. For the purposes of the material presented here. we consider systems in which the flow field may be modeled by that of a plug flow profile (e.g. uniform velocity as in

turbulent flow), as shown in Figure 2.16. That is, there is no radial variation in reaction rate and the reactor is referred to as a plug-flow reactor (PFR).

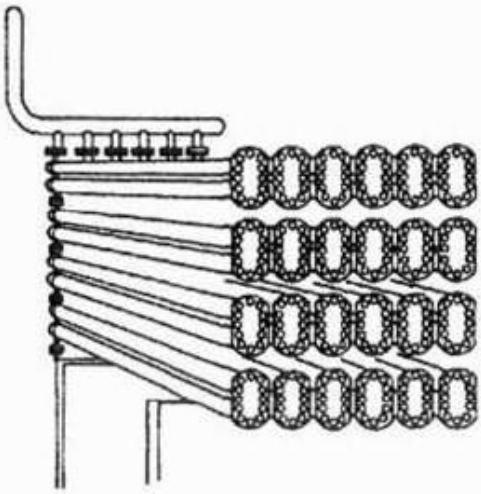

Figure 2.16a Tubular reactor schematic, Longitudinal tubular reactor [21].

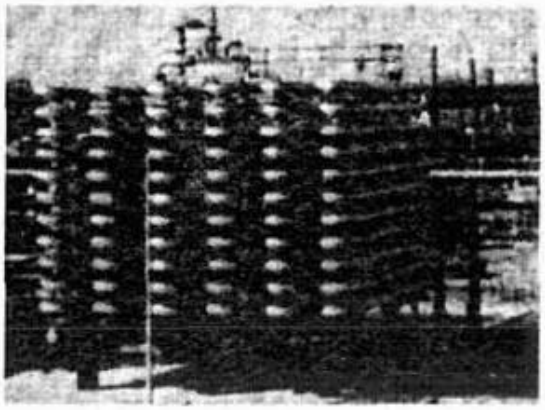

Figure 2.16b Tubular reactor photo [21].

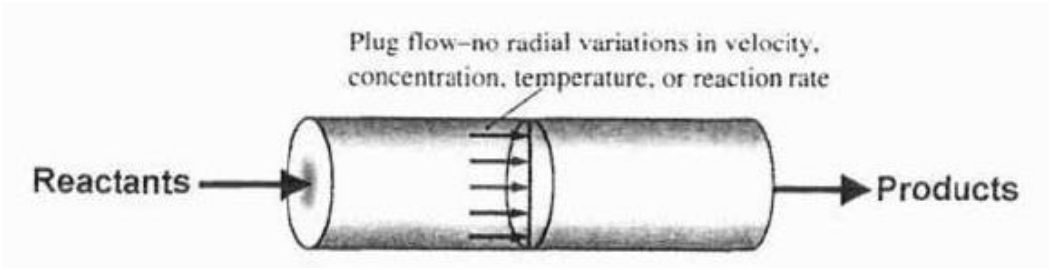

Figure 2.16 Plug-flow tubular reactor. [21].

The equation we will use to design PFRs at steady state can be developed in two ways: (1) directly from Equation (2-34) by differentiating with respect to volume *V*, or (2) from a mole balance on species *j* in a differential segment of the reactor volume ΔV. Let us choose the second way to arrive at the differential form of the PFR mole balance. The differential volume shown, ΔV, in Figure 2-17, will be chosen sufficiently small such that there are no spatial variations in reaction rate within this volume. Thus the generation term, ΔG_j, is

$$\Delta G_j = \int^{\Delta V} r_j dV = r_j \Delta V$$

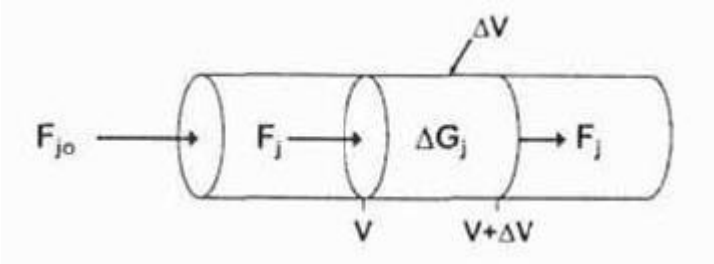

Fig. 2.17 Mole balance on species j in volume ΔV [21].

$$\begin{bmatrix} Molar\ flow \\ rate\ of\ species\ j \\ In\ at\ V \end{bmatrix} - \begin{bmatrix} Molar\ flow \\ rate\ of\ species\ j \\ Out\ at\ (V + \Delta V) \end{bmatrix} + \begin{bmatrix} Molar\ rate\ of \\ Generation \\ of\ species\ j \\ within\ \Delta V \end{bmatrix} = \begin{bmatrix} Molar\ rate\ of \\ Accumulation \\ of\ species\ j \\ within\ \Delta V \end{bmatrix} \quad (2\text{-}38)$$

In	-	**Out**	+	**Generation**	=	**Accumulation**
$\boldsymbol{F_j\vert_V}$	-	$\boldsymbol{F_j\vert_{V+\Delta V}}$	+	$\boldsymbol{r_j \Delta V}$	=	**0**

Dividing by ΔV and rearranging:

$$\left[\frac{F_j|_{V+\Delta V} - F_j|_V}{\Delta V}\right]$$

the terms in brackets resemble the definition of the derivative

$$\lim_{\Delta x \to 0}\left[\frac{f(x+\Delta x) - f(x)}{\Delta x}\right] = \frac{df}{dx}$$

Taking the limit as AV approaches zero, we obtain the differential form of the steady state mole balance on a PFR

$$\frac{dF_j}{dV} = r_j \quad (2\text{-}39)$$

We could have made the cylindrical reactor on which we carried out our mole balance an irregular shaped reactor, such as the one shown in Figure 2.18, for reactant species A.

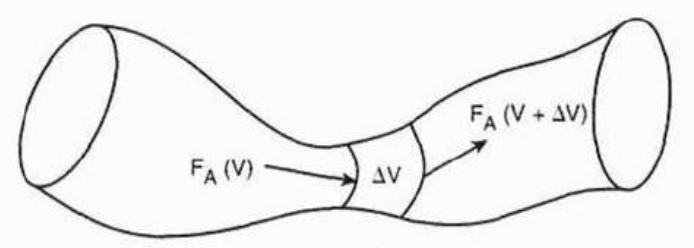

Figure 2.18 Pablo Picasso's reactor [21].

However, we see that by applying Equation (2-38), the result would yield the same equation (i.e. Equation [2-39]). For species A, the mole balance is:

$$\frac{dF_A}{dV} = r_A \tag{2-40}$$

Consequently, we see that Equation (2-39) applies equally well to our model of tubular reactors of variable and constant cross-sectional areas, although it is doubtful that one would find a reactor of the shape shown in Figure 2-18, unless it were designed by Pablo Picasso. The conclusion drawn from the application of the design equation to Picasso's reactor is an important one: the degree of completion of a reaction achieved in an ideal plug-flow reactor (PFR) does not depend on its shape, only on its total volume. Again consider the isomerization A → B, this time in a PFR. As the reactants proceed down the reactor. A is consumed by chemical reaction and B is produced. Consequently, the molar Raw rate of A decreases and that of B increases, as shown in Figure 2-19.

$$V = \int_{F_A}^{F_{A0}} \frac{dF_A}{-r_A}$$

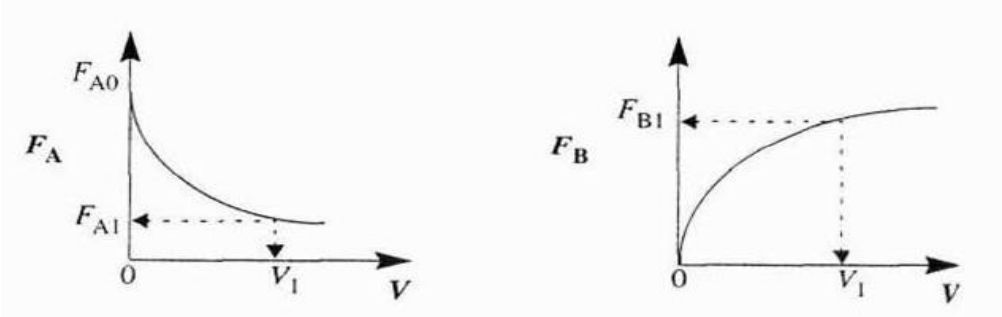

Figure 2.19 Profiles of molar flow rates in a PFR [21].

We now ask what is the reactor volume *V*, necessary to reduce the entering molar flow rate of A from F_A, to F_{A1}. Rearranging Equation (2-40) in the form:

$$dV = \frac{dF_A}{r_A}$$

and integrating with limits at $V = 0$, then $F_A = F_{A0}$ and at $V = V_1$ then $F_A = F_{A1}$.

$$V_1 = \int_{F_{A0}}^{F_{A1}} \frac{dF_{A1}}{r_A} = \int_{F_{A1}}^{F_{A0}} \frac{dF_A}{-r_A} \qquad (2\text{-}41)$$

V_1 is the volume necessary to reduce the entering molar flow rate F_A, to some specified value F_{A1} and also the volume necessary to produce a molar flow rate of B of F_{B1}.

2.3.2.3 Packed-Bed Reactor

The principal difference between reactor design calculations involving homogeneous reactions and those involving fluid-solid heterogeneous reactions is that for the latter, the reaction takes place on the surface of the catalyst. Consequently, the reaction rate is based on the mass of the solid catalyst. *W*, rather than on reactor volume, *K* For a fluid-solid heterogeneous system, the rate of reaction of a substance A is defined as

$$-r'_A = \textit{mol A reacted/s•g catalyst}$$

The mass of thesolid catalyst is used because the amount of the catalyst is what is important to the rate of product formation. The reactor volume that contains the catalyst is of secondary significance. Figure 2-20 shows a schematic of an industrial catalytic reactor with vertical tubes packed with catalyst.

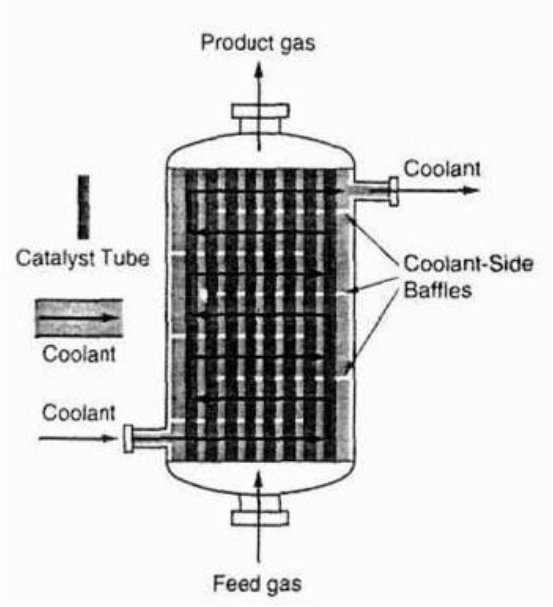

Figure 2.20 Longitudinal catalytic packed-bed reactor [21].

In the three idealized types of reactors just discussed (the perfectly mixed batch reactor, the plug-flow tubular reactor (PFR), and the perfectly mixed continuous-stirred rank reactor (CSTR), the design equations (i.e. mole balances) were developed based on reactor volume. The derivation of the design equation for a packed-bed catalytic reactor (PRR) will be carried out in a manner analogous to the development of the tubular design equation. To accomplish this derivation, we simply replace the volume coordinate in Equation (2-38) with the catalyst weight coordinate *W* (Figure 2-21).

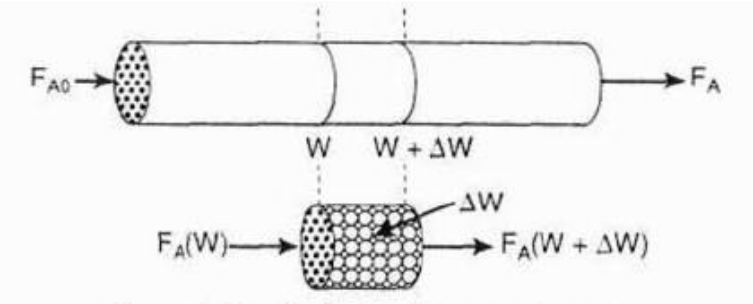

Figure 2.21 Packed-bed reactor schematic. [21].

As with the PFR, the PBR is assumed to have no radial gradients in concentration, temperature, or reaction rate. The generalized mole balance on species A over catalyst weight ΔW results in the equation:

In	**-**	**Out**	**+**	**Generation**	**=**	**Accumulation**
$\boldsymbol{F_A\|_W}$	**-**	$\boldsymbol{F_A\|_{W+\Delta W}}$	**+**	$\boldsymbol{r'_A \Delta W}$	**=**	**0**

(2-42)

The dimensions of the generation term in Equation (2-42) are

$$(r'_A)\Delta W \equiv \frac{mole\ A}{(time)(mass\ of\ catalyst)} \cdot ((mass\ of\ catalyst)) \equiv \frac{mole\ A}{time}$$

which are, as expected, the same dimensions of the molar flow rate F_A. After dividing by ΔW and taking the limit as $\Delta W \rightarrow 0$, we arrive at the differential form of the mole balance for a packed-bed reactor:

$$\frac{dF_A}{dW} = r'_A \tag{2-43}$$

When the pressure drop through the reactor and catalyst decay are neglected, the integral form of the packed-cataIyst-bed design equation can be used to calculate the catalyst weight.

$$W = \int_{F_{A0}}^{F_A} \frac{dF_A}{r'_A} = \int_{F_A}^{F_{A0}} \frac{dF_A}{-r'_A} \tag{2-44}$$

W is the catalyst weight necessary to reduce the entering molar flow rate of species A, F_{A0}, to a flow rate F_A.

CHEPTER 3

METHODOLOGY

This research was divided into three parts. Firstly, select the proper kinetic equations of esterification reaction. Secondly, reactor sizing, Finally, find the proper condition for operate process which factor affecting conversion will be investigated.

3.1 Select the proper kinetic equations of esterification reaction

This primary work will be carried out to find the proper kinetic equations of the esterification reaction. The kinetic equation of the esterification reaction for reactants that have free fatty acids reacted with methanol over the solid acid catalyst was considered.

In this research, the three different kinetic models were used to validate the model proper for using in modeling a continuous packed bed. The result that obtained from simulated each models were compared to the experimental results from literature. In detail, models 1 and 2 are the esterification of oleic acid in soybean oil and methanol using amberlyst 15 resins as a catalyst, while model 3 uses myristic acid in paapeseed oil, methanol and sulfated zirconia as a catalyst. Operative conditions are shown in Table 3.1 and the kinetic equations of 3 models are explained as following:

The first model (model 1, PH:OA) is based on a simple pseudo-homogeneous reversible reaction. The assumptions of this model are (i) the presence of two liquid phases can be neglected; (ii) the solid phase (the catalyst) is lumped into the single hypothetical phase; and (iii) the effects related to the vapor–liquid equilibrium are neglected. On the basis of these assumptions, the kinetic equation of this model is as follows:

$$r_{cat} = k_{cat} C_A C_M - k_{-cat} C_E C_W$$

where r_{cat} is the reaction rate for the catalyzed reaction, k_{cat} and k_{-cat} represent the kinetic constants of the forward and the reverse reaction respectively, that can been calculated in an Arrhenius Equation.

The second model (model 2, ER) is based on the Elay-Rideal mechanism. It mainly consisted of 5 elementary reactions (S denotes an active site):

$$A + S \Leftrightarrow A{\cdot}S \quad (3\text{-}1)$$

$$M + S \Leftrightarrow M{\cdot}S \quad (3\text{-}2)$$

$$A{\cdot}S + M \Leftrightarrow E{\cdot}S + W \quad (3\text{-}3)$$

$$W + S \Leftrightarrow W{\cdot}S \quad (3\text{-}4)$$

$$E{\cdot}S \Leftrightarrow E + S \quad (3\text{-}5)$$

This mechanism could be described as follows: firstly, oleic acid was adsorbed onto the surface of the catalyst and produced an intermediate molecule (3-1), which reacted with methanol coming from the bulk phase to produce FAME and water (3-3). Finally, FAME desorbed from surface of catalyst (3-5), which methanol and water could also adsorbed on surface of catalyst during reaction(3-2) and (3-4).

Equation (3-1), (3-2), and (3-4) were the adsorption reaction, (3-3) the surface reaction and (3-5) the desorption reaction. Under the following assumptions: (i) the catalyst was considered as a heterogeneous catalyst on which surface adsorption of methanol, water, oleic acid and methyloleate occurred according to a Langmuir isotherm. The triglycerides was presented and considered as non-adsorbing compound; (ii) the adsorption equilibrium constants were assumed as independent temperature - in range of (333-393 K); (iii) the rate-determining step in the overall reaction rate was surface reaction (Eley-Rideal step). As mentioned earlier, the kinetic rate law was described as follows:

$$r_{cat} = \frac{k_{cat} b_A C_A C_M - k_{-cat} b_E C_E C_W}{1 + b_A C_A + b_M C_M + b_E C_E + b_W C_W}$$

where b_i are the adsorption equilibrium constants related to each component, A is oleic acid, B is methanol, E is methyl oleate and W is water. The corresponding values were reported by Tesser et al. (2010), as shown in Table 4.1.

The Third model (model 3, PH:MA) is also represented by a simple pseudo-homogeneous reaction with model 3 using myristic acid in paapeseed oil, methanol and sulfated zirconia as a catalyst. Therefore, the kinetic equation can be shown as follows:

$$r_{cat} = k_1 C_{MA} C_M - k_{-1} C_E C_W$$

where C_{MA}, C_M, C_E and C_W are the concentrations of myristic acid, methanol, myristic acid methyl ester and water respectively, k_1 is the forward rate constant and k_{-1} is the backward rate constant.

Table 3.1 Operative conditions.

Run.	Temperature (°C)	Amount of catalyst (g)	Amount of oleic acid (g)	Amount of methanol (g)
T1	80	5.0781	100.8	91.2
T2	100	5.0074	99.8	90.5
T3	100	10.0037	104.4	94.7
T4	120	0.9027	3.6158	21.7662
T5	150	0.9039	3.6147	21.7662
T6	170	0.9124	3.6667	21.7662

3.2 Reactor sizing

This part is work on a sizing reactor, including model geometry and mass balance in the continuous packed bed reactor

3.2.1 Model geometry

The scheme configuration of a packed bed reactor for this investigation is presented in Fig 3.1. Free fatty acid and methanol were fed to a packed bed at an inlet simultaneously. The esterification reaction occurred in the packed bed region only, of which Amberlyst 15 resin was used as solid acid catalyst. Reactants and products were obtained at outlet. The internal diameter of reactor was 2.5 cm, catalytic bed length was varied from 100 cm, catalyst loading was 10 g. The developed model were based on the assumptions as follows; (1) this reactor operated as isothermal along reactor length, (2) no pressure drop along reactor length, and (3) ideal gas behavior was applied to all gas components. The developed mathematical model was coded in COMSOL® program.

3.2.2 Mass balance in the continuous packed bed reactor

In the continuous packed bed reactor, the mass balance for each component can be written as:

$$\nabla \cdot (-D_i \nabla c_i) + u \cdot \nabla c_i = R_i$$

where ∇ is gradient $\left(\frac{\partial}{\partial x}, \frac{\partial}{\partial y}, \frac{\partial}{\partial z}\right)$, D_i is the diffusion coefficient (m^2/s), R is a reaction term ($mol/m^3 \cdot s$), u is the inlet velocity and c is the total concentration (mol/m^3).

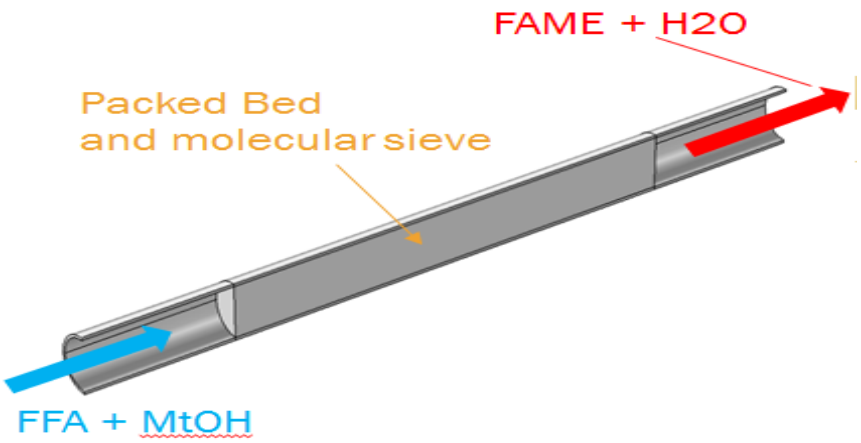

Figure 3.1 Scheme of packed bed reactor.

3.3 Find the proper conditions for operating process

This work was carried out to find the effect of conversion on operating parameters in a packed bed reactor. The simulation steps are as follows:

- Review the literature to find the governing equations applicable to this study.
- Define the parameters in an equation used for biodiesel production in a packed bed reactor.
- Design the three-dimensional configuration of the packed bed reactor.
- Study the effects of operating parameters that include flow rate, concentration and inlet temperature.
- Summarize the results.

CHAPTER 4

RESULTS AND DISCUSSION

In this chapter, a continuous packed bed operation was investigated as alternative method for biodiesel production from reactants that have high free fatty acids. Based on the esterification reaction, a mathematical model of a continuous packed bed was developed and coded in COMSOL® software.

4.1. Study and validate kinetics for modeling of continuous packed bed

To validate the model that is proper for using in modeling a continuous packed bed, the results obtained from the simulation each of model were compared to the results in the literature.

Figs. 4.1 and 4.3 show the simulate data that obtained from simulated, while Figs. 4.2 and 4.4 are experimental data from the literature. When compared Fig. 4.1 with Fig. 4.2 at same conditions, it can be seen that model 2 is more appropriate than model 1 because it gives comparable results to literature. Table 4.1 also shows that model 2 presents higher value of the correlation coefficient R^2 and lower value of a root mean square error than model 1. Fig 4.3 represents that model 3 can also be used since the simulate data are closed to experimental data. Based on this validation, model 2 will be applied for further study since oleic acid is the suitable model compound of vegetable oil fatty acid rather than myristic acid.

Table 4.1 Results of the kinetic study for catalyzed esterification [13].

Model	NP	Kinetic parameter				Absorption parameter				Statistics		
		k_{cat}^{rif}	E_A^{cat}	k_{-cat}^{rif}	E_A^{-cat}	b_M	b_A	b_W	b_B	RMS	R^2	F_{test}
1(PH)	4	185.0	15.78	212.6	$6.3x10^{-6}$	-	-	-	-	10.71	0.81	113
2(ER)	8	131.6	17.83	161.8	8.76	49.16	3.38	3537	1.59	7.28	0.91	266

NP = no. of parameter. $[k_{cat}^{rif}]$, $[k_{-cat}^{rif}]$ (for PH model) = $cm^6mol^{-1}g_{cat}^{-1}min^{-1}$; (for ER model) = $cm^3g_{cat}^{-1}min^{-1}$. $[E_A^{cat}]$,$[E_A^{-cat}]$ = kcal mol^{-1}. $[b_i]$ = cm^3mol^{-1}

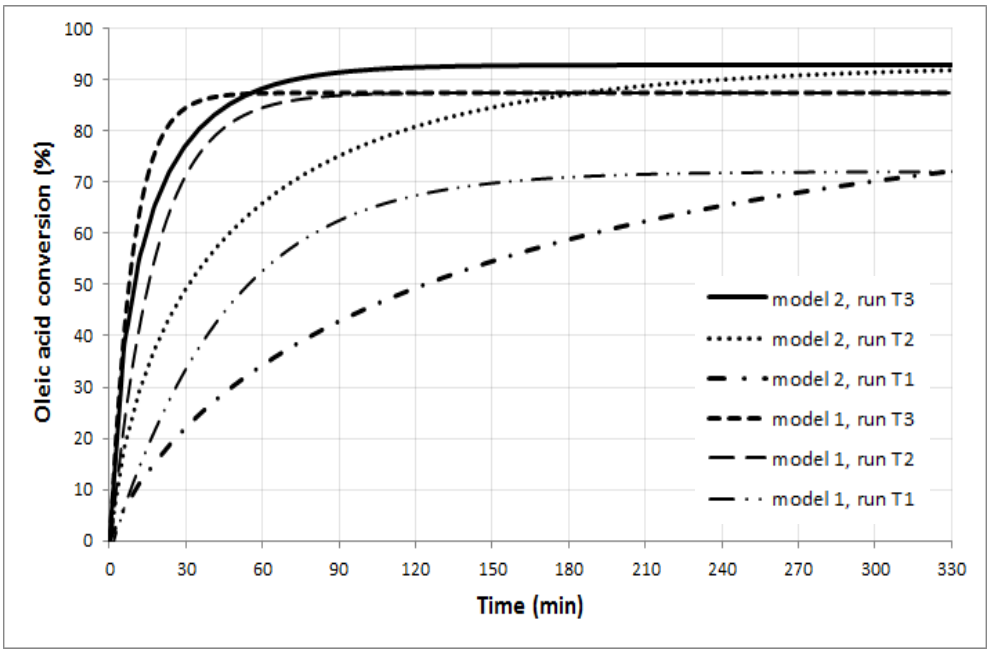

Figure 4.1 Simulation packed bed run. MeOH: oleic acid ratio = 8:1, flow rate = 1 L/h.

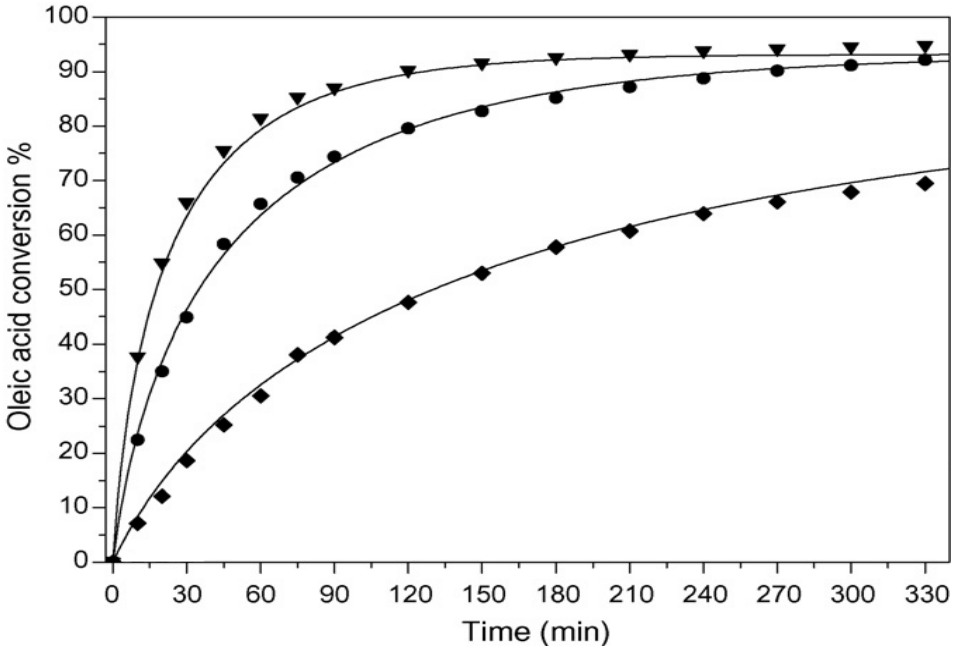

Figure 4.2 Experimental batch run. MeOH: oleic acid ratio = 8:1, flow rate = 1 L/h. (♦) Run T1, (●) Run T2, (▼) Run T3.

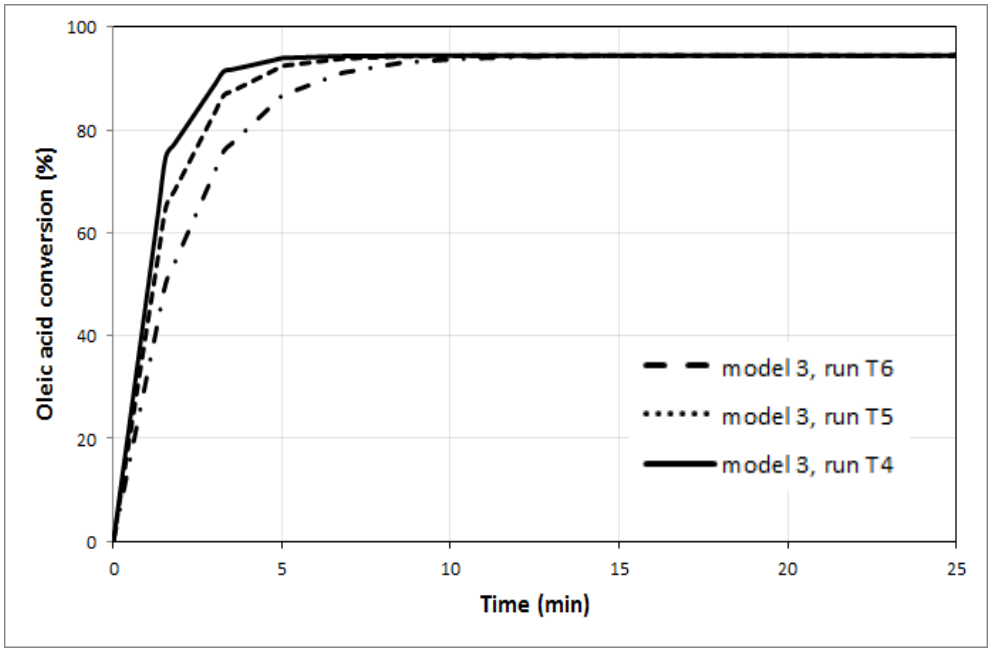

Figure 4.3 Simulation packed bed run. Methanol: oleic acid molar ratio = 42:1 and flow rate = 1 L/h.

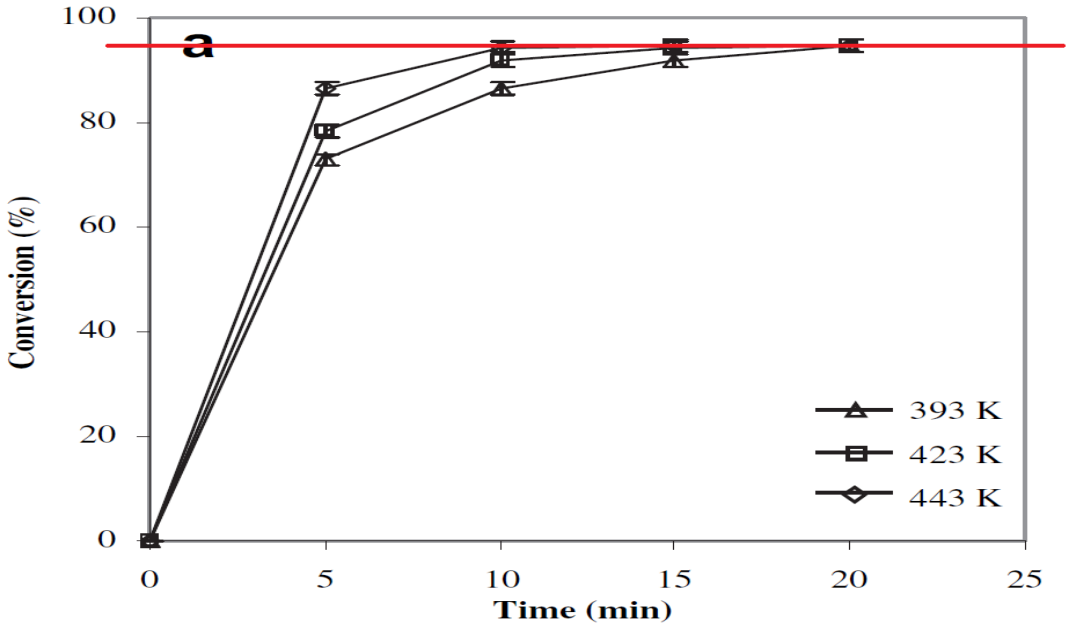

Figure 4.4 Experimental batch run. Methanol: oleic acid molar ratio = 42:1. (Δ) Run. T4, (□) Run T5, (◊) Run T6.

4.2 Effect of operating conditions

Firstly, the model was simulated at reference conditions, of which the operating temperature and pressure were fixed at 100 °C and 6 bar, while the methanol/oleic acid molar ratio in the inlet was 8:1. This inlet feed was introduced to the packed bed reactor with flow rate of 1 L/h. Under these conditions, the effects of catalyst weight, temperature, methanol/fatty acid ratio on the conversion of fatty acid were investigated.

Table 4.2 Operative conditions at different catalyst weights.

Run.	Temperature (°C)	Amount of catalyst(%wt)	Amount of oleic acid (g)	Molar ratio (M/O)	Flow rate (L/h)
T7	100	1	100	8	1
T8	100	4	100	8	1
T9	100	7	100	8	1
T10	100	10	100	8	1
T11	100	15	100	8	1
T12	100	20	100	8	1
T13	100	50	100	8	1

4.2.1 Effect of catalyst weight

Fig. 4.5 presents the conversion of oleic acid along the reactor length at different amounts of catalyst base on oleic acid weights (1%wt, 4%wt, 7%wt, 10%wt, 15%wt, 20%wt and 50%wt of catalyst). It can be seen that the conversion of oleic acid increased immediately at entrance of the packed bed reactor and reached to constant. Using 10%wt of catalyst, it shows the rapid and highest conversion rate. Therefore, 10%wt of catalyst weight was chosen for further studies since its high conversion rate can lower the requirements of the long reactor system.

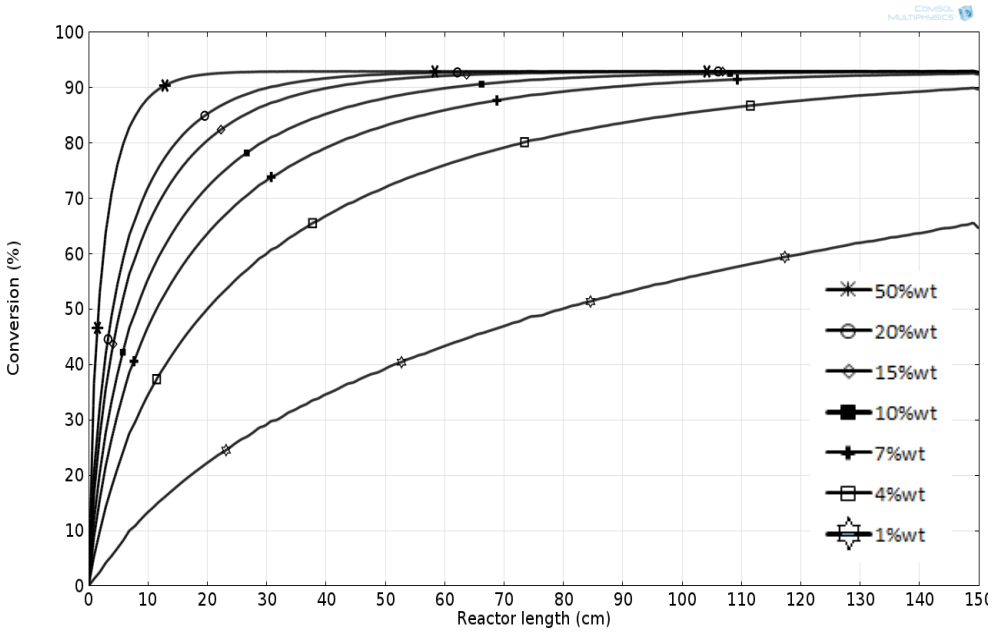

Figure 4.5 Conversion of oleic acid vs. reactor length at different catalyst weights. (Simulated condition: temperature = 100°C, MeOH: Oleic acid ratio = 8:1 and flow rate = 1 L/h).

4.2.2 Effect of reaction temperature

Reaction temperature is one factor that influences the esterification rate. The esterification reaction is favored by high temperature, and hence, oleic acid conversion should increase. Fig. 4.6 shows the effects of temperature from 60°C to 120°C on oleic acid conversion. It demonstrates that the reaction rate (conversion) could be rapidly sped up by a rising the temperature. The conversion increased up to 95.95% when esterified at 120°C. Figs. 4.7-4.10 present the profiles of reactants and products along the reactor at different operating temperatures. Clearly, FAME and water are generated along the length of the reactor, whereas fatty acid and methanol steadily decrease. It is noted that although the use of high temperature can enhance high conversion rate, it also requires high energy input to maintain the reaction temperature along the operation. Therefore, in this study, 100°C is selected for further optimization.

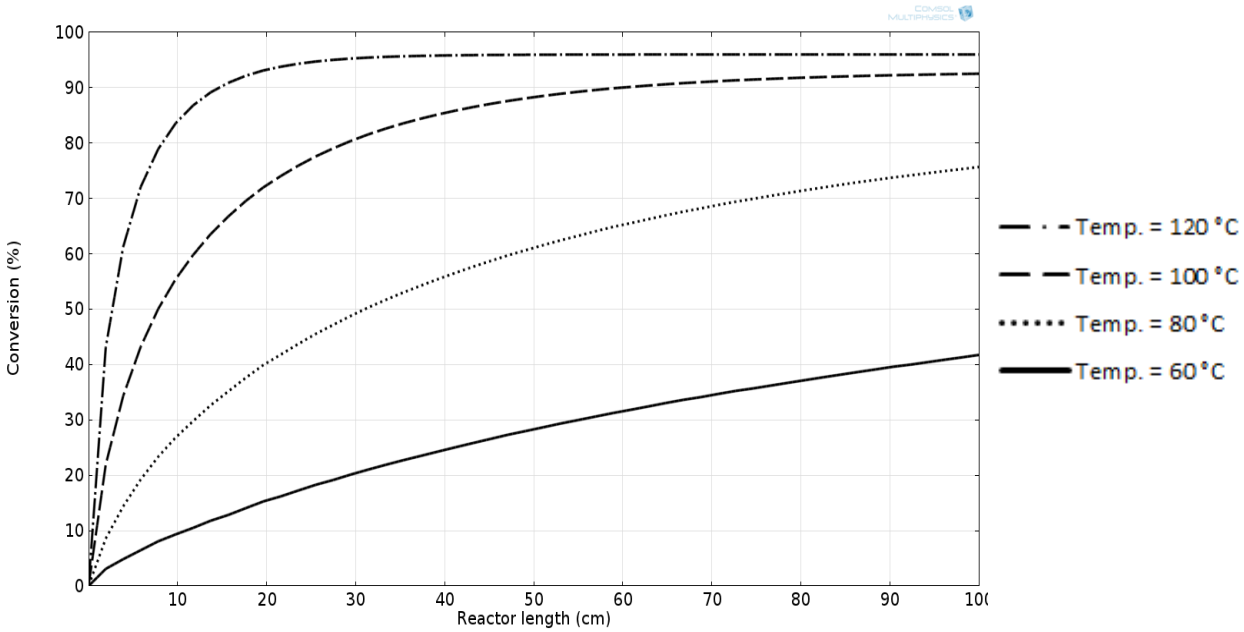

Figure 4.6 Conversion of oleic acid vs. reactor length at different temperatures. (Simulated condition: MeOH: Oleic acid ratio = 8:1 and flow rate = 1 L/h)

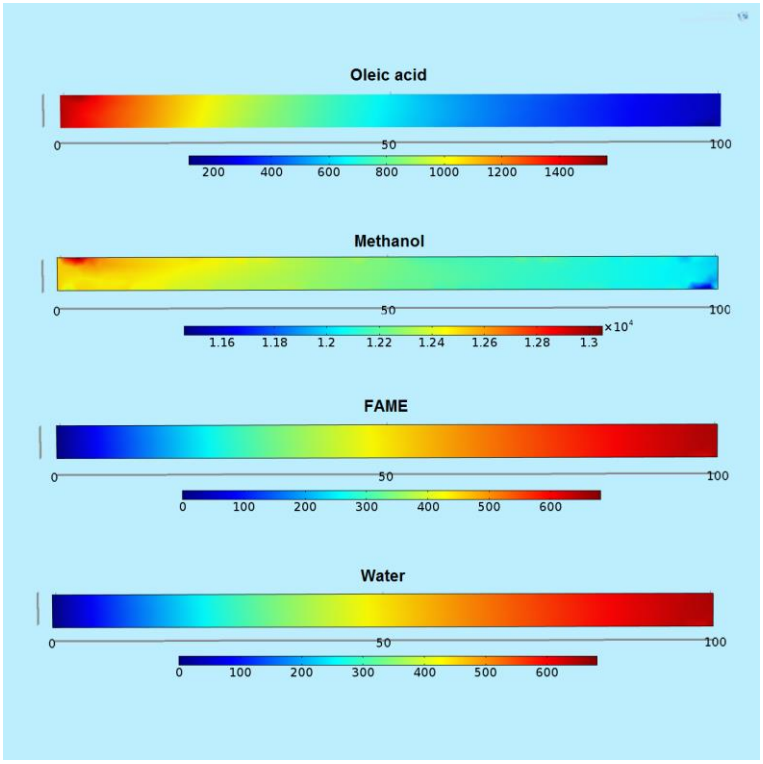

Figure 4.7 Concentration profiles of Oleic acid, Methanol, FAME and Water at temperature = 60 °C.

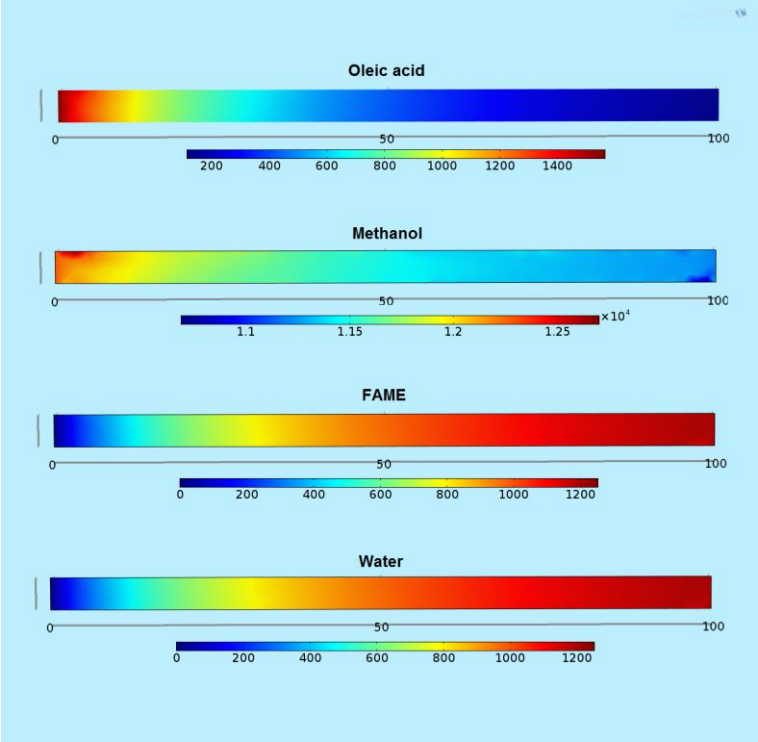

Figure 4.8 Concentration profiles of Oleic acid, Methanol, FAME and Water at temperature = 80 °C.

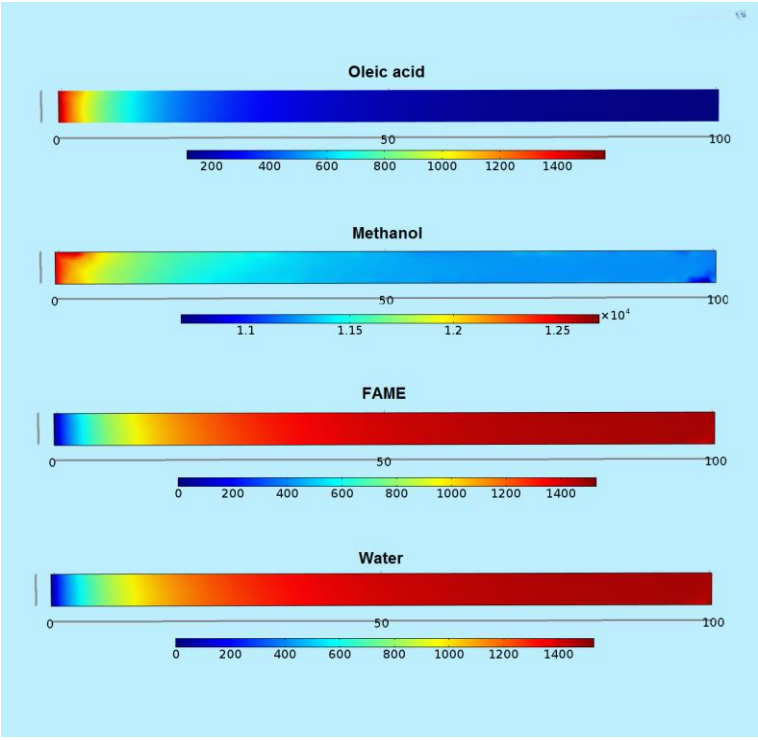

Figure 4.9 Concentration profiles of Oleic acid, Methanol, FAME and Water at temperature = 100 °C.

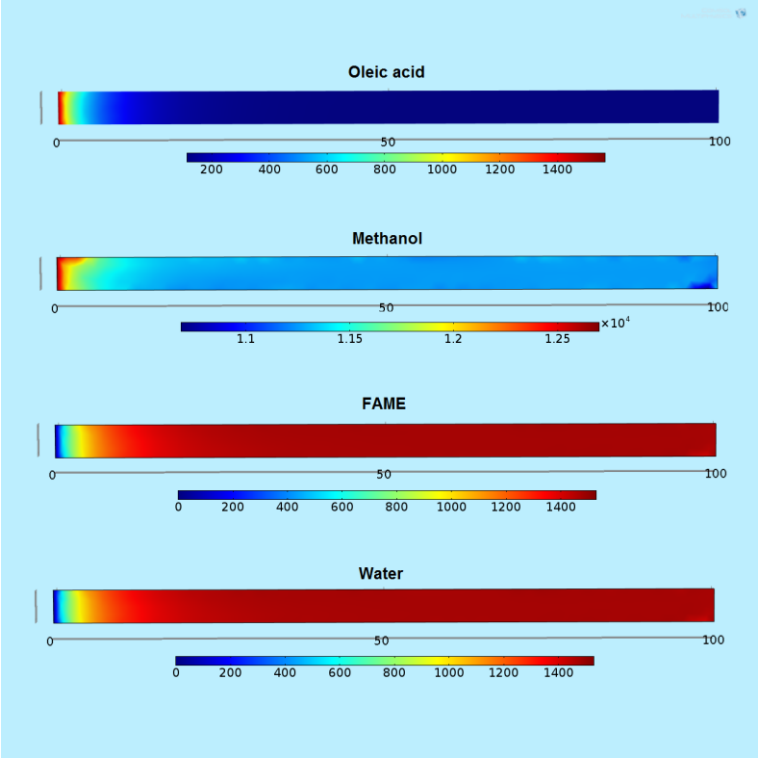

Figure 4.10 Concentration profiles of Oleic acid, Methanol, FAME and Water at temperature = 120 °C.

4.2.3 Effect of Methanol: Oleic acid molar ratio

Fig 4.11 shows the effect of methanol/oleic acid molar ratio on the conversion of oleic acid, while Figs 4.12-4.15 present the profiles of reactants and products along the reactor at different methanol/oleic acid molar ratios. It can be seen that the conversion increased with increasing mole ratio. When methanol concentration increased, the equilibrium of the esterification reaction shifted towards the side of the products i.e. FAME and water, resulting in higher conversion of oleic acid to FAME. Furthermore, by increasing the methanol to molar ratio, an excess of methanol could speed up the reaction and thus the viscosity of the reacting mixture decreased. This in turn promoted better mixing between reactants and catalyst as well as enhanced the mass transfer rate leading to a higher conversion**.**

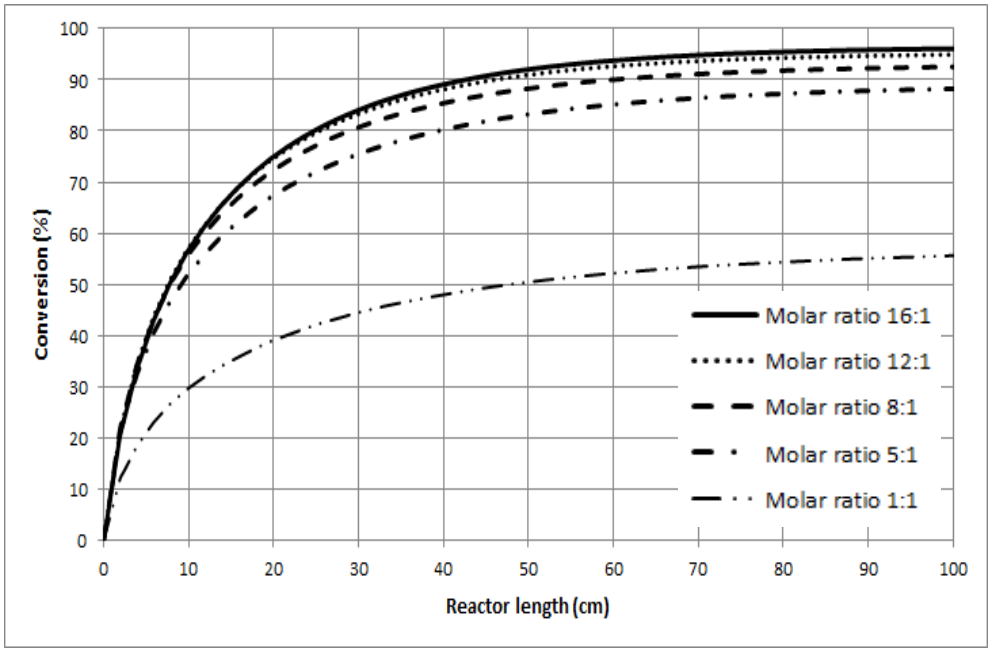

Figure 4.11 Conversion of oleic acid versus reactor length at different molar ratios. (Simulated conditions: at temperature = 100°C and flow rate = 1 L/h)

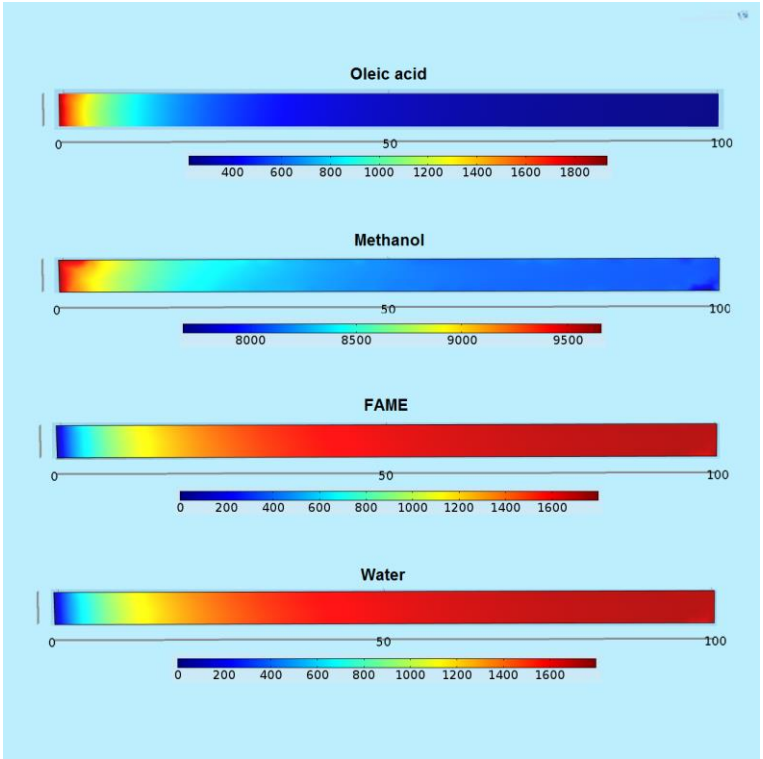

Figure 4.12 Concentration profiles of Oleic acid, Methanol, FAME and Water at MeOH: Oleic acid ratio = 5:1.

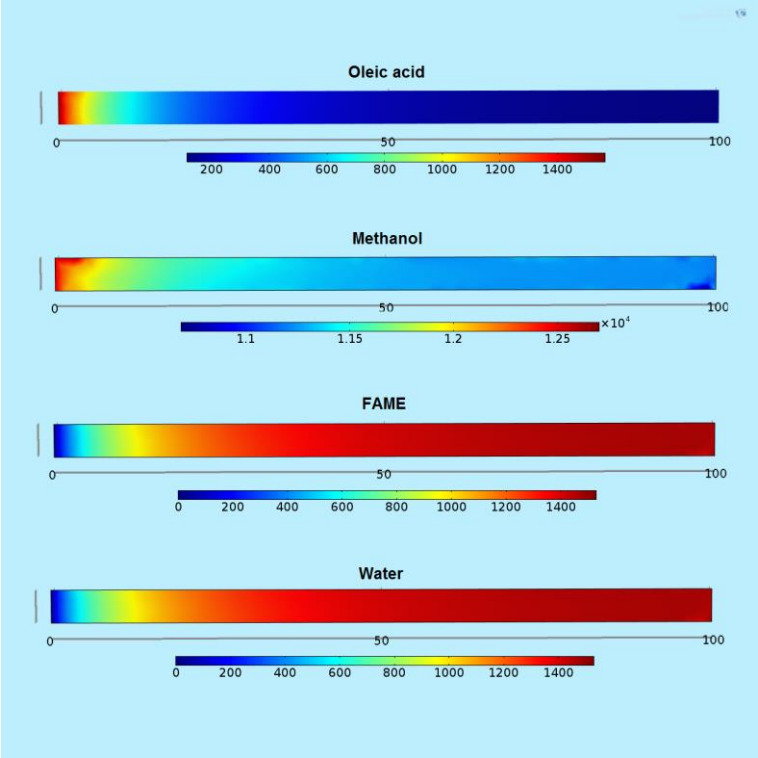

Figure 4.13 Concentration profiles of Oleic acid, Methanol, FAME and Water at MeOH: Oleic acid ratio = 8:1.

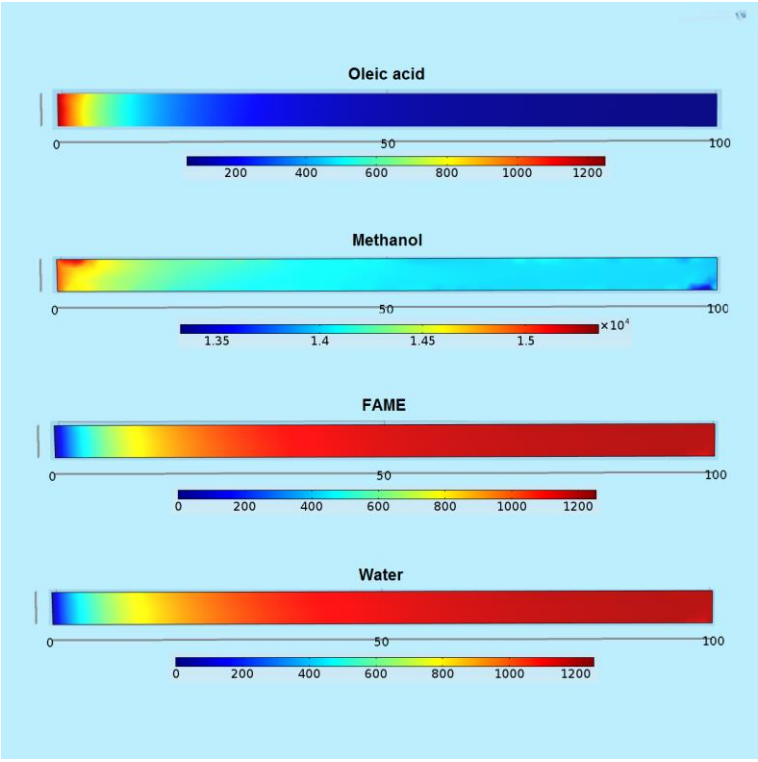

Figure 4.14 Concentration profiles of Oleic acid, Methanol, FAME and Water at MeOH: Oleic acid ratio = 12:1.

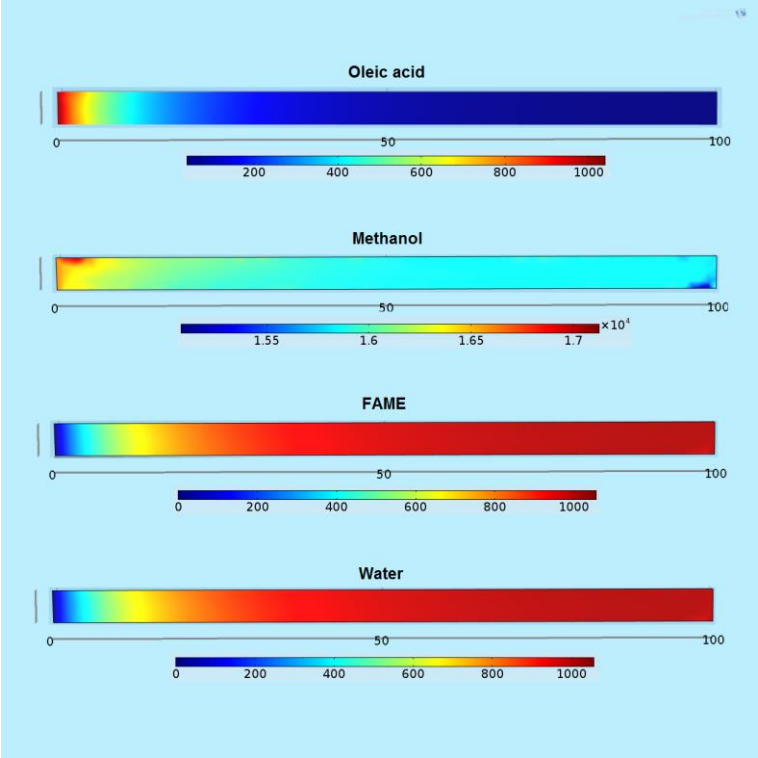

Figure 4.15 Concentration profiles of Oleic acid, Methanol, FAME and Water at MeOH: Oleic acid ratio = 16:1.

4.2.4 Effect of flow rate

Figure 4.16 demonstrates that the feed flow rate directly affected the conversion of oleic acid, while Figs 4.17-4.20 present the profiles of reactants and products along the reactor at different feed flow rates. When decreasing of feed flow rate, the conversion of oleic acid increased and reached lower steady state rate at the end of the reactor. Especially at the lowest flow rate of 1 L/h, the conversion of oleic acid rapidly increased since the contact time of the reactants inside the reactor is much longer. This implied that the oleic acid could react with methanol longer or oleic acid could be higher adsorbed on the specified catalyst surface due to the longer residence time in the reactor, resulting in higher conversion. However, when flow through 100 cm of reactor length, the conversion of oleic acid was reached to constant according to the lower amount of oleic acid. The other case, 2, 3 and 4 L/h showed the same relationship between feed flow rate and conversion of oleic acid, also taking the fact that the longer residence time in reactor or the lower feed flow rate to reactor could obtain the higher conversion.

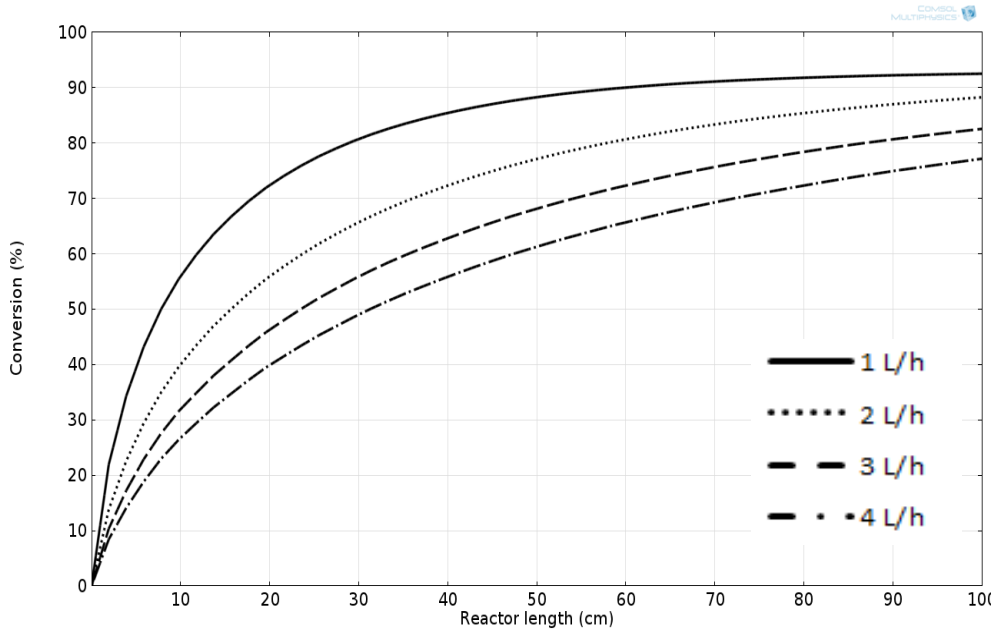

Figure 4.16 Conversion of oleic acid versus reactor length at different feed flow rates. (Simulated conditions: temperature = 100°C and MeOH: Oleic acid ratio = 8:1)

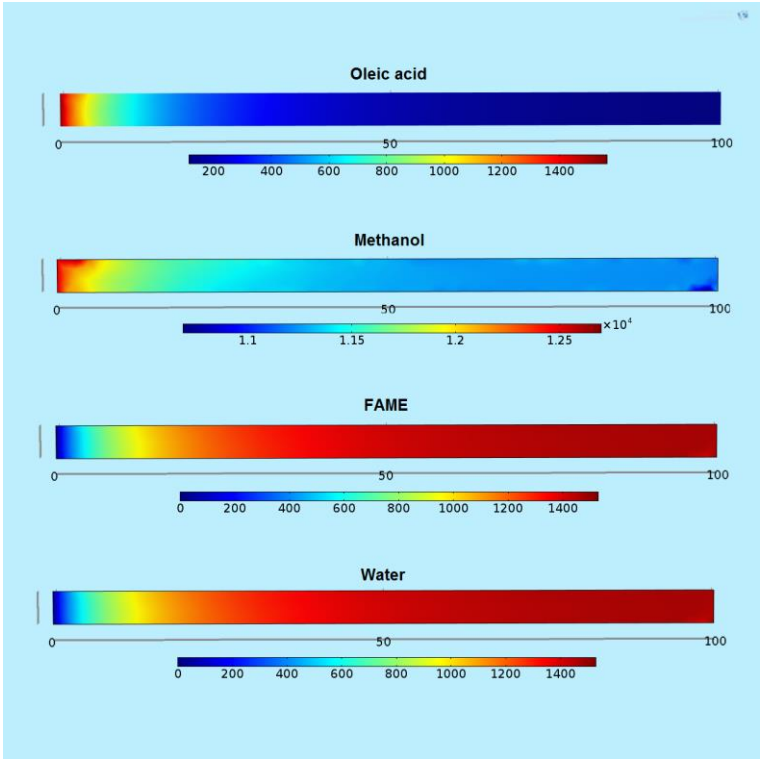

Figure 4.17 Concentration profiles of Oleic acid, Methanol, FAME and Water at flow rate = 1 L/h.

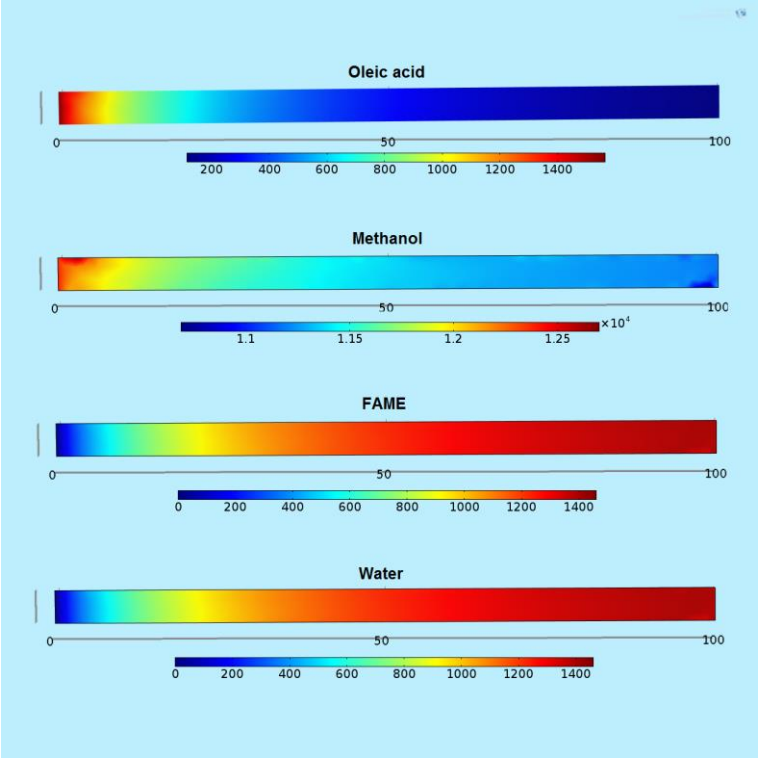

Figure 4.18 Concentration profiles of Oleic acid, Methanol, FAME and Water Water at flow rate = 2 L/h.

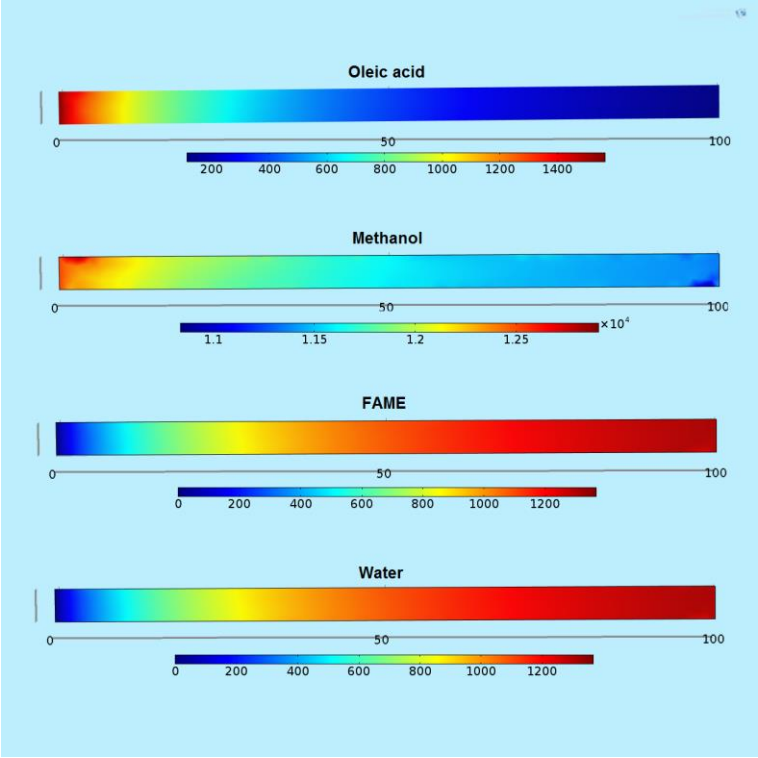

Figure 4.19 Concentration profiles of Oleic acid, Methanol, FAME and Water Water at flow rate = 3 L/h.

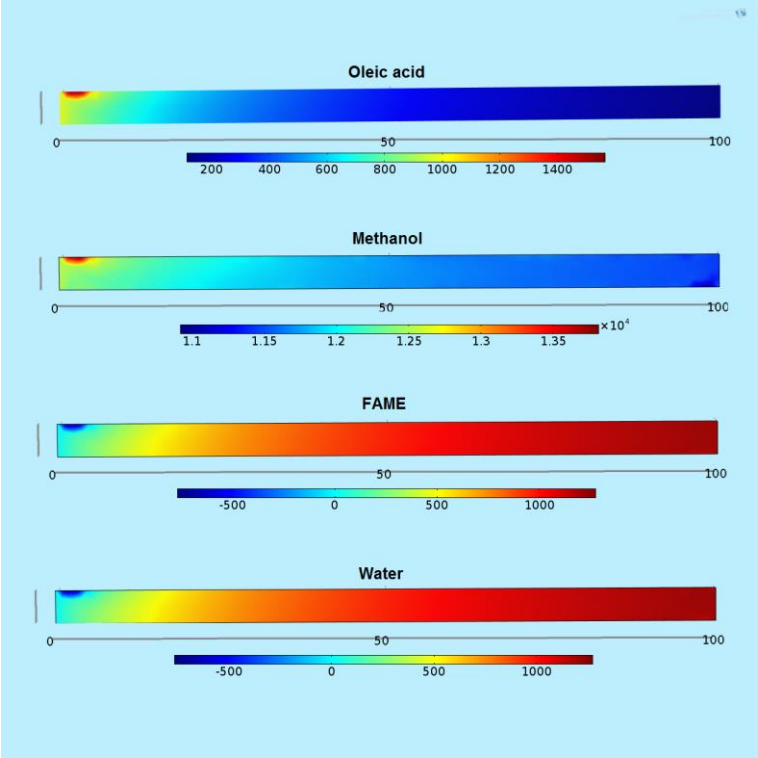

Figure 4.20 Concentration profiles of Oleic acid, Methanol, FAME and Water Water at flow rate = 4 L/h.

In summary, Table 4.3 shows the reactor length required to enhance the highest steady state conversion rate for each operating condition. To enhance the highest conversion of fatty acid, the operation conditions include the operating temperature of 100°C with methanol/fatty acid molar ratio of 16:1 and flow rate of 1 L/h.

Table 4.3 Operative conditions and simulated results of effect of temperature, molar ratio and flow rate at 10% of catalyst.

Run.	**Temp. (°C)**	**Flow rate (**L/h**)**	**Molar ratio M/O**	**Reactor Length (cm)**	**(%) conversion of oleic acid**
1	120	1	8	100	95.94
2	120	1	8	150	95.95
3	100	1	8	100	92.43
4	100	1	8	150	92.88
5	100	1	8	200	92.93
6	80	1	8	100	76.06

Table 4.3 Operative conditions and simulated results of effect of temperature, molar ratio and flow rate at 10% of catalyst (Cont').

Run.	Temp. (°C)	Flow rate (L/h)	Molar ratio M/O	Reactor Length (cm)	(%) conversion of oleic acid
7	80	1	8	150	82.03
8	80	1	8	200	84.84
9	80	1	8	250	86.17
10	80	1	8	300	86.85
11	60	1	8	100	41.95
12	60	1	8	150	50.54
13	60	1	8	200	56.66
14	60	1	8	300	64.62
15	60	1	8	500	72.53
16	60	1	8	750	76.31
17	60	1	8	1000	77.68
18	100	2	8	100	86.17
19	100	2	8	150	91.42
20	100	2	8	200	92.44
21	100	2	8	250	92.77
22	100	3	8	100	82.47
23	100	3	8	200	90.72
24	100	3	8	250	91.89
25	100	3	8	300	92.44
26	100	4	8	100	78.96
27	100	4	8	300	91.58
28	100	4	8	400	92.49
29	100	1	5	100	88.24
30	100	1	12	100	94.92
31	100	1	16	100	96.08

4.3 Integrated model of esterification in the presence of a molecular sieve

To improve the model of the continuous packed bed to be more efficient in biodiesel production, making the equilibrium of the esterification reaction shift toward the side of the products is an alternative option. The method to shift the equilibrium of the esterification reaction toward the side of product was removed water as by-product from the system. In this work, use of molecular sieve as desiccant could separate and adsorb water that was produced during operating reaction along reactor length, which molecular sieve type used was 3A that has 3Å of pore diameter. This molecular sieve 3A is highly suitable for use in this study because the molecule size of water about 2.8 Å, which was smaller than pore diameter of molecular sieve whereas molecule size of oleic acid, methanol and FAME was larger than 3 Å . Performance of the molecular sieve used to adsorb the water was presented in term of water sorption isotherm, which AL-ASHEH et al., 2004 reported isotherm equation that be showed as below;

$$X = \frac{X_m C K a_W}{[(1 - K a_W)(1 + (C - 1) K a_W)]} \qquad (4-6)$$

In this work, the investigation of the effect of a molecular sieve on the conversion of oleic acid by comparing percentage conversion obtained from the simulation model with and without a molecular sieve. Fig. 4.21 represents effect of amount of molecular sieve, it can be seen that mass of molecular sieve is not a significant factor for speed up adsorption rate of water but mass of molecular sieve must enough for adsorb water in system . Fig. 4.22, 4.27 and 4.32 show conversion of oleic acid that obtained from simulated with molecular sieve. When compared with Figs. 4.6, 4.11 and 4.16, it is clear that adding a molecular sieve along the length of a reactor can provide a higher conversion of oleic acid, for which conversion can reach to 99%. Furthermore, molecular sieve can increase conversion rate, resulting in the shortening of reactor length required to obtain the highest conversion as shown in Table 4.4. At Run.41, the result showed that conversion increased from 77.68% (Run.17) to 99% and length of reactor decreased from 1000(Run.17) cm to 700 cm. All operative conditions for simulation effect of molecular sieve are summarized in Table 4.4.

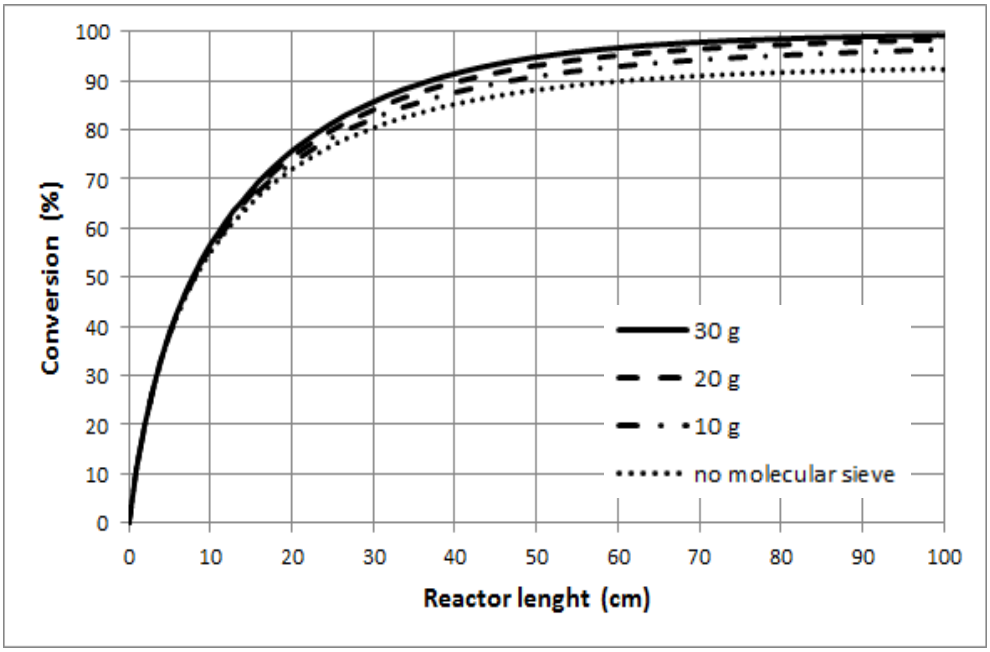

Figure 4.21 Conversion of oleic acid versus reactor length at different masses of the molecular sieve. (Simulated at temperature = 100°C, molar ratio = 8:1 and flow rate = 1 L/h).

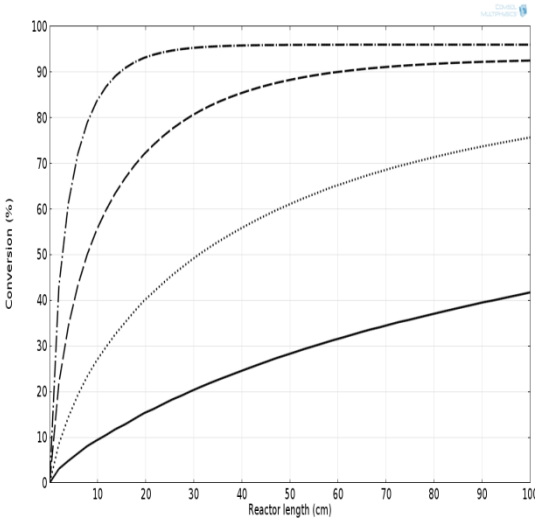

Figure 4.6 Conversion of oleic acid without a molecular sieve.

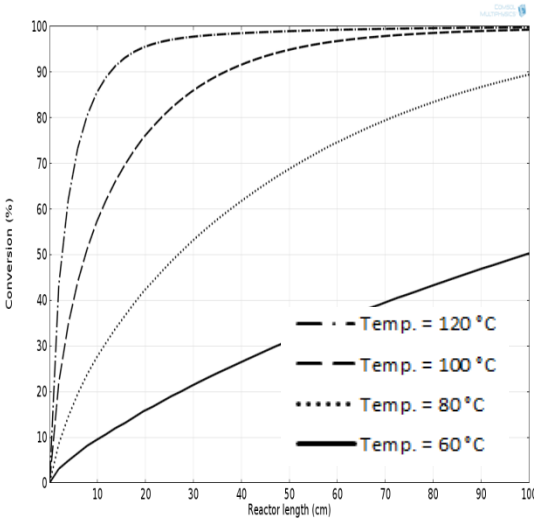

Figure 4.22 Conversion of oleic acid with a molecular sieve.

(Simulated conditions: MeOH: Oleic acid ratio = 8:1 and flow rate = 1 L/h)

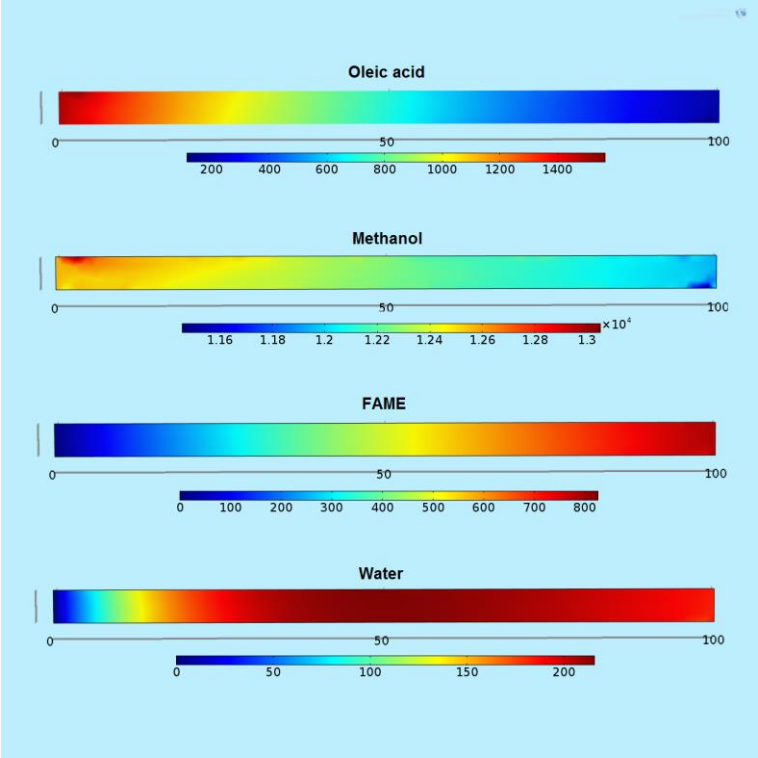

Figure 4.23 Concentration profiles of Oleic acid, Methanol, FAME and Water at temperature = 60°C. (Simulated with a molecular sieve)

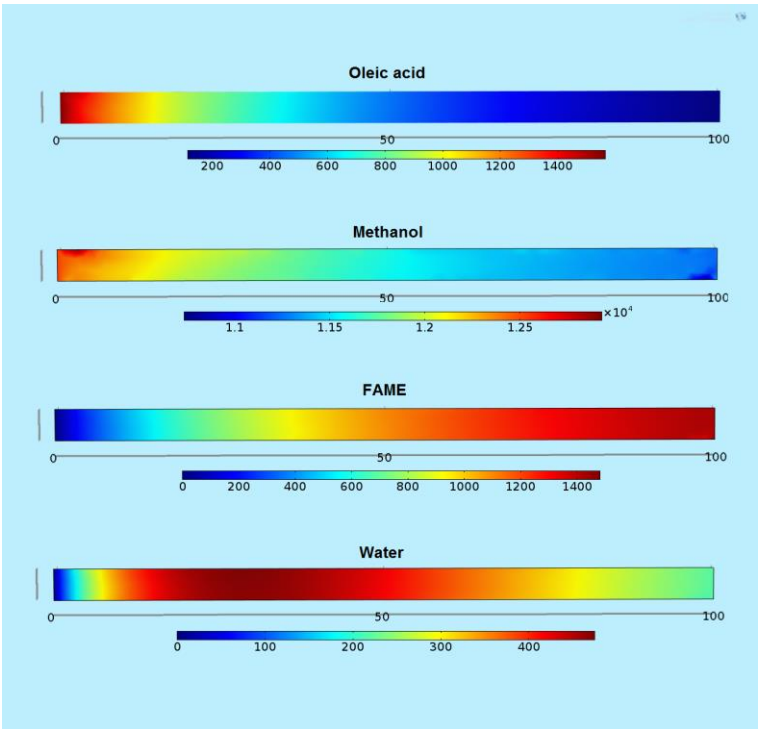

Figure 4.24 Concentration profiles of Oleic acid, Methanol, FAME and Water at temperature = 80°C. (Simulated with a molecular sieve)

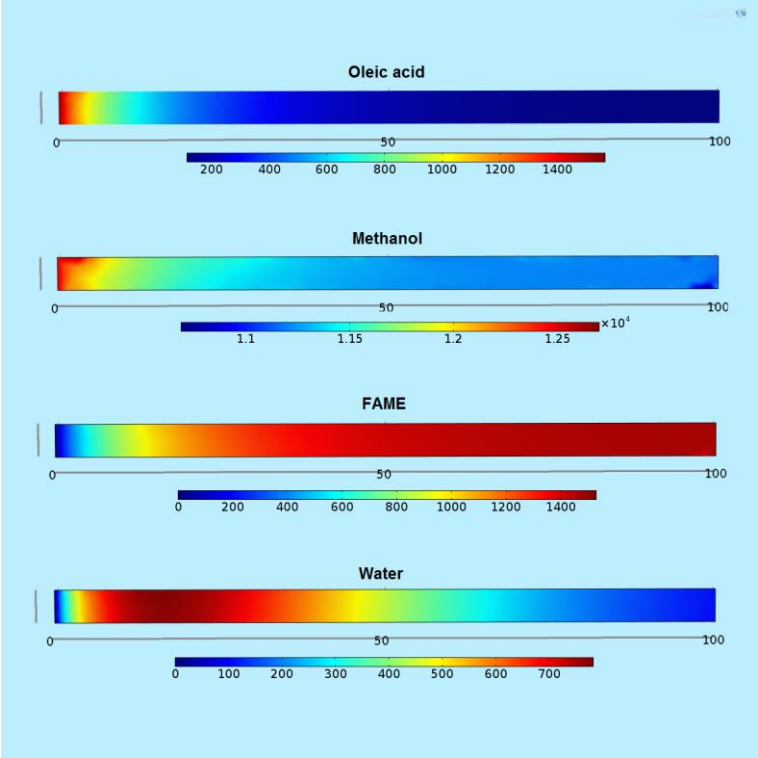

Figure 4.25 Concentration profiles of Oleic acid, Methanol, FAME and Water at temperature = 100°C. (Simulated with a molecular sieve)

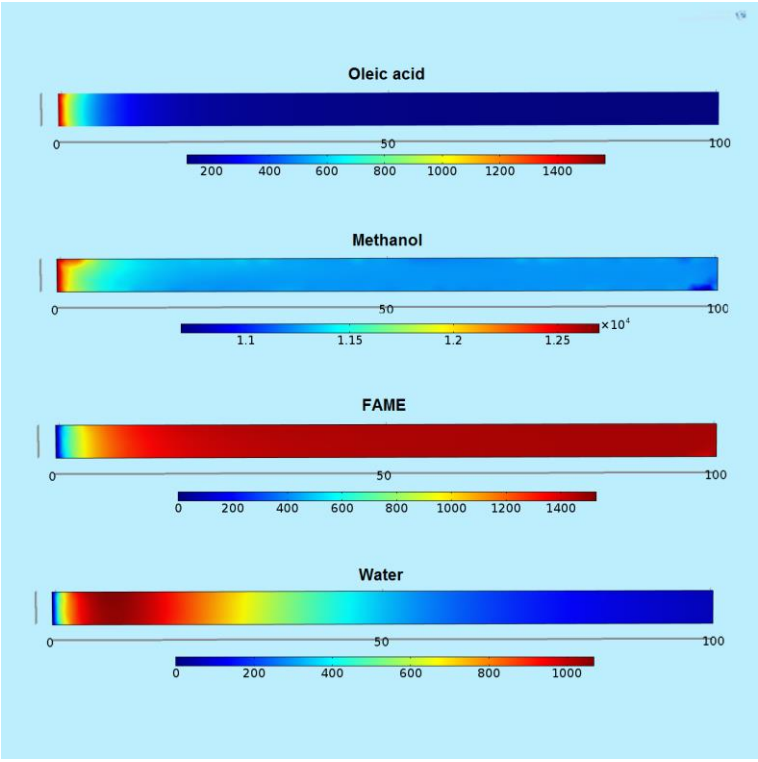

Figure 4.26 Concentration profiles of Oleic acid, Methanol, FAME and Water at temperature = 120°C. (Simulated with a molecular sieve)

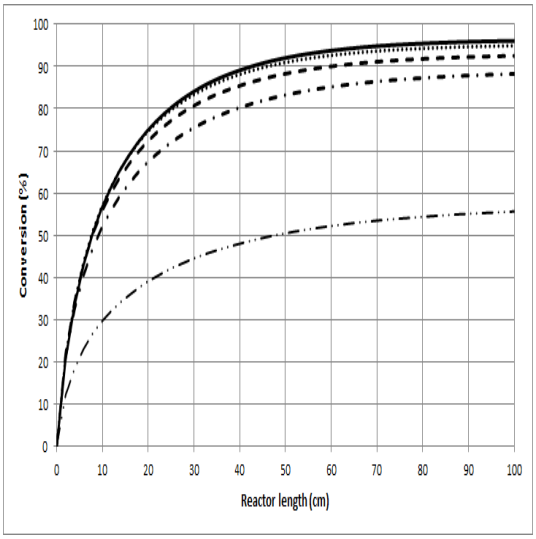

Figure 4.11 Conversion of oleic acid without a molecular sieve.

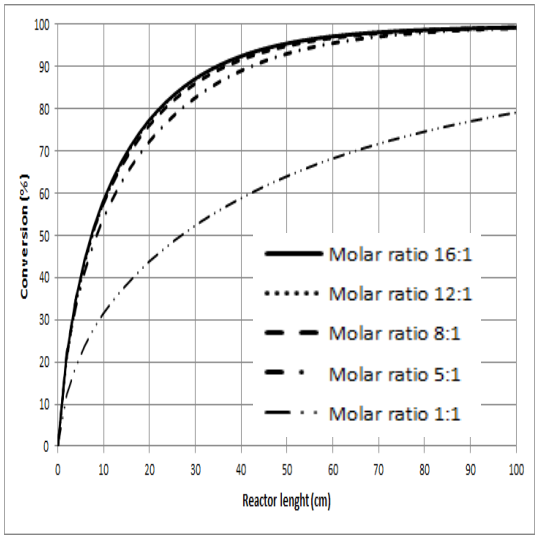

Figure 4.27 Conversion of oleic acid with a molecular sieve.

(Simulated conditions: temperature = 100 °C and flow rate = 1 L/h)

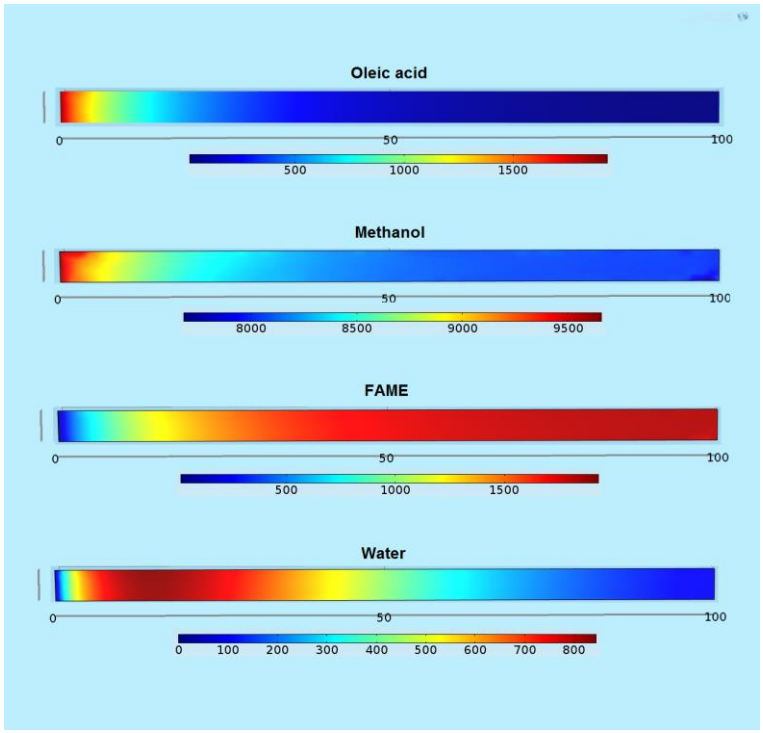

Figure 4.28 Concentration profiles of Oleic acid, Methanol, FAME and Water at MeOH: Oleic acid ratio = 5:1. (Simulated with a molecular sieve)

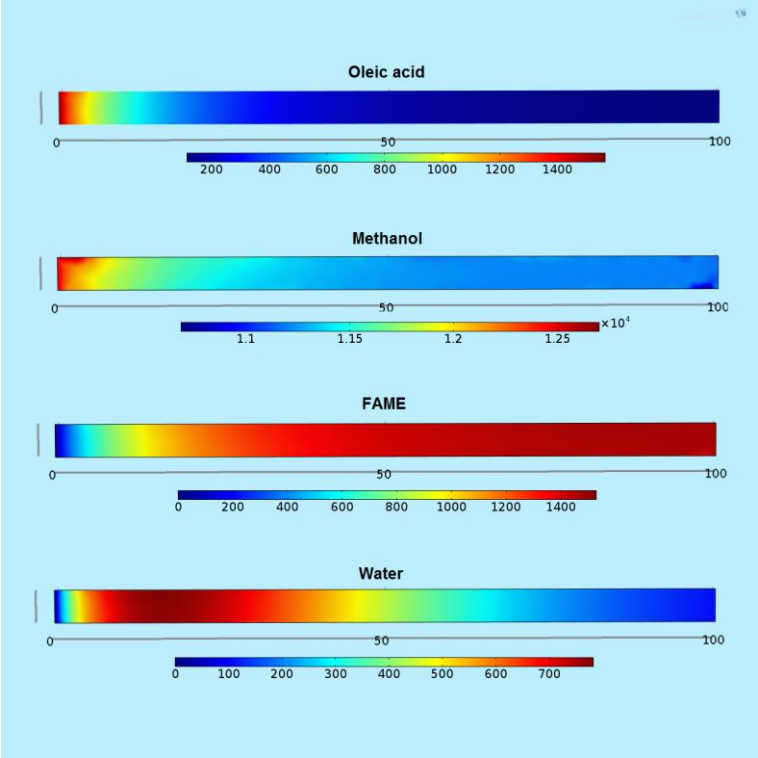

Figure 4.29 Concentration profiles of Oleic acid, Methanol, FAME and Water at MeOH: Oleic acid ratio = 8:1. (Simulated with a molecular sieve)

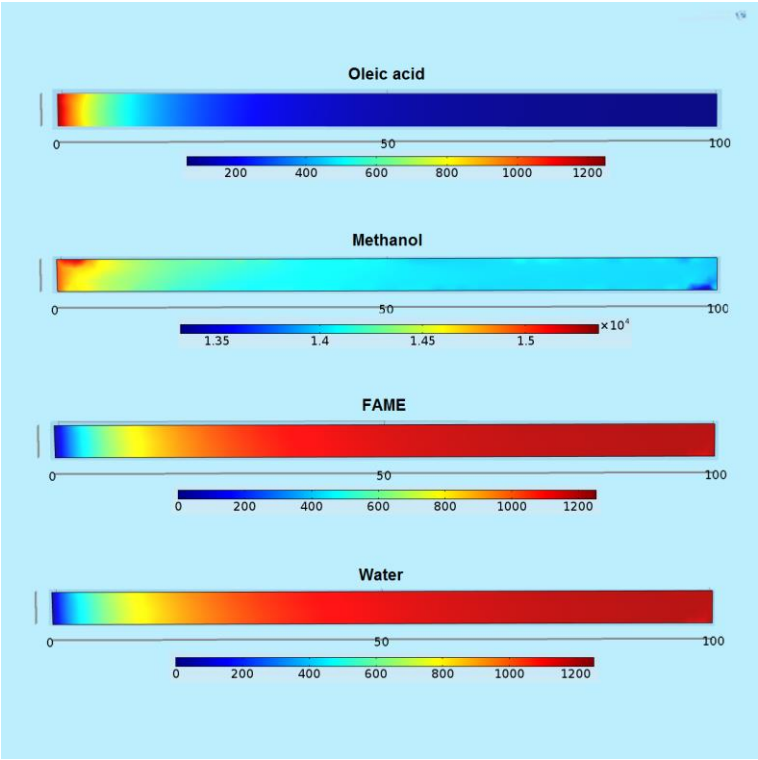

Figure 4.30 Concentration profiles of Oleic acid, Methanol, FAME and Water at MeOH: Oleic acid ratio = 12:1. (Simulated with a molecular sieve)

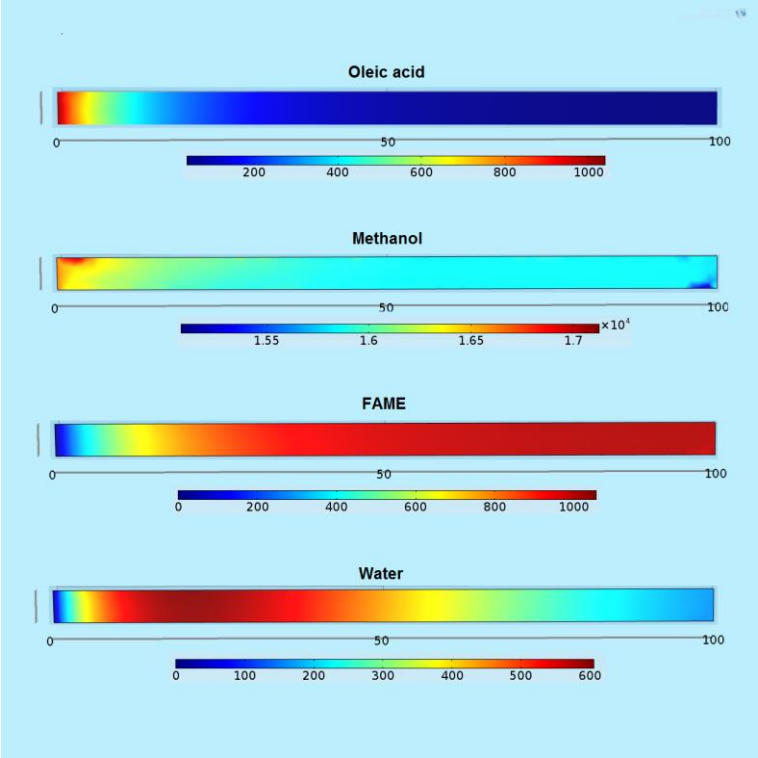

Figure 4.31 Concentration profiles of Oleic acid, Methanol, FAME and Water at MeOH: Oleic acid ratio = 16:1. (Simulated with a molecular sieve)

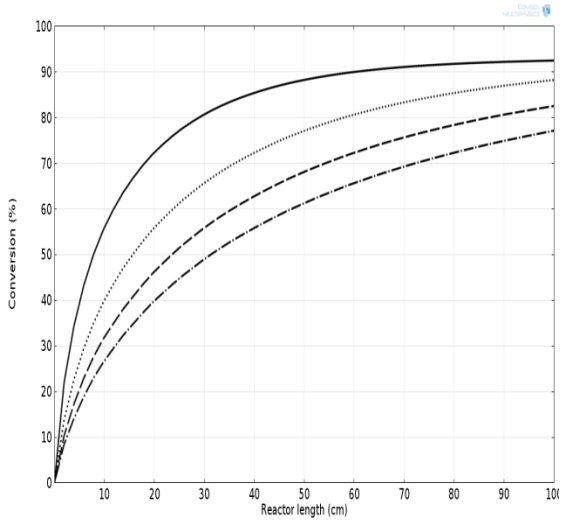

Figure 4.16 Conversion of oleic acid without a molecular sieve.

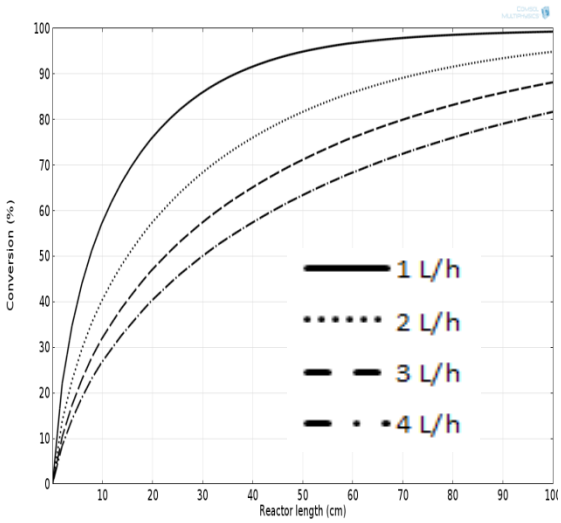

Figure 4.32 Conversion of oleic acid with a molecular sieve.

(Simulated conditions: temperature = 100 °C and MeOH: Oleic acid ratio = 8:1)

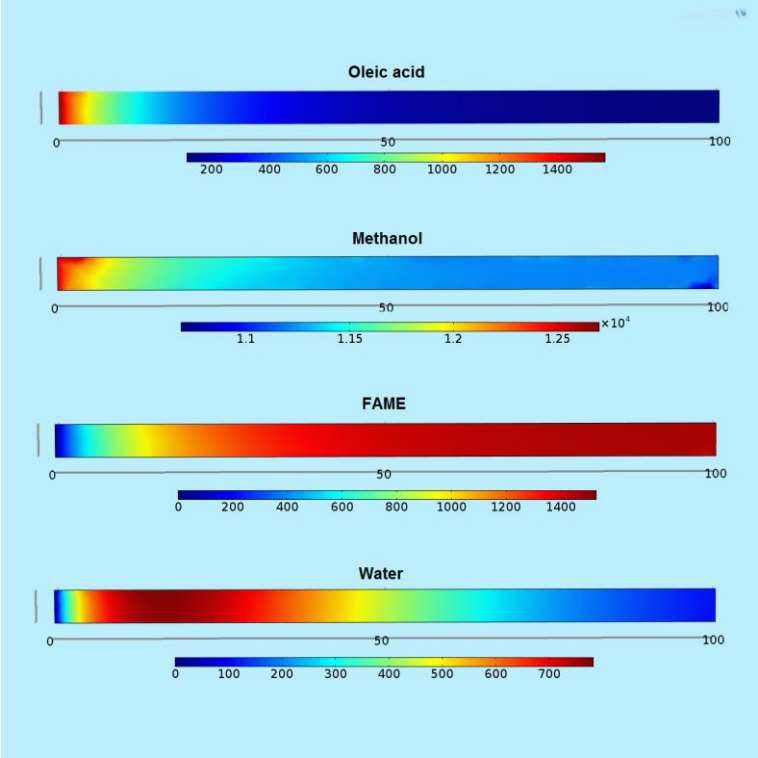

Figure 4.33 Concentration profiles of Oleic acid, Methanol, FAME and Water at flow rate = 1 L/h. (Simulated with a molecular sieve)

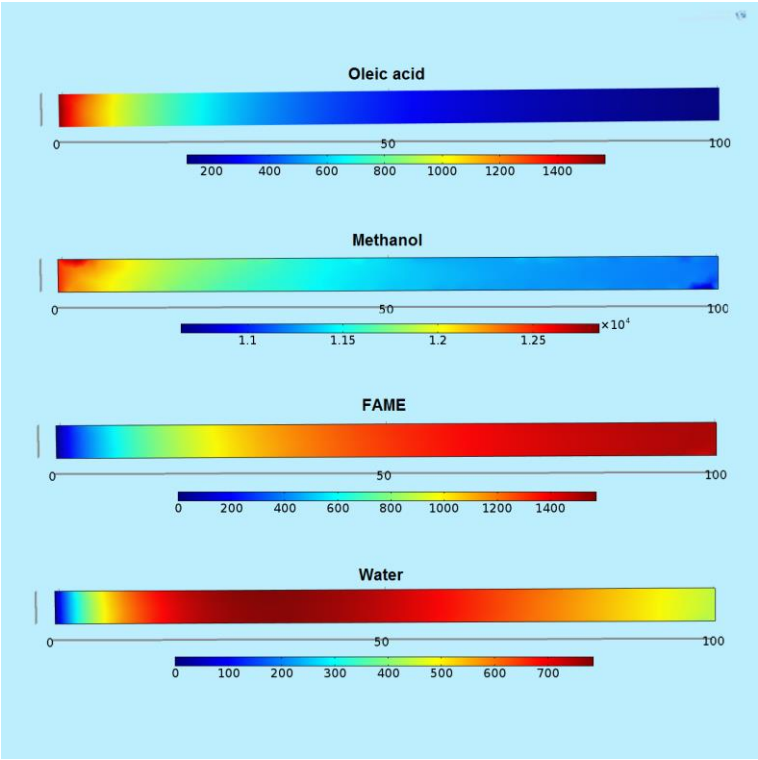

Figure 4.34 Concentration profiles of Oleic acid, Methanol, FAME and Water at flow rate = 2 L/h. (Simulated with a molecular sieve)

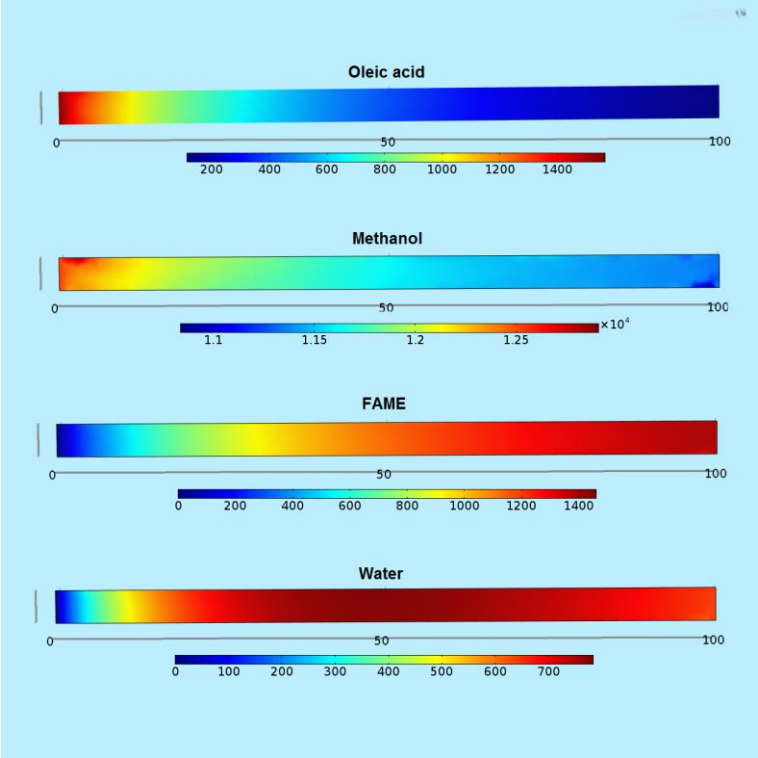

Figure 4.35 Concentration profiles of Oleic acid, Methanol, FAME and Water at flow rate = 3 L/h. (Simulated with a molecular sieve)

.

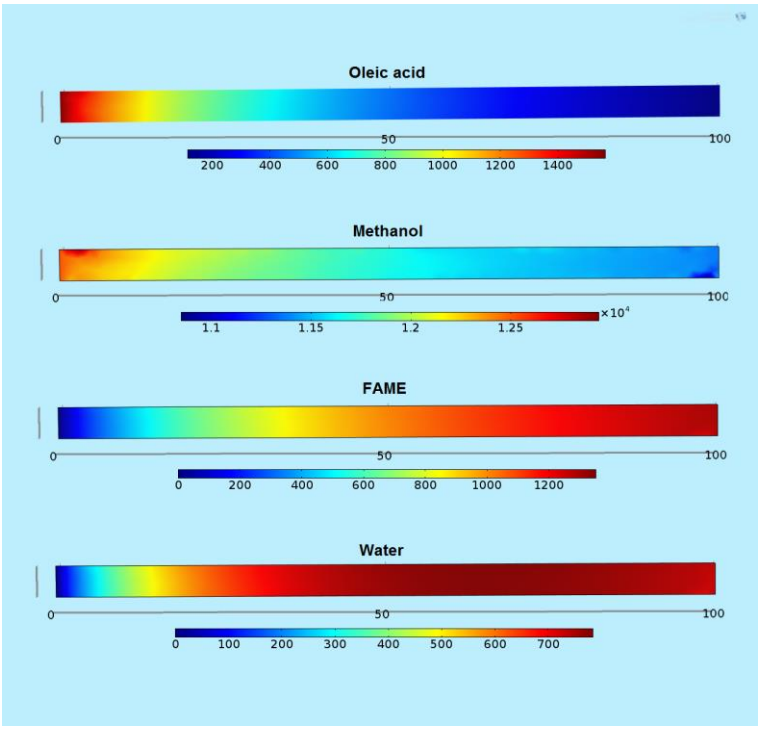

Figure 4.36 Concentration profiles of Oleic acid, Methanol, FAME and Water at flow rate = 4 L/h. (Simulated with a molecular sieve)

Table 4.4 Operative conditions and simulated results of effect of temperature, molar ratio and flow rate at 10%wt of catalyst and 30 g of molecular sieve.

Run.	Temp. (°C)	Flow rate (L/h)	Molar ratio M/O	Reactor Length (cm)	(%) conversion of oleic acid
33	**120**	**1**	**8**	**100**	**99.82**
34	**100**	**1**	**8**	**100**	**99.32**
35	80	1	8	100	90
36	80	1	8	150	97.05
37	**80**	**1**	**8**	**200**	**99.16**
38	60	1	8	100	50.68
39	60	1	8	200	75.16
40	60	1	8	500	97.48
41	**60**	**1**	**8**	**700**	**99.49**
42	**100**	**1**	**16**	**100**	**99.61**
43	**100**	**1**	**12**	**100**	**99.58**
44	**100**	**1**	**5**	**100**	**99.13**
45	100	2	8	100	95.05
46	100	2	8	150	98.32
47	**100**	**2**	**8**	**200**	**99.3**
48	100	3	8	100	88.45
49	100	3	8	200	97.63
50	**100**	**3**	**8**	**300**	**99.29**
51	100	4	8	100	82.03
52	100	4	8	200	94.97
53	100	4	8	300	98.29
54	**100**	**4**	**8**	**400**	**99.29**

From Table 4.4, the conditions that can be used in modeling a continuous packed bed to obtain percentage conversion higher than 99% were run. 33, 34, 37, 41, 42, 43, 44, 47, 50 and 54.

4.4 Optimization by response surface methodology (RSM)

To find the optimal conditions to operate a packed bed reactor, the RSM was used. The conditions that used to plot the 3D surfaces graphs are 60 – 120 °C of temperature, 1 – 5 L/h of flow rate and 1:5 – 1:17 of oleic acid/methanol molar ratio. However, the 3D surfaces can plot when it is in form of z = f(x,y) (1 independent and 2 dependent variable), for this reason, it was plotted by fixed oleic/methanol molar ratio at 1:1, 1:15, 1:9 and 1:17. For optimal conditions was being shown in case of operation with and without a molecular sieve.

4.4.1 Optimal conditions for operation without molecular sieve adding

Figures 4.37a - 4.37e show the 3D surface graphs where x-axis is the flow rate and y-axis is the temperature. From these figure, the summary of all operative conditions and results is shown in Table 4.5, which the highest conversion (98.11%) of oleic acid is corresponded with experimental that can obtained at 1:17 of molar ratio, 1 L/h of flow rate and 120 °C of temperature while optimal conditions were chosen at 2 L/h of flow rate.

Table 4.5 Operative conditions and results without a molecular sieve adding from RSM.

Run.	Molar ratio M/O	Flow rate (L/h)	Temp. (°C)	(%) conversion of oleic acid
55	1	1	60	20.01
56	1	1	75	34.18
57	1	1	90	47.54
58	1	1	105	57.30
59	1	1	120	63.71
60	1	2	60	13.28
61	1	2	75	25.89
62	1	2	90	40.29
63	1	2	105	53.25
64	1	2	120	62.54
65	1	3	60	10.00
66	1	3	75	21.13

Table 4.5 Operative conditions and results without a molecular sieve adding from RSM (Cont').

Run.	Molar ratio M/O	Flow rate (L/h)	Temp. (°C)	(%) conversion of oleic acid
67	1	3	90	35.08
68	1	3	105	49.07
69	1	3	120	60.36
70	1	4	60	8.00
71	1	4	75	17.98
72	1	4	90	31.25
73	1	4	105	45.49
74	1	4	120	57.95
75	1	5	60	6.63
76	1	5	75	15.71
77	1	5	90	28.30
78	1	5	105	42.48
79	1	5	120	55.61
80	5	1	60	37.45
81	5	1	75	61.84
82	5	1	90	81.08
83	5	1	105	89.86
84	5	1	120	93.27
85	5	2	60	25.24
86	5	2	75	47.59
87	5	2	90	70.89
88	5	2	105	86.94
89	5	2	120	93.14
90	5	3	60	19.27
91	5	3	75	39.21

Table 4.5 Operative conditions and results without a molecular sieve adding from RSM (Cont').

Run.	Molar ratio M/O	Flow rate (L/h)	Temp. (°C)	(%) conversion of oleic acid
92	5	3	90	62.70
93	5	3	105	82.41
94	5	3	120	92.37
95	5	4	60	15.62
96	5	4	75	33.61
97	5	4	90	56.41
98	5	4	105	77.83
99	5	4	120	90.93
100	5	5	60	13.13
101	5	5	75	29.54
102	5	5	90	51.46
103	5	5	105	73.63
104	5	5	120	89.07
105	9	1	60	40.71
106	9	1	75	68.18
107	9	1	90	87.76
108	9	1	105	94.37
109	9	1	120	96.37
110	9	2	60	26.80
111	9	2	75	52.02
112	9	2	90	77.42
113	9	2	105	92.34
114	9	2	120	96.33
115	9	3	60	20.12
116	9	3	75	42.50

Table 4.5 Operative conditions and results without a molecular sieve adding from RSM (Cont').

Run.	Molar ratio M/O	Flow rate (L/h)	Temp. (°C)	(%) conversion of oleic acid
117	9	3	90	68.58
118	9	3	105	88.41
119	9	3	120	95.98
120	9	4	60	16.11
121	9	4	75	36.15
122	9	4	90	61.65
123	9	4	105	84.03
124	9	4	120	95.10
125	9	5	60	13.41
126	9	5	75	31.55
127	9	5	90	56.13
128	9	5	105	79.82
129	9	5	120	93.77
130	13	1	60	40.82
131	13	1	75	70.13
132	13	1	90	90.31
133	13	1	105	96.09
134	13	1	120	97.52
135	13	2	60	26.17
136	13	2	75	52.73
137	13	2	90	79.54
138	13	2	105	94.28
139	13	2	120	97.49
140	13	3	60	19.31
141	13	3	75	42.58

Table 4.5 Operative conditions and results without a molecular sieve adding from RSM (Cont').

Run.	Molar ratio M/O	Flow rate (L/h)	Temp. (°C)	(%) conversion of oleic acid
142	13	3	90	70.19
143	13	3	105	90.46
144	13	3	120	97.23
145	13	4	60	15.27
146	13	4	75	35.87
147	13	4	90	62.82
148	13	4	105	86.05
149	13	4	120	96.50
150	13	5	60	12.58
151	13	5	75	31.06
152	13	5	90	56.95
153	13	5	105	81.72
154	13	5	120	95.31
155	17	1	60	39.79
156	17	1	75	70.38
157	17	1	90	91.45
158	17	1	105	96.99
159	17	1	120	98.11
160	17	2	60	24.87
161	17	2	75	52.04
162	17	2	90	80.05
163	17	2	105	95.16
164	17	2	120	98.09
165	17	3	60	18.07
166	17	3	75	41.51

Table 4.5 Operative conditions and results without a molecular sieve adding from RSM (Cont').

Run.	Molar ratio M/O	Flow rate (L/h)	Temp. (°C)	(%) conversion of oleic acid
167	17	3	90	70.19
168	17	3	105	91.22
169	17	3	120	97.85
170	17	4	60	14.13
171	17	4	75	34.64
172	17	4	90	62.46
173	17	4	105	86.63
174	17	4	120	97.13
175	17	5	60	11.54
176	17	5	75	29.76
177	17	5	90	56.33
178	17	5	105	82.11
179	17	5	120	95.95

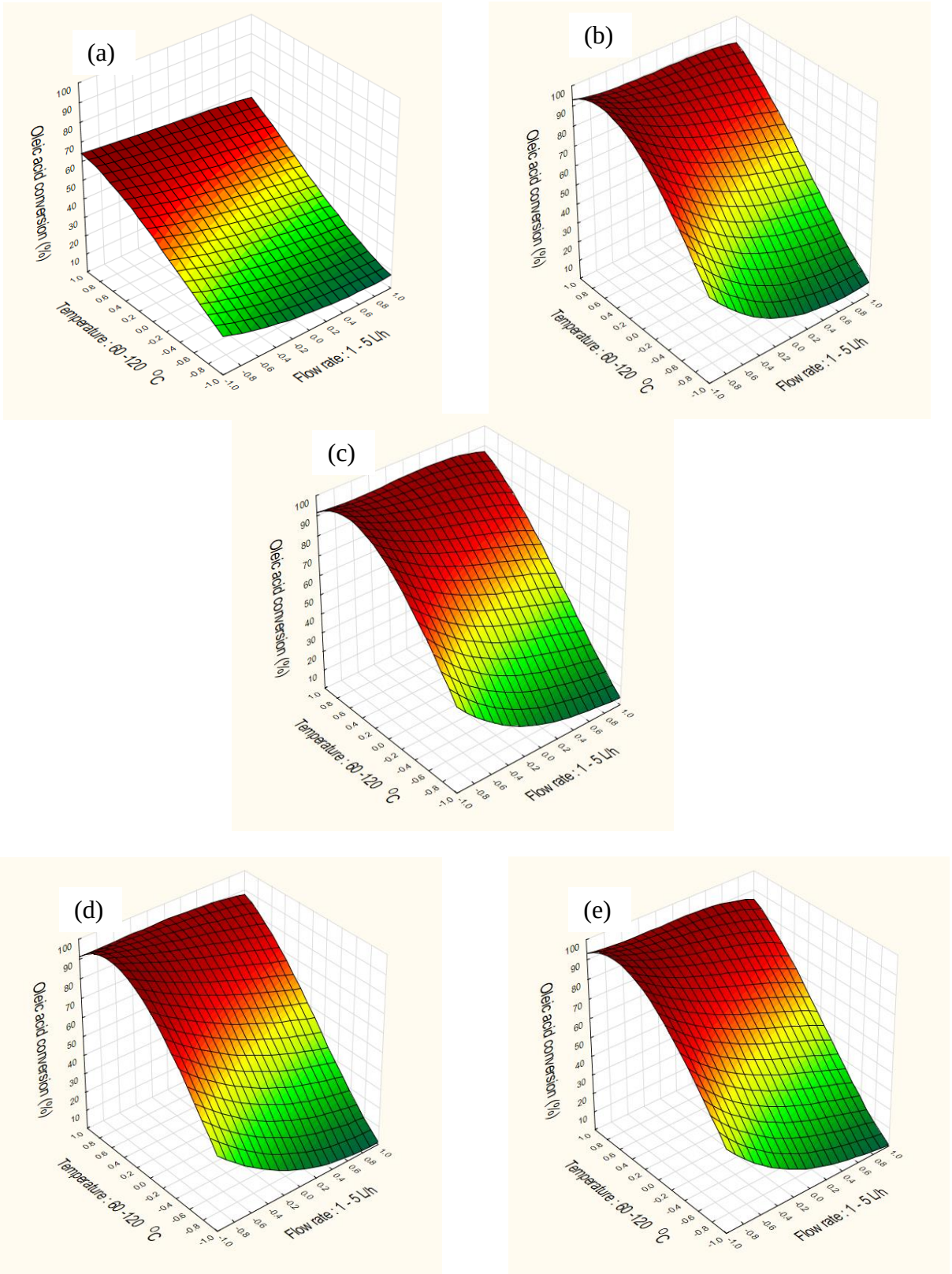

Figure 4.37 Conversion profiles of Oleic acid at different molar ratios without a molecular sieve. (a) O:M = 1:1, (b) O:M = 1:5, (c) O:M = 1:9, (d) O:M = 1:13 and (e) O:M = 1:17.

4.4.2 Optimal conditions for operation with a molecular sieve adding

Table 4.6 shows all the operative conditions and results summarized from Figures 4.38a – 4.34e, which the highest conversion (99.81%) of oleic acid can obtain at 1:17 of molar ratio, 1 L/h of flow rate and 120 ℃ of temperature. For optimal condition was optimized to 1:5 of molar ratio and 100 ℃ of temperature, which the next study will use this condition to simulate model of continuous biodiesel production that using waste cooking oil as reactants.

Table 4.6 Operative conditions and results with a molecular sieve from RSM.

Run.	Molar ratio M/O	Flow rate (L/h)	Temp. (°C)	(%) conversion of oleic acid
180	1	1	60	28.25
181	1	1	75	50.21
182	1	1	90	69.49
183	1	1	105	82.05
184	1	1	120	88.98
185	1	2	60	16.25
186	1	2	75	33.05
187	1	2	90	51.92
188	1	2	105	67.98
189	1	2	120	78.80
190	1	3	60	11.46
191	1	3	75	25.13
192	1	3	90	42.27
193	1	3	105	58.87
194	1	3	120	71.64
195	1	4	60	8.84
196	1	4	75	20.52
197	1	4	90	36.15
198	1	4	105	52.56

Table 4.6 Operative conditions and results with a molecular sieve from RSM (Cont').

Run.	Molar ratio M/O	Flow rate (L/h)	Temp. (°C)	(%) conversion of oleic acid
199	1	4	120	66.38
200	1	5	60	7.17
201	1	5	75	17.45
202	1	5	90	31.88
203	1	5	105	47.87
204	1	5	120	62.24
205	5	1	60	48.39
206	5	1	75	79.65
207	5	1	90	96.60
208	5	1	105	99.44
209	5	1	120	99.81
210	5	2	60	29.12
211	5	2	75	56.16
212	5	2	90	82.16
213	5	2	105	95.66
214	5	2	120	98.57
215	5	3	60	21.15
216	5	3	75	44.07
217	5	3	90	70.31
218	5	3	105	89.81
219	5	3	120	97.02
220	5	4	60	16.70
221	5	4	75	36.71
222	5	4	90	61.83
223	5	4	105	83.91
224	5	4	120	95.17

Table 4.6 Operative conditions and results with a molecular sieve from RSM (Cont').

Run.	Molar ratio M/O	Flow rate (L/h)	Temp. (°C)	(%) conversion of oleic acid
225	5	5	60	13.82
226	5	5	75	31.68
227	5	5	90	55.51
228	5	5	105	78.64
229	5	5	120	92.98
230	9	1	60	44.17
231	9	1	75	78.46
232	9	1	90	97.01
233	9	1	105	99.45
234	9	1	120	99.74
235	9	2	60	26.11
236	9	2	75	55.54
237	9	2	90	84.64
238	9	2	105	97.57
239	9	2	120	98.99
240	9	3	60	18.59
241	9	3	75	43.35
242	9	3	90	73.35
243	9	3	105	92.95
244	9	3	120	98.18
245	9	4	60	14.40
246	9	4	75	35.74
247	9	4	90	64.69
248	9	4	105	88.87
249	9	4	120	97.21
250	9	5	60	11.70

Table 4.6 Operative conditions and results with a molecular sieve from RSM (Cont').

Run.	Molar ratio M/O	Flow rate (L/h)	Temp. (°C)	(%) conversion of oleic acid
251	9	5	75	30.48
252	9	5	90	57.97
253	9	5	105	83.23
254	9	5	120	95.85
255	13	1	60	46.77
256	13	1	75	80.33
257	13	1	90	97.35
258	13	1	105	99.48
259	13	1	120	99.76
260	13	2	60	27.98
261	13	2	75	57.39
262	13	2	90	85.40
263	13	2	105	97.50
264	13	2	120	99.13
265	13	3	60	20.11
266	13	3	75	45.10
267	13	3	90	74.28
268	13	3	105	93.66
269	13	3	120	98.57
270	13	4	60	15.70
271	13	4	75	37.41
272	13	4	90	65.74
273	13	4	105	88.94
274	13	4	120	97.82
275	13	5	60	12.84
276	13	5	75	32.09

Table 4.6 Operative conditions and results with a molecular sieve from RSM (Cont').

Run.	Molar ratio M/O	Flow rate (L/h)	Temp. (°C)	(%) conversion of oleic acid
277	13	5	90	59.12
278	13	5	105	84.23
279	13	5	120	96.67
280	17	1	60	48.89
281	17	1	75	81.46
282	17	1	90	97.46
283	17	1	105	99.51
284	17	1	120	99.79
285	17	2	60	29.49
286	17	2	75	58.35
287	17	2	90	85.28
288	17	2	105	97.15
289	17	2	120	99.21
290	17	3	60	21.37
291	17	3	75	46.02
292	17	3	90	74.07
293	17	3	105	93.68
294	17	3	120	98.77
295	17	4	60	16.80
296	17	4	75	38.35
297	17	4	90	65.60
298	17	4	105	88.02
299	17	4	120	98.08
300	17	5	60	13.84
301	17	5	75	33.05
302	17	5	90	59.09

Table 4.6 Operative conditions and results with a molecular sieve from RSM (Cont').

Run.	**Molar ratio M/O**	**Flow rate (L/h)**	**Temp. (°C)**	**(%) conversion of oleic acid**
303	17	5	105	84.06
304	17	5	120	96.95

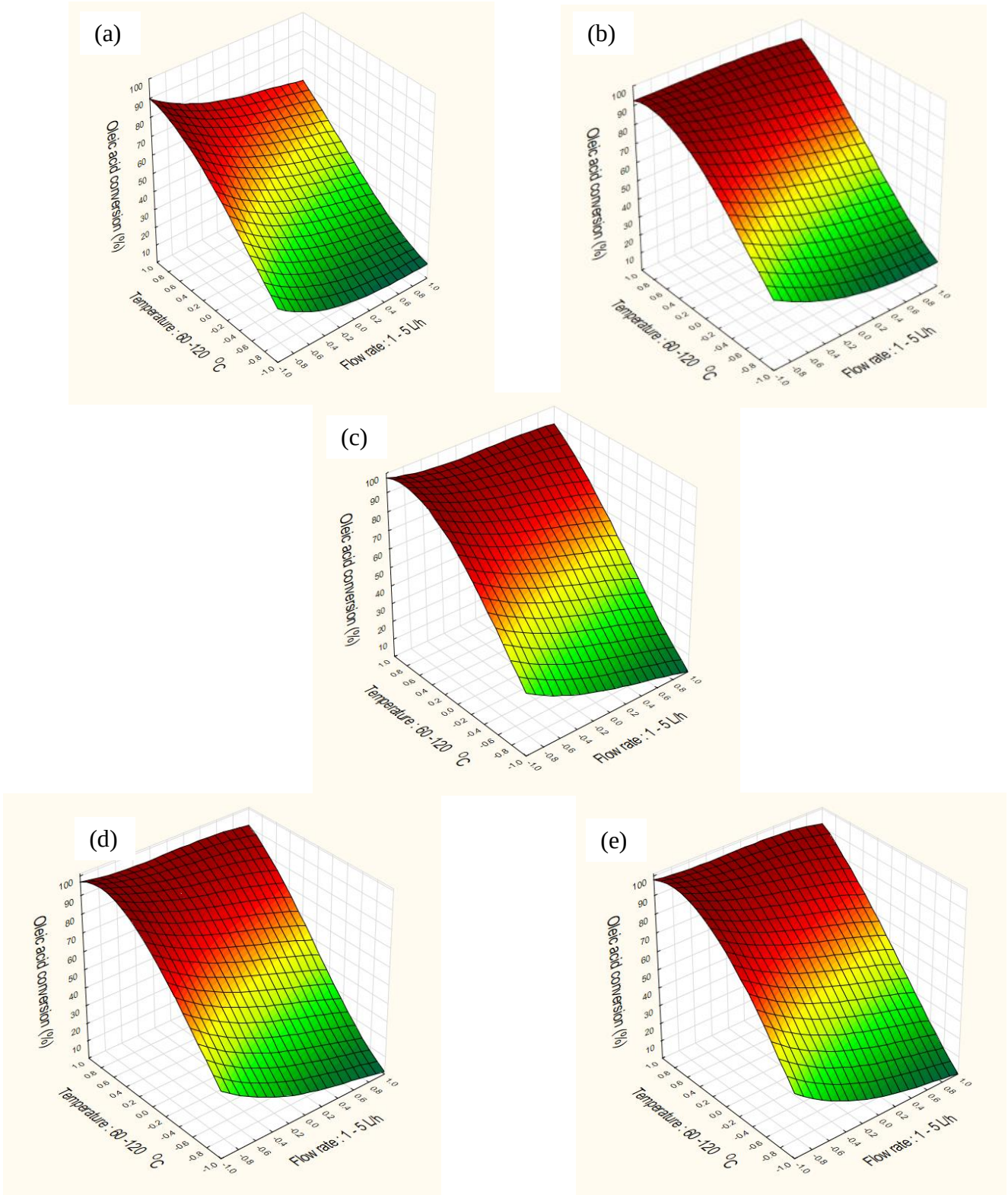

Figure 4.38 Conversion profiles of Oleic acid at different molar ratios with a molecular sieve. (a) O:M = 1:1, (b) O:M = 1:5, (c) O:M = 1:9, (d) O:M = 1:13 and (e) O:M = 1:17.

4.5 Applying the model for converting waste cooking oil to FAME

Lastly, the simulation under selected operating conditions was applied to convert waste cooking oil to biodiesel. In detail, the percentage weight composition of fatty acid (determined by GLC analysis) in waste cooking oil include oleic acid (43.46%), palmitic acid (31.3%), linoleic acid (15.40), stearic acid (3.49%), Lauric acid (2.51), myristic acid (1.43), linolenic acid (1.22%) and other (1.19%). The operate conditions were 10%wt of catalyst weight, 100 °C, 5:1 of methanol/oleic acid molar ratio and 1 L/h of feed flow rate. Figure 4.39 shows that the conversion of fatty acid was 98%, which is applicable in the real application.

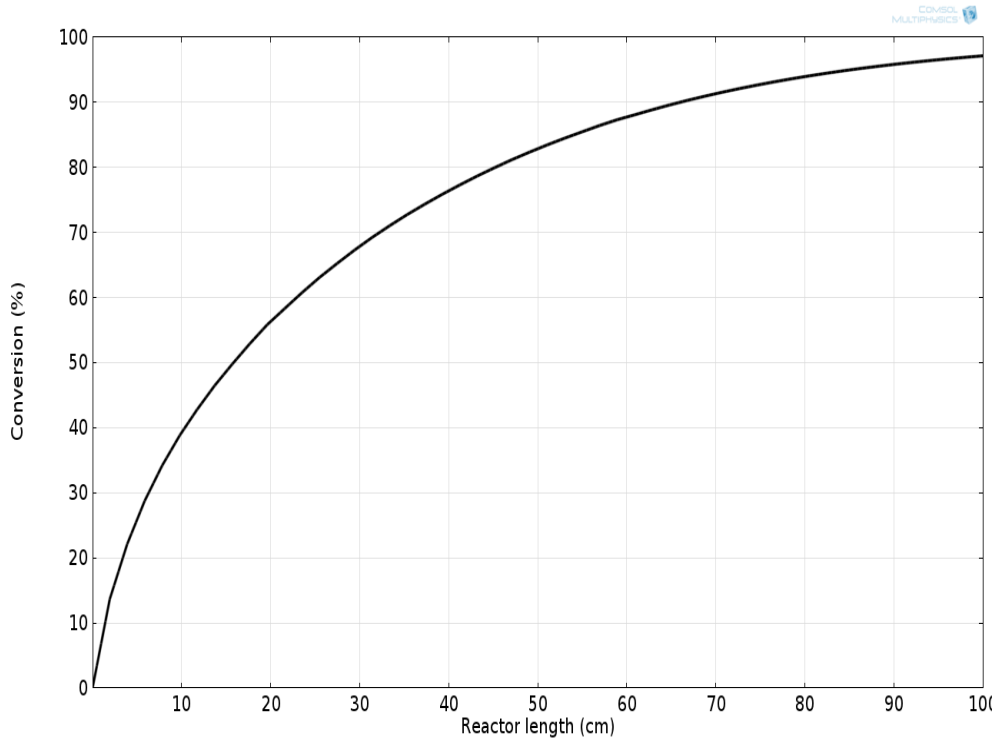

Figure 4.39a Conversion of fatty acid along reactor length

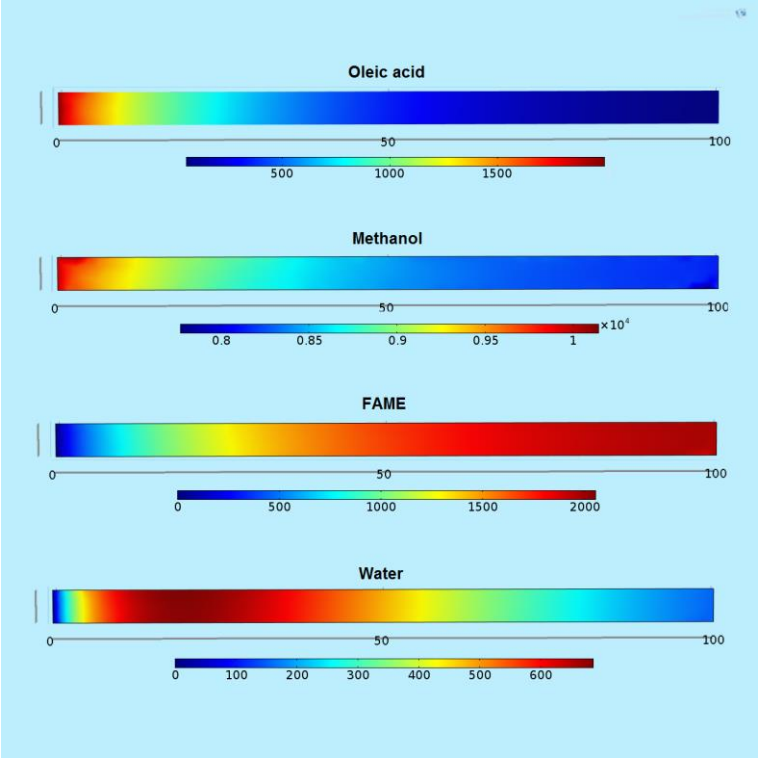

Figure 4.39b Concentration profiles of Oleic acid, Methanol, FAME and Water along reactor length

CHAPTER 5

CONCLUSION AND RECOMMENDATIONS FOR FUTURE WORK

5.1 Conclusion

In this present work, a three dimensional model of continuous biodiesel production (the internal diameter and length of reactor were 2.5 cm and 100 cm) by esterification of oleic acid and methanol in presence of Amberlyst 15 as solid acid catalyst was developed based on isothermal process and no pressure drop along reactor length. The simulation results of effects of amount of catalyst base on oleic acid weight showed that with increasing of catalyst weight from 1%wt to 50%wt can increase the conversion of oleic acid, which conversion reached to constant at 10%wt. For the effect of temperature and effects of methanol/oleic molar ratio, the simulation results showed that conversion of oleic acid increased with increment of temperature and methanol/oleic acid molar ratio, while the simulation results of effects of feed flow rate indicated that the conversion increased with decreasing of flow rate. Therefore, we concluded here that the highest conversion of oleic acid can be obtained by using 10%wt of catalyst, 120 °C of temperature, 16:1 of methanol/oleic acid molar ratio and 1 L/h of feed flow rate.

Then, continuous biodiesel production model was improved to obtain the conversion more than 99% by adding of molecular sieve along reactor length. The simulation results suggested that molecular sieve can increase conversion of oleic acid and speed up conversion rate. Therefore, the above results could be optimized to 100 °C with methanol/oleic acid molar ratio of 5:1, which was chose as an optimal condition. Finally, the optimal conditions were applied to simulate continuous biodiesel production by using waste cooking oil. The simulation results showed that the conversion of fatty acid close to the conversion of oleic acid.

5.2 Recommendations

For a future study, the model of continuous biodiesel production should be developed into a multi-configuration. Thus is useful when a molecular sieve absorbs water

at full capacity which required shutting down the process for regenerating the molecular sieve. It can switch feed to other configurations.

REFERENCES

[1] Demirbas, A. 2002, "Biodiesel from vegetable oils via transesterification in supercritical methanol", **Energy Convers Manage**, 43, 2349 -2356.

[2] Jitputti, J., B. Kitiyanan, P. Rangsunvigit, K. Bunyakiat, L. Attanatho and P. Jenvanitpanjakul.,2005, "Transesterification of crude palm kernel oil and crude coconut oil by different solid catalysts",**Chemical Engineering Journal**, 116, 61-66.

[3] Kandpal, J.B. and M. Madan, 1994, "Jatropha curcas a renewable source of energy for meeting future energy needs", **Technical Note**, 6, 159-160.

[4] Ma, F., L.D. Clements and M.A. Hanna.,1998,"The effect of catalyst, free fatty acids, and water on transesterification of beef tallow", **Transactions of the American Society of Agricultural Engineers**, 41(5),1261-1264.

[5] Ma, F., L.D. Clements and M.A. Hanna. 1999 "The effect of mixing on transesterification of beef tallow", **Bioresource Technology**, 69,289-293.

[6] Madras, G., C. Kolluru and R. Kumar. 2004," Synthesis of biodiesel in supercritical fluids", **Fuel**, 83, 2029-2033.

[7] Marchetti, J.M., V.U. Miguel and A.F. Errazu, 2005, "Possible methods for biodiesel production", **Renewable and Sustainable Energy Reviews**. 20, 280-28

[8] Meher, L.C., D. Sagar and S.N. Naik, 2004, "Technical aspects of biodiesel production by Transesterification-a review", Renewable **and Sustainable Energy Reviews**, 10,1-21.

[9] Ramadhas, A.S., S. Jayaraj and C. Muraleeharan, 2005, "Biodiesel production from high FFA rubber seed oil", **Fue,**.84, 335-340.

[10] Srivastava, A. and R. Prasad, 1999, "Triglycerides based diesel fuels", **Renewable and Sustainable Energy Review**, 4, 111-133.

[11] GAN Mengyu, PAN Deng, MA Li**,** 2009, "The Kinetics of the Esterification of Free Fatty Acids in Waste Cooking Oil Using Fe2(SO4)3/C Catalyst" , ***Chinese Journal of Chemical Engineering*****, 17**, 83-87.

[12] Suyin Gan,Hoon Kiat Ng , Park Hinn Chan, Fook Lim Leong,2012, "Heterogeneous free fatty acids esterification in waste cooking oil using ion-exchange resins", **Fuel Processing Technology**, 102, 67-72.

[13] R.Tesser, L.Casale, D.Verde, M.Di Serio, E. Santacesaria∗, 2009, "Kinetics of free fatty acids esterification: Batch and loop reactor modeling", **Chemical Engineering Journal ,154 , 25–33**.

[14] Alpio C. Carmo Jr,Luiz K.C. de Souza,Carlos E.F. da Costa, E. Longo, Jos R. Zamian, Geraldo N.da Rocha Filho, 2009, "Production of biodiesel by esterification of palmitic acid over mesoporous aluminosilicate Al-MCM-41", **Fuel**, 88, 461-468.

[15] R. Tesser, L. Casale, D. Verde, M. Di Serio, E. Santacesaria,2010, "Kinetics and modeling of fatty acids esterification on acid exchange resins", **Chemical Engineering Journal, 157 ,** 539–550,

[16] Fukuda, H., A. Kondo and H. Noda., 2001, "Biodiesel fuel production by transesterification of oils", **Journal of Bioscience and Bioengineering**, 92,405-416.

[17] J.M. Marchetti, V.U. Miguel, A.F. Errazu, 2007, "Possible methods for biodiesel production", **Renewable and Sustainable Energy Reviews,** 11, 1300-1311

[18] Demirbas. A, 2005, "Biodiesel production from vegetable oils via catalytic andnon-catalytic supercritical methanol transesterification methods", **Progress in Energy and Combustion Science**, 31, 466-487

[19] W.W. Christie, 1993, "Preparation of ester derivatives of fatty acids for chromatographic analysis", **in Advances in Lipid Methodology**, 2, 69-111

[20] Gordon M. Harris, 1966. "Chemical Kinetics", Michigan, Heath.

[21] H. Scott Fogler, 2009. "Elements of Chemical Reaction Engineering", Massachusetts, Person Education, Inc.